Biomechanical analysis of different aspects in virtual reality : application

Jingtao Chen

Communauté
UNIVERSITÉ Grenoble Alpes

THÈSE

Pour obtenir le grade de

DOCTEUR DE L'UNIVERSITÉ DE GRENOBLE ALPES

Spécialité : **Mouvement et comportement pour la santé et l'autonomie**

Arrêté ministériel : 7 août 2006

Présentée par

Jingtao CHEN

Thèse dirigée par : **M. Peter MITROUCHEV**
Mme. Sabine COQUILLART
M. Franck QUAINE

Préparée au sein du **Laboratoire GIPSA**
Dans l'**Ecole doctorale EDISCE**

Biomechanical analysis of different aspects in virtual reality. Application

Thèse soutenue publiquement le : 30/01/2017
devant le jury composé de :

M. Georges DUMONT
Professeur, Ecole normale supérieure de Rennes, Rapporteur
M. Pierre PORTERO
Professeur, Université Paris – Est Créteil, Rapporteur
M. Marc SARTOR
Professeur, INSA Toulouse, Président
M. Michel TOLLENAERE
Professeur, Grenoble INP, Examinateur

M. François MOUTET
Professeur, Centre Hospitalier Universitaire, CHU Grenoble, Invité

Dedication

To my parents,

my wife and my son

Acknowledgment

Foremost, I would like to express my special appreciation and thanks to Dr. Peter Mitrouchev, Dr. Franck Quaine and Dr. Sabine Coquillart for their continuous support of my PhD research, for their patience, motivation, enthusiasm and immense knowledge. I would like to express my sincere gratitude to Grenoble Alpes University for providing the free and friendly research environment.

I wish to thank all members of the jury for the attention they have kindly given to this work: Prof. SARTOR Marc for doing me honors to chair this jury, Prof. DUMONT Georges and Prof. PORTERO Pierre for accepting the burden to be Reviewers and Prof. TOLLENAERE Michel for allowing me the honor to consider it. I want to thank them for their brilliant comments and suggestions.

I would especially like to thank prof. François MOUTET, Chef of Hand surgery center, who provide me the advice about the CRPS and the chance for conducting the experiment in his department. I would like also to thank the members of physical rehabilitation team: Mathieu JEAN-PIERRE, François ARRAMY and Manuel FRANÇOIS for giving me their valuable suggestions about our research.

I would like to thank Mr. Silvain GERBERS from GIPSA laboratory, for helping me to perform the statistical analysis and giving his suggestions on the data analysis. I would like to thank Charles-Henry DUTEFEL for developing the application used in CHU and helping me debug the program of pseudo-haptic experiment. My sincere thanks also go to Mr. Thierry Henocque from GINOVA laboratory, for supporting me with the device for simulation. I would like to thanks the staff of GIPSA Laboratory, G-SCOP Laboratory and INRIA for their good reception. I also want to thank all people who participated in my experiments. They generously donated their time to my research.

I would like to thank the LabEx PERSYVAL-lab *(ANR--11-LABX-0025)* for awarding me a scholarship and providing me with the facilities to complete this thesis.

At the end, I would like express appreciation to my beloved wife Min GONG who was always my support in the moments when there was no one to answer my queries.

Table of content

Part II Application in CRPS rehabilitation

List of the tables

List of figure

List of the articles

I. Related with the Ph.D. thesis

International journals

1. Jingtao Chen, Peter Mitrouchev, Sabine Coquillart, Franck Quaine. Disassembly task evaluation by muscle fatigue estimation in Virtual reality environment. The International Journal of Advanced Manufacturing Technology, 2016, <10.1007/s00170-016-8827-6

International conferences

1. P. Mitrouchev , J.T. Chen, S. Coquillart and F. Quaine, Length perception in virtual reality environment, MIT 2016 Conference Proceedings, Fiesa, Slovenia, 05-07 September, 2016, pp. 56-62.

In preparation

1. Jingtao Chen, Peter Mitrouchev, Sabine Coquillart, Franck Quaine. Towards a better understanding of pseudo-haptics: A force analysis during stiffness discrimination task.

II. Others

International Conferences

1. Peter Mitrouchev, Cheng-gang Wang, Jing-tao Chen, Disassembly Process Simulation in Virtual Reality Environment, in *Advances on Mechanics, Design Engineering and Manufacturing,* Lecture Notes in Mechanical Engineering, DOI 10.1007/978-3-319-45781-9_63, Ressorter International Publishing AG 2017, B. Eynard et al. (eds.), JCM 2016 Conference, 14-16 September, 2016, Catania, Italy, pp 631-638.

2. P. Mitrouchev J. Chen, F. Maffray, Y. Zheng, Enumeration of driving mechanisms in robotics by combinatorial analysis method, in: Mechanisms and Machine Science 37, Robotics and mechatronics, The 4th IFTOMM International Symposium on Robotics and Mechatronics, 2015 Poitiers (France), Ed. Ressorter, ISBN: 978-3-319-22367-4, Chapitre 5, pp 41-49.

3. Peter Mitrouchev, Cheng-gang Wang, Jing-tao Chen, Virtual disassembly sequences generation and evaluation, 6th CIRP Conference on Assembly Technologies and Systems (CATS), Goteborg, Sweden, Ed. Elsevier, Procedia CIRP 44 (2016) 347 – 352.

General Introduction

Human behavior is the subject of a lot of studies in numerous fields, spanning the social, natural, technological sciences and beyond. Being defined as the *capacity of mental, physical, emotional, and social activities experienced during the five stages of a human being's life*, important progress in understanding human behavior can only be achieved through a multidisciplinary community effort. The study we carried out aims to foster that effort by trying to understand basic human behavior and perception. It was realized in the frame of LABEX Persyval-Lab, Work package (WP2) *Authoring Augmented Reality*, research axis *Real-time capture and simulation of the real world. Representation and editing of virtual prototypes. Natural interaction with the augmented world*. Thus, the study federated skills in mechanics, bio-mechanics and computer sciences in order to better understand how virtual reality (VR) technologies, influence on human behavior with using biomechanical analysis methods in general and its application for Complex Regional Pain Syndrome (CRPS) rehabilitation in particular.

Fatigue in human is a natural response observed in workers or during sport activities. Understanding and evaluating fatigue remains a great challenge in physiology and biomechanics. Fatigue depends on several factors, such as: motivational, physiological and nervous, and it may be defined as the failure to maintain the required or expected force. Poorly designed working station or reduced rest can result in fatigue, accidents, injuries and illnesses. Fatigue reduces human reactions, decreases information processing accuracy, induces lack of attention and can be the cause of major accidents. In that way, evaluating fatigue of human operator during disassembly operation is of great importance. Disassembly operation is a very important issue often considered in the different stages of Product Life Cycle starting by its initial design and ending by its end of life. Note, that evaluating disassembly sequence with considering ergonomic factors, which influence the manufacturing and recycling efficiency, is also an important question in different industrial fields in general and in recycling activities in particular. Comparing with evaluation in real environment after product prototyping, it is more convenient and low-cost to evaluate the disassembly operation in VR environment which provides a potential way for creating a real-time visual/audio/haptic experience with computer systems [GoZa99, JiPu06, LaFP10, AlCa10, PKVD13]. As haptic device can provide force feedback to users, disassembly operation simulation with using haptic device in VR

environment is broadly used in operation training, ergonomic design verification etc. [AGLN09].

The importance of haptic sensation in real environment being high, simulating haptic feedback in virtual reality (VR) environment is a domain worth of exploring. Haptic feedback simulation provides the sense of touch to user by applying forces and vibrations or using information coming from other sensory modalities. Several industrial applications have utilized the simulated haptic feedback to create more realistic scenarios of training and operation simulations. Thus, coupling Haptic feedback simulations with biomechanical techniques may be useful to better understand human movement, especially the motor strategy for the muscle recruitment during a given task.

In order to avoid disturbing oscillations, *1000* Hz is necessary for the system who provide the haptic rendering. Comparing with the minimal updating frequency of haptic real-time loop, the visual scene-graph loop requires a lower minimal frequency of *60* Hz. Then some researchers tried to use the visual feedback to simulate the haptic feedback. Srinivasan et al. [SrBB96], Wu et al. [WuBS99] and [LCKR00] have influenced subject's perception of stiffness by manipulating the visual feedback in different amounts. Pseudo-haptics being "*the generation, augmentation or deformation of haptic sensations by information coming from other sensory modalities*" [LBCC01], Lécuyer et al. used it in order to provide the haptic sensations to subjects during spring stiffness estimation. This provides a new method to explore the possibilities for simulating the haptic feedback in VR environment. In [Lécu01], pseudo-haptic feedback allows "*to combine visual feedback with a passive haptic information related to or caused by a user action"* while perceiving the stiffness of pseudo-haptic spring. Several physical properties have been simulated by using the pseudo-haptic feedback such as: stiffness, friction, texture, weight, force field amongst others. Comparing with haptic device, pseudo-haptic feedback can use less computation resource to provide a high frequency haptic sensation.

Virtual reality has been proved to be a relevant technique in healthcare through surgery training and simulation, psychological treatment or robotic surgery. In health domain, there exist some diseases which influence patient's motor behavior. Complex Regional Pain Syndrome (CRPS), for instance, is one of those diseases. It is characterized by specific symptoms and often accompanied with motor disorders. Although the reasons of CRPS are not clear yet, it is believed that it is caused by the damages of the central nervous system. One of the key physiological symptoms of CRPS is the prolonged pain which can be unbearable in

some extremely cases. Different levels of pain, provoked by this disease, not only change the motor strategy of painful muscle, but also change the synergistic muscles while performing dynamic exercises [EFAG05]. When CRPS patient is performing some painful movements, peripherical adaptation may happen on movement-involved muscles. This implies that the pain can create alterations in skeletal muscle. Another symptom frequently observed in CRPS is the limited range of movement and the maladaptation due to abnormal posture of the affected limb. Structural alterations in skeletal muscle tissue and pain-induced adaptations may contribute to a deficient muscle activation in CRPS patient [BPMB13]. In order to prevent deterioration of CRPS on patient, encouraging them to actively participate in physical therapy is an important issue today. The virtual reality technology may be a useful tool which can respond this issue.

Research problematic

Human behavior and perception under the influence of VR-based application is an important issue, and investigation in this area can help researchers and professionals to understand and better utilize VR technology. In this context, one part of our research was conducted in order to better understand how haptic simulation applications will influence on human behavior and perception with using biomechanical analysis methods. As visual feedback can influence the physiological aspect of human [GPRS14], we try to manipulate this feedback by using computer-based application in order to improve the rehabilitation performance of CRPS patients.

For evaluating disassembly sequences with considering ergonomic factors, different tools and VR human-computer interfaces are proposed [GoZa99, RaMS99]. Platforms with haptic device, which can provide force feedback, are the example of those different tools. However, many of the platforms using haptic device are facing difficulties for evaluating muscles fatigue induced while performing disassembly operations.

Previous existing methods for evaluating disassembly sequences include the calculation of the energy expenditure [TLKC12], predicting the muscle fatigue associated with a specific task [RoFD04, DNHÅ11], predicting the energy consummation associated with a specific task [BSHG11] and modeling the work-recovery ratios [RNHK14]. However, most of these methods either use parameters obtained in too subjective way without corresponding physical considerations either require some physiological parameters with poor availability. Due to the complexities of the existing models and the necessity of requiring too many input data, their

usages are often limited. Hence, another method of evaluating the fatigue levels associated with different disassembly operations in VR environment is necessary.

A few research started to investigate pseudo-haptic influence on user's motor behavior, muscle involvement and limb coordination. Stiffness simulation, for instance, is an aspect for the experience in VR. Although there are many works investigating how the human perception may change with the influence of the pseudo-haptic feedback, to our knowledge how does pseudo-haptics influence subject's motor behavior in stiffness discrimination has not been investigated yet. Some previous works investigated finger forces applied in stiffness discrimination with real springs [Endo16, Fuji04]. However, the force during pressing on spring simulated by using pseudo-haptic feedback is not known yet. From biomechanical point of view, two questions arise:

- how does the pseudo haptic feedback influence the perception and force applied on the spring during stiffness discrimination task?
- can pseudo-haptic feedback induce different muscle activities in general and different muscle involvements in particular?

For improving the motor function of affected limb and reducing the pain, CRPS patients are encouraged to participate in physical therapy. One of the existing methods in such a therapy is mirror therapy which requires patient to fix the orientation of his/her head to the mirror and ignore his/her healthy limb. Those requirements limit patients to actively use the affected limbs and to associate mirror reflection with the movement of the affected limbs.

In VR rehabilitation platforms, visual feedback plays an important role in motor control [MoAr13, SMRB09], restoring brain function [RaAl09] and perception of physical properties. Virtual reality has been applied in rehabilitation tasks for many diseases, such as: stoke, phantom limb, … ([MJBT02, MPCH06]). Hoffman et al. mentioned in [HDPC00] that during treating the pain, virtual reality can be used to distract the patients and provide them relaxation and encouragement.

As we are aware the visual feedback can influence some physiological characteristics of humans. Thus, we try to manipulate the visual feedback to improve the rehabilitation performance of patients with CRPS on upper limbs. In order to manipulate the relationship between the motion of patients' physical limb and the rendered avatar hand motion, it is

necessary to track and reconstruct their hand motion. It is also necessary to test whether amplification of the movement can benefit the patient in rehabilitation.

Research contribution

In this context, our research attempts to understand how VR-based application will influence on human behavior and perception with using biomechanical analysis methods. It will enable to help researchers and professionals to understand and utilize VR technology better. Thus, we propose to amplify the hand movement of the patient in order to study the benefit of this amplification in the rehabilitation.

Thus, our contribution consists of:

- The development of a new method for evaluating the fatigue associated with a disassembly task. The fatigue evaluation is based on metabolic energy expenditure and electromyography (EMG) signal analysis. For this purpose, a VR application is developed and applied for disassembly task simulation which confirmed the efficiency of the proposed method.
- A better understanding on how does pseudo haptic feedback influences: the perception of stiffness; some kinematic parameters; force and EMG (surface electromyogram), signals during perceiving stiffness. For this purpose, we proposed a similar stiffness discrimination task as in [LCKR00] consisting in discriminating the stiffness of one amongst three real springs, with eleven virtual ones (pseudo-haptic spring). Through analyzing and comparing the pressing force, the kinematic parameters and the EMG signals recorded from subjects' arms during stiffness discrimination task, we firstly found that pressing forces on both real and virtual springs have similar behavior and the muscle co-activation induced by pseudo-haptic spring behaves as in dynamic movement task, even if the subjects' fingers were almost static.
- Proposing the first steps toward an application for hand rehabilitation for CRPS patients. Thus, new rehabilitation application based on low-cost device with acceptable accuracy of hand tracking is developed. Based on the Leap Motion and Unity3D, the application provides an avatar of the user's hand with an amplified or reduced motion. For this purpose, a pilot study for testing the feasibility of this application was conducted at the Central University Hospital (CHU) in Grenoble (France) in the Service of hand surgery. Some feedback from the involved subjects (a hospital practitioner, two physical therapists, a patient and a health subject) during the experiment have been collected. It

has been shown that all subjects had no uncomfortable feeling with using the application. The medical staff expressed interest in pursuing this work for potential rehabilitation applications.

Application area

Concerning the proposed method for evaluating the fatigue levels associated with different disassembly tasks, it is useful to provide a reference for product designers allowing them to estimate which disassembly sequence, among all the possible ones, induces least fatigue.

The results related to the pseudo-haptics, show that the force and the muscle co-activation behavior may be useful to better understand the pseudo-haptic feedback in stiffness discrimination task.

The application for CRPS patients' rehabilitation based on the Leap motion can be useful in kinesiological therapy. When the motion of the avatar hand is amplified, one hypothesis is that it may encourage patients to overcome the limited range of their movements due to pain or stiffer joint. On the other hand, when the motion of the avatar hand is reduced, one hypothesis is that it can help patients to amplify the range of their hand movements.

Limits of the work

- Concerning the model for evaluating the fatigue associated with a disassembly task, as the energy consumption of rotation movement is not considered, it only evaluates the fatigue levels associated with translation movement of disassembly tasks simulation. Since the method is proposed toward considering the muscle fatigue factor with one hand disassembly operation simulation in the initial stage of product design, it might not be adapted for the disassembly operation simulation during a real disassembly task which often involves two-hand gestures and different body positions.

- Concerning the biomechanical analysis of pseudo-haptics, only its influence on hand behavior during stiffness discrimination task was investigated. Other potential influences of pseudo-haptic feedback to simulate friction, force field are not investigated in the frame of our study.

- Concerning the feasibility test of application developed toward CRPS rehabilitation, it involves with the medical staff of Hand Surgery department at CHU Grenoble and one patient which is not enough to ensure the safety usage of the developed application. Due to the limited accuracy of Leap Motion device, the avatar hand motion is not stable. Consequently, this instability results in the dissatisfaction during using the application.

Structure of the manuscript

The manuscript consists of two parts:

The first part (Part I), entitled "Biomechanical analysis of haptic-based concepts and tasks" consists of two chapters:

A new method for disassembly task fatigue evaluation based on metabolic energy expenditure and muscle fatigue estimation is presented in Chapter 1. The analytical model for mechanical energy expenditure is presented in details where the required mechanical work is used as main parameter thus allowing to compare relationships among different fatigue levels associated with different disassembly operations in VR environment. The fatigue levels are evaluated by analyzing the recorded EMG signals on operator' arm. The proposed method is validated by a set of experimental loading tests performed in the realized Virtual Reality environment allowing to simulate rehabilitation tasks. Finally, the analytical and experimental results are compared thus showing very good correlation between them.

Chapter 2 focusses on the force, kinematic parameters and the EMG signal on flexors and extensors of subject's forearm induced by the pseudo-haptics during stiffness discrimination task. The performed series of tests for stiffness discrimination between real spring and virtual spring (with pseudo-haptic feedback) are presented. The materials and the method including measurement items, experiment protocol, participants and data analysis are detailed then. The results concerning the perception under different stiffness, the pressing force, the kinematic parameters, and EMG signals and co-activation are also presented and then analyzed. Finally, how the pseudo-haptic feedback underestimates the stiffness and how the muscle co-activation levels change under the influence of pseudo-haptic feedback are discussed.

The second part (Part II), entitled "Application in CRPS rehabilitation", consists in one chapter.

Chapter 3 introduces the basic notions and situations of CRPS including its symptoms, the traditional physical therapy and some existing physical methods for rehabilitation. The mirror neuron system and the mirror therapy as one of the effective methods for treatment are presented. Comparing with the traditional method for physical therapy, some virtual reality environments and platforms for CRPS rehabilitation applications in general, and for hand movement reconstruction in particular are presented in this chapter as well. The developed platform for CRPS patients' rehabilitation, based on Leap Motion, and the series of pilot tests performed with patients and Hand surgery medical staff in Grenoble University Hospital are presented. The range of hand movement of subject-controlled avatar during the experiments, under different conditions, were reported and their feedbacks were analyzed thus allowing to improve the performances of the platform in future.

This Ph.D. thesis work was realized in a multidisciplinary collaborative environment in the frame of LABEX PERSYVAL Lab (Pervasive Systems and Algorithms) (http://www.persyval-lab.org/index.html) where G-SCOP (Sciences for Design, Optimisation and Production Laboratory of Grenoble), GIPSA Lab (Grenoble Images Speech Signal and Control) Grenoble, and INRIA (National research Institute in Computer sciences and Automation) Grenoble, are involved. The whole work during the Ph.D. is under the co-direction of Dr. Peter MITROUCHEV associate professor HDR at University Grenoble Alpes (UGA), Dr. Franck QUAINE associate professor HDR at UGA and Dr. Sabine COQUILLART research director at INRIA. The experimental part presented in Chapter 1 was conducted in Gi-Nova Plateforme Technologique, Systèmes de Production, AIP-PRIMECA, Dauphiné-Savoie, Grenoble. The experiments presented in Chapter 2 were conducted in Biomechanical platform of GIPSA Lab, SAIGA Team, Grenoble. The experiments presented in Chapter 3 were conducted in CHU (Centre Hospitalier Universitaire) Grenoble under the supervision of prof. François MOUTET, Chef of Hand surgery center.

Part I

Biomechanical analysis of haptic-based concepts and tasks

This part presents two researches which are related with evaluating the fatigue levels associated with VR-based application for disassembly task evaluation in VR environment, and biomechanical analysis of pseudo-haptics in the aspect of human perception and behavior.

Disassembly operation simulation in VR environment is a novel way to evaluate the disassembly sequences in the initial design stage, product maintenance and product recycling process. First, we evaluate the muscle fatigue levels associated with different disassembly tasks simulated in VR environment using haptic device. For this purpose: i). a new method for disassembly task fatigue evaluation based on metabolic energy expenditure and muscle fatigue estimation is proposed; ii). the fatigue levels are evaluated by EMG (electromyography) signals analysis when performing disassembly task. The proposed method is validated by a set of experimental loading tests performed in a Virtual Reality environment.

Usually Pseudo-haptics utilizes not only visual feedback, but also information from the other sensory modalities to provide perception of different physical properties such as: shape or texture without providing the same physical existence in reality. Secondly, we focus on force induced by pseudo-haptics during stiffness discrimination task. For this purpose, series of tests for stiffness discrimination between real spring and virtual spring (with pseudo-haptic feedback) are performed. Thus, the materials and the method including measurement items, experimental protocol, participants and data analysis are presented. Then, the results concerning: the perception under different stiffness, the pressing force, the kinematic parameters, and EMG (Electromyography) signals and co-activation are presented. Finally, how does the subject underestimate the stiffness of pseudo-haptic spring and how does the Pseudo-haptic induce different muscle co-activation levels are discussed.

Chapter 1

Evaluation of fatigue levels during disassembly task

This chapter presents a new method for disassembly task fatigue evaluation based on metabolic energy expenditure and muscle fatigue estimation. A new analytical model for mechanical energy expenditure is proposed where the required mechanical work is used as main parameter allowing to compare relationships among different fatigue levels when performing disassembly task. Then, the fatigue levels are evaluated by analyzing the recorded EMG (electromyography) signals on some muscles of the operator' arm. The proposed method is validated by a set of experimental loading tests performed in a specially realized Virtual Reality environment. Then the analytical and experimental results are compared showing a very good correlation between them.

1.1 Introduction

Simulations closely related with Assembly/Disassembly (A/D) operations represent important research subject today. These A/D operations are often considered in the initial stage of product design.

Virtual reality is "*a simulation in which computer graphics is used to create a realistic looking world"* [BuCo03]. It creates a real-time visual/audio/haptic experience with computer systems [PKVD13] and provides a potential way for A/D operation simulation [GoZa99, JiPu06, LaFP10, AlCa10]. In order to evaluate disassembly sequences in the initial stage of product design, different tools and VR human-computer interfaces are proposed [GoZa99, RaMS99]. As the Virtual reality set-up can be easily modified, designer can quickly adjust the design of product [PSBM13].

As previously said, preliminary evaluation of disassembly sequences during product design is a very important issue. Thus, for disassembly task of complex products, two questions are arising, namely:

- disassembly sequence generation,

- disassembly sequence evaluation.

This chapter is focusing on the second one. In this context, it considers the operator's muscle fatigue factors in evaluation of fatigue associate with disassembly task. Thus, the new method for evaluating the fatigue associated with disassembly task by utilizing metabolic energy expenditure is presented here below.

The two principal parameters for carrying out the calculation of metabolic energy expenditure for disassembly tasks, which potentially may be used for different applications are:

- the *weights* of the components,

- the *disassembly paths* of the components.

For this purpose, disassembly experiments in VR were performed in order to evaluate fatigue with EMG analysis during performing disassembly tasks.

Our method shows that using EMG data can give relevant information about the subject muscle state, which could be of interest in the field of evaluation of disassembly task. The proposed method aims to give a fatigue level rank of disassembly task operations.

The results of the study of this chapter may be useful for product designers as a decision-making tool allowing them to evaluate the muscle fatigue level while performing different disassembly sequences.

1.2 Previous work

The literature analysis carried out within this study shown that certain existing approaches for disassembly evaluation, some integrated in VR, were proposed by taking into account different criteria such as:

- visibility score [Wang14, WMLL15, MiWC16],
- set of directions for removal (SDR) [PPTC04, LXGK13, WMLL15],
- stability of sub-assembly [AlCa10, MiWC16],
- disassembly time [GuGu97] ,
- Combination of multiple ergonomic factors [YoAE11],
- disassembly cost [MoZG09],
- number of necessary tools for disassembly [MWLL15].
- …….

However, they do not take into account the muscle fatigue of the operator for different conditions of requests (postures, efforts), which in our opinion is highly influencing work's efficiency and very important today with the increasing of the retire age of the operators.

For disassembly sequences evaluation *disassembly cost function* was proposed in by using parameters such as:

- removing time of component and fasteners [DeMi03, CDPS07],
- accessibility and orientation factors [JJSK06, SmCh11],
- disassembly distances [SrFG99, TsYH11].

However, simply multiplying or dividing a subjective weight value with a factor being considered in disassembly operation does not promise to obtain a convincing analytical model without corresponding physical essence.

The *total time* for disassembly was proposed as main evaluation indicator for disassembly operations' evaluation in [GuGu97, KoGu05, GiFa07] by considering the disassembly direction and the joint type. However, using the total time for disassembly is not an appropriate indicator because the operator may expend different amount of energy for moving a given component with different velocities, i.e. with different powers.

Trying to avoid uncertainty of disassembly operation process, Tian et al. [TLKC12] proposed a method to calculate the probability of disassembly energy's distribution and the minimal energy expenditure in a disassembly sequence. The minimal energy for each disassembly sequence is estimated. However, the authors pointed out that the probable energy expenditure intervals of several disassembly sequences had the possibility to overlap with each other. In this context, a new method is needed for choosing the less-energy-spending disassembly sequence.

In order to model work-recovery ratios for optimizing the recovery time during tasks, Rose et al. [RNHK14] presented data from empirical study regarding how maximal pushing force, endurance time, recovery time and perceived discomfort vary with loading level and loading time. During the tests, subjects were asked to perform two trials which included a loading and a recovery trial. The results of the experiments show that:

- shorter endurance time is found in high loading level, compared with low loading level;
- subjectively perceived discomfort increases linearly with the increase of loading level;
- recovery time does not monotonically vary with loading levels.

However, this work does not present a general model allowing to describe the working-recovery ratios.

Some bio-mathematical models of fatigue (BMMF) based on work hours data have been proposed in [DNHÅ11] to predict the levels of fatigue associated with a pattern of work. *Fatigue Audit Inter Dyne* (FAID) is one of the BMMFs which has been commercially used to estimate work related fatigue. The hours of work are the input in the model allowing to estimate the work related fatigue associated with shift workers' duty schedules [RoFD04]. The output fatigue score represents a predicted sleep opportunity. One of the benefits of FAID model is the good availability of hours of work, which is the input data in the organizational records.

Predicting metabolic energy consumption associated with a disassembly sequence can be a criterion for evaluating the fatigue level induced by a disassembly sequence. In this optic Bisi [BSHG11] proposed an EMG (Electromyography[1]) *driven model* for predicting metabolic energy consumption during physical effort. It includes EMG signals from active muscles associated with some kinematic joint parameters. For using this method to predict the metabolic energy consumption of all the possible disassembly operation, it needs to measure the EMG signal of certain muscles and kinematic parameters of certain task-related muscles and joints during performing disassembly operation. However, it is too complex to be applied in the disassembly operation evaluation, because it is quite time consuming to perform erery disassembly sequence and predict its metabolic energy consumption which requires a motion capture analysis system coupled with EMG data processing.

A long time repeatedly performed training may activate the neural adaption of muscles by changing their activation mode. Rube and Secher [RuSe91] performed leg task experiment in three phases. During the first one all subjects were asked to perform one hundred and fifty maximum voluntary contractions (MVCs) in isometric leg extension task. On the second phase, subjects were assigned into two groups: one performing a training task with one-leg, the other performing the same training with two-legs. During five weeks, one-leg and two-leg trainings have been respectively performed by each group. After training, both groups were asked to perform once again one hundred and fifty MVCs in isometric one- and two- legged extension task, which was the third phase of the experiment. The results of comparison between the MVCs values before and after training shown that one-legged group of subjects was less tired when performing one-legged task, and two-legged group was less tired during two-legged task. It was mentioned in [Roge01] that the effect of training on fatigue depends on training mode. For a disassembly sequence, for instance, loading level, loading time and operation posture are not always the same.

Note, that evaluating disassembly sequence is also an important question in the industrial manufacture and recycling. Considering the ergonomic factor during the disassembly task, many works focus on:

- calculating the energy expenditure [TLKC12],
- predicting the muscle fatigue associate with the specific task [RoFD04, DNHÅ11],
- predicting the energy assumption associate with the specific task [BSHG11],

[1] All the EMG below means surface EMG after normalization

- modeling the work-recovery ratios [RNHK14].

1.3 Summary synthesis and critical analysis

The bibliographical analysis shows that the existing methods for disassembly sequence evaluation; developed so far, as we are aware, satisfy only partially the needs of designers and professionals.

The aim of disassembly sequence evaluation is to evaluate the cost of carrying out disassembly sequence. Different considerations for evaluating the disassembly cost product different evaluation methods. According to the applied techniques two large groups of methods for disassembly cost emerge, namely: *disassembility, time cost* and *physiological cost*.

The review of current approaches, a part of which was briefly presented here, and other works we have studied, leads to the following remarks:

- Considering the disassembility mainly evaluate the disassembly sequence by taking into account the disassemblility of disassembled components in each sequence. The parameters used in this type method includes the visibilities of component, removing time of component and fasteners, accessibility and orientation, disassembly distances etc. In order to calculate a disassemblility score for each disassembly sequence, subjective coefficients should be allocated to parameters to indicate their importance in disassembility. Without providing the corresponding physical meaning of value of subjective coefficient, the calculation has a potential to be subjective value which can't be used in disassembly sequence evaluation.

- Considering disassembly time is a direct method to evaluate the cost for disassembly sequence. In the case of automatic manufacturing or recycling, this method is effective.

- Considering physiological cost require to evaluate the fatigue or metabolic energy consumption associated with disassembly sequence. This type method is suitable for the case where human participant is real important for the process such as design verification, or manually performed manufacturing or maintenance. However, those existing methods always require hard-obtained data of human body.

The fatigue being an important factor which can affect the efficiency of performing the disassembly task, how to evaluate the level of fatigue in the muscles is also a part of our work. Muscle fatigue refers to the acute impairment of performance due to physical activity [Roge01].

The level of muscle fatigue and the mechanism underlying the development of fatigue depend on several parameters such as: type of muscle exercise, contraction intensity, sustained or intermittent contraction or isometric and dynamic movement [EnSt92]. Mechanisms contributing to fatigue are metabolic subtracts and acidification into the muscle [Vøll95] as well as impairment of activation [Mert54]. One possibility for this evaluation is to calculate the decreasing slope of median frequency of EMG signals [SoKn00]. The more the slope of median frequency decreases, the more muscle fatigue there is [DGBA99]. It was proven that the peak value of EMG signals after root mean square (RMS) processing is also an index of fatigue [BoGu14] when subjects are performing the task at the same level of force. However, it is not convenient for designer to evaluate the fatigue from EMG signals recorded for each possible disassembly sequence. Hence, another method of predicting the fatigue during disassembly task in simulating environment is necessary.

Hence, a new method of predicting the fatigue during disassembly task in VR environment should be proposed. As we are aware, in the literature there are not methods involving muscle fatigue to evaluate disassembly task.

There exists some previous works which focus on comparing the motor control, fatigue and motor adaptations while performing task in real and virtual environment [Koch08, KSCK09, PDSM14]. However, it is not the object of our study since we propose to focus more on a method for fatigue evaluation in virtual reality environment without direct comparison with the real environment.

1.4 Method for fatigue level evaluation

While performing disassembly task in VR environment subject interacts with the virtual object with or without force feedback. In the next of this chapter, we consider that the disassembly task provides force feedback. The method for evaluation of fatigue associated with disassembly task, proposed here, is based on metabolic energy expenditure estimation model.

1.4.1 Hypotheses and basic principles

Considering muscle fatigue factor in disassembly task evaluation, a rank of fatigue levels should be available for designers and operators allowing them to choose a disassembly task inducing less fatigue. As the operator uses his/her the arm to perform the disassembly operation simulation, only the consumption of the energy on the arm is taken into account of the model.

For this purpose, the arm's energy expenditure is used as indicator for muscle fatigue estimation. The method presented here below is built upon the following hypotheses [CMCQ16]:

Hypothesis 1: The more mechanical energy is required to complete the disassembly task, the more metabolic energy will be consumed in the human arm.

Hypothesis 2: The arm muscles, involved in the disassembly task, perform in an environment with constant temperature. The task is performed in continuous way. The fatigue accumulated in the muscle is a monotonically increasing function of the metabolic energy expenditure.

Hypothesis 3: During the disassembly task, the operator is moving the virtual objects with a given velocity in all allowed disassembly directions. The disassembly trajectory (path) is not a closed loop.

Hypothesis 4: Under the conditions of Hypotheses 1, 2 and 3, if the consumed metabolic energy for performing disassembly task 1 is bigger than this for disassembly task 2, then disassembly task 1 induces more fatigue than 2.

The reason why the hypothesis 1 cannot be obviously established is that the mechanical work is only a part of the energy consumed in the arm. Exerting force to move an object is not the only part that consumes the muscle metabolic energy. Let $\dot{E}$ (in *Jules/kg*) be the total energy expenditure rate for a muscle. It can be expressed as [ZBHR11]:

$$\dot{E} = \dot{h_a} + \dot{h_m} + \dot{h_{sl}} + \dot{w_{ce}} \tag{1-1}$$

where: - $\dot{h_a}$ is the muscle activation heat rate,

- $\dot{h_m}$ is the maintenance heat rate,
- $\dot{h_{sl}}$ is the shortening/lengthening heat rate,
- $\dot{w_{ce}}$ the mechanical energy rate.

The relationship between the increase of $\dot{w}_{ce}$ and the variations of $\dot{h}_a + \dot{h}_m + \dot{h}_{sl}$ is not evident. Thus, hypothesis 1 is proposed, and its proof is presented in the next section.

1.4.1.1 Proof for ***hypothesis 1***

Let $\eta = \frac{\dot{w_{ce}}}{\dot{E}}.100\%$ is the percentage of mechanical energy expenditure. Then one has:

$$\dot{h_a} + \dot{h_m} + \dot{h_{sl}} = \dot{w_{ce}} \frac{1-\eta}{\eta} \tag{1-2}$$

Let $\frac{1-\eta}{\eta} = f(\eta)$. It is easy to prove that $f(\eta)$ is a monotonically decreasing function of η.

However, the experimental results presented in [BrKP03] indicate that η is a monotonically decreasing function of $\dot{w_{ce}}$. Then it can be proved that $\dot{w_{ce}} \frac{1-\eta}{\eta}$ is a monotonically increasing function of $\dot{w_{ce}}$ ($\frac{d(\dot{w_{ce}} \frac{1-\eta}{\eta})}{d\dot{w_{ce}}} > 0$). Since $\dot{w_{ce}} \frac{1-\eta}{\eta}$ is equivalent with $\dot{E}(1-\eta)$, consequently $\dot{E}(1-\eta)$ is also a monotonically increasing function of $\dot{w_{ce}}$. Thus, $\dot{E} = \dot{E}(1-\eta) + \dot{w_{ce}}$ is a monotonically increasing function of $\dot{w_{ce}}$.

For example, from Figure 1.1 ([BrKP03]) is seen that the mechanical work and the total energy of a muscle increase with the increase of the mechanical work during the simulation and experimental phases.

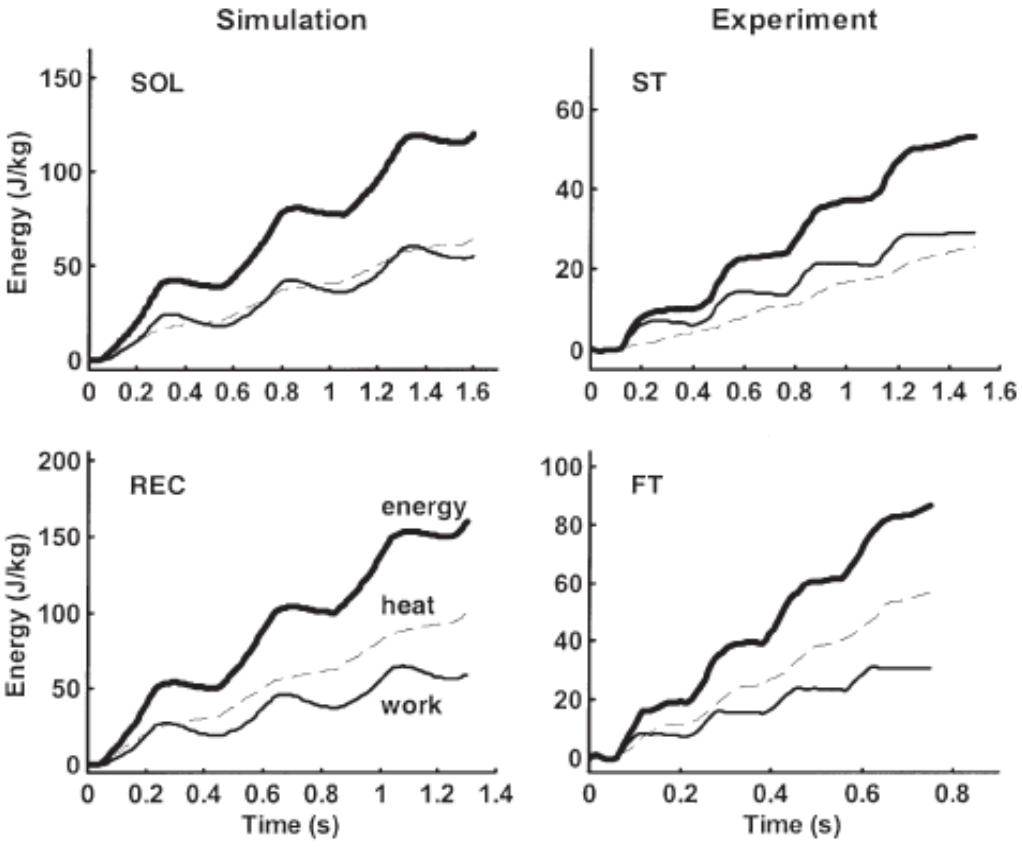

Figure 1.1. Work, heat and total energy liberation during simulated and experimental cyclic concentric contractions [BrKP03].

Simulation data are shown for soleus (*2 Hz*) and rectus femoris (*2.5 Hz*) muscles. ST and FT are respectively the data for Slow Twitch and Fast Twitch fibers [BrKP03].

1.4.1.2 Proof of hypothesis 2

In the conclusions of [Lind00, Vern29] it is stated that:

- *i).* The level and duration time of exerted tension varies with the changes of the successive contractions and the external temperature (in [Lind00] the muscles are immersed in water on two places with different temperatures);
- *ii).* The durations of muscle's contraction in *18℃* are much greater than ones in *34℃.*

Based on those two statements, duration time between two contractions is set to zero and the ambient temperature is fixed while performing disassembly task.

According to Hypothesis 2, the fatigue accumulated in the muscle is a monotonically increasing function of the metabolic energy expenditure. In addition, according to the conclusions in [SHWP15], the force generation capacity after the exercise is monotonically decreasing with the increase of force level and consequently can be used as an index of fatigue level estimation. Thus, we may do the hypothesis that the fatigue accumulated in the muscle is monotonically increasing with the increasing of the force level.

A consequence of Hypothesis 1 is that the mechanical energy is monotonically increasing with the increase of force level. The results in [RNHK14] clearly concluded that higher load level leads to statistically significant shorter endurance time and recovery time increases with increasing loading time. Both shorter endurance time and longer recovery time indicate the accumulation of more fatigue.

We present the fatigue as $FA = f(FA_c, FA_p)$, where FA_c and FA_p are respectively the fatigue in *central* nervous system and *peripheral* system (muscle). Note, that central nervous system fatigue is not taken into account in the proposed method. The metabolic energy expenditure *E* being considered as a function of *F*, *t* and *v*, then the FA_p can be expressed as:

$$FA_p = f(E(F, t, v)) \tag{1-3}$$

where: $F \in (0, F_{max}]$ is the loading level,

$t \in (0, t_{max}]$ is the loading time,

$v = (0, v_{max}]$ is the velocity of the end of hand (arm).

Based on the muscle mechanical model [SHWP15], maximal muscle fatigue may be reached for different values of *F*, *t* and *v*. Thus, the boundary conditions are respectively:

- If *F* is near *0*, *t* and *v* can respectively arrive at t_{max} and v_{max}.

- If F is equal to F_{max} , *t* and *v* tend to *0* (zero).

The FA_p derivative of F is: $\frac{dFA_p}{dF} = \frac{\partial FA_p}{\partial E} \cdot \frac{\partial E}{\partial F}$. Thus, based on the data presented in [RNHK14] the FA_p is a monotonically increasing function of *F*, *which* means that $\frac{dFA_p}{dF} > 0$. It is obvious that $\frac{\partial E}{\partial F} > 0$ and consequently $\frac{\partial FA_p}{\partial E} > 0$ is correct in the range of loading level tested in [RNHK14] which are in agreement with those observed in our disassembly task. It means that FA_p is a monotonically increasing function of *E*.

1.4.2 Mechanical work for performing disassembly task

A long time repeatedly performed training may activate the neural adaption of muscles by changing their activation mode. That is the reason why we consider the effect of long-time task training on fatigue evaluation.

Based on the proof for *Hypothesis 1* (Section *1.3.1.1*), if the mechanical work consumed to perform the disassembly task can be calculated, it can indicate which disassembly task consumes more metabolic energy and consequently induces more fatigue in the muscles.

Note that for disassembling a target component from an assembly, there may be many possible disassembly sequences. Consequently, different disassembly sequences can be used as different disassembly tasks. Evaluating the fatigue levels associated with different disassembly sequences can also be applied in the evaluation of fatigue levels associated with different disassembly tasks. In disassembly task, the principal involved movement is to move the virtual object. The mechanical energy expenditure for component disassembling execution and the operator's arm movements are presented in the following content of this chapter.

1.4.2.1 Mechanical energy expenditure for moving disassembly components

The mechanical work spent by the muscular force required to perform the task (moving an object) will transfer into potential and kinetic energies. Suppose that the i-th component should

be disassembled in disassembly sequence (task) 1. The variation of the total mechanical energy ΔE_i is:

$$\Delta E_i = \Delta E_{ki} + \Delta E_{pi} = \frac{1}{2} m_i ({v_i}^2 - {v_{i0}}^2) + m_i g h_i \quad (1\text{-}4)$$

where: - ΔE_{ki} and ΔE_{pi} are respectively the variations of kinetic and potential energy,

- m_i is the mass of the component,
- v_i and v_{i0} are respectively the velocity of the component at *ending point* and *starting point*,
- h_i is the vertical displacement of the component.

The system is evolving in Earth gravity field (gravity vector g is supposed in negative vertical direction). Let h_{iu} and h_{id} be respectively the total vertical displacement of the mass center of the ith disassembled component along the positive (up) and negative (down) directions. The velocities v_i and v_{i0} are both equal to *0 m/s*, then equation (1-4) can be written as:

$$\Delta E_i = m_i g (h_{iu} - h_{id}) \quad (1\text{-}5)$$

Consider the disassembled component as an isolated system, and let ΔE_{iu} and ΔE_{id} be respectively the variation of mechanical energy when the component moves upward and downward:

$$\Delta E_{iu} = m_i g h_{iu} \quad (1\text{-}6)$$

$$\Delta E_{id} = -m_i g h_{id} \quad (1\text{-}7)$$

Although ΔE_{iu} and ΔE_{id} have opposite signs, they cannot offset with each other when calculating the mechanical energy expenditure of the arm. If the component is only affected by the gravity, the variation of its potential energy should be equal to the variation of the kinematic energy. But when the component is stopping at a highest or lowest point of the disassembly path, the kinetic energy is zero, which corresponds to the starting point of the disassembly path. The reason why the potential energy does not fully transform into kinetic energy is because of the mechanical work done by the arm. Hence, for disassembling the ith component, the mechanical work done by the arm is:

$$\Delta E_{iu} + |\Delta E_{id}| = m_i g (h_{iu} + h_{id}) \quad (1\text{-}8)$$

1.4.2.2 Mechanical energy expenditure for moving the operator's arm

The variation of mechanical energy of operator's arm from the starting point of the ith component to the position of the next disassembled component, ΔE_{ai}, can be express as:

$$\Delta E_{ai} = \Delta E_{aki} + \Delta E_{api} = \frac{1}{2} m_a \left(v_{qi}^2 - v_{ai0}^2\right) + m_a g h_{ai} \quad (1\text{-}9)$$

where: - m_a is the mass of the arm,

- h_{ai} is the vertical displacement of the mass center of the arm between the starting point of the ith component and the position of the next component;
- ΔE_{aki} and ΔE_{api} are respectively the variation of the kinetic and potential energies of operator's arm.

Similarly, as the mechanical energy of the disassembly component (eq. (1-8)), ΔE_{ai} can be written as:

$$\Delta E_{ai} = m_a g (h_{aiu} - h_{aid}) \quad (1\text{-}10)$$

where: h_{aiu} and h_{aid} are respectively the total vertical displacement of the arm's mass center along the positive and negative direction of ith component.

The mechanical work, done by the shoulder, to move the arm is:

$$E_{haiu} + |E_{haid}| = m_a g (h_{aiu} + h_{aid}) \quad (1\text{-}11)$$

Assuming that there are n components to be disassembled in sequence S (task). Thus, the required arm's mechanical energy is:

$$\Delta \mathrm{E_{S1}} = \sum_{\mathrm{i=1}}^{\mathrm{n}} (\Delta \mathrm{E_i} + \Delta \mathrm{E_{ai}}) \quad (\mathrm{i} = 1,2,3 \ldots n) \quad (1\text{-}12)$$

When the operator's arm is coming back to the initial position after performing the task: $h_{aiu} = h_{aid}$. Thus, eq. (1-8) can be rewritten as:

$$\Delta E_{S1} = \sum_{i=1}^{n} [m_i g (h_{iu} + h_{id}) + 2 m_a g h_{aiu}] \quad (i = 1,2,3 \ldots \mathrm{n}) \quad (1\text{-}13)$$

Note that h_{iu} and h_{id} should be the real vertical displacements of the end point of the hand in the real world, not the vertical displacement of avatar's hand in the VR world (see details in Section 1.4.1).

1.4.2.3 Vertical displacement of the arm's mass center

The vertical displacement of the center of the arm's mass h_{aiu} (see eq. (1-13)) is also a parameter, which has to be calculated. The arm can be geometrically abstracted as a two DOF (degrees of freedom) mechanism with three segments as shown in Figure 1.2. Note that the first segment is the operator's body, supposed to be the frame of the mechanism.

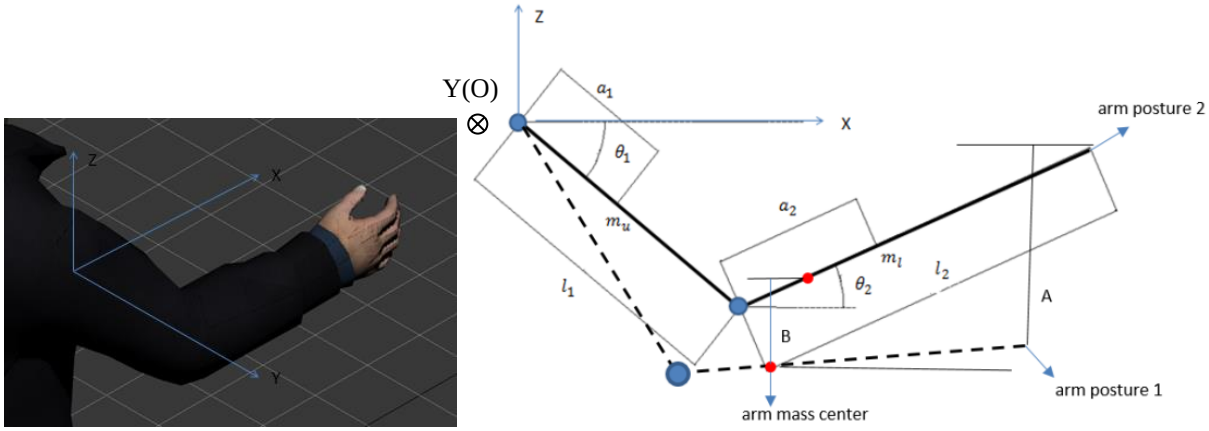

Figure 1.2 Arm and its associated two joints mechanism

Assume that the shoulder only rotates around ***Y*** axis. Consequently, the forearm and upper arm form the plane of ZOX. Let:

- l_1 and l_2 be respectively the length of upper and lower arms;

- a_1 and a_2 the relative position of mass center of upper and lower arms;

m_u and m_l respectively the mass of the upper and lower arm;

θ_1 and θ_2 the absolute rotation angles of each segment (upper and lower arms) related to the horizontal frame axe **X.**

It is also assumed that the center of mass of each segment is stable inside each segment. Thus, the coordinates *x* and *z* of arm's mass center are:

$$x = \frac{m_u a_1 cos\theta_1 + m_l(l_1 \cos\theta_1 + a_2 \cos\theta_2)}{m_u + m_l} \quad (1\text{-}14)$$

$$z = -\frac{m_u a_1 sin\theta_1 + m_l(l_1 \sin\theta_1 + a_2 \sin\theta_2)}{m_u + m_l} \quad (1\text{-}15)$$

For a given disassembly path of the ith component, the vertical displacement of the hand end point A_i between two dates t_0 and t_1 is:

$$A_i = l_1\left(sin\theta_{1i}^{t_1} - \sin\theta_{1i}^{t_0}\right) + l_2\left(sin\theta_{2i}^{t_1} - \sin\theta_{2i}^{t_0}\right) \quad (1\text{-}16)$$

The vertical displacement of the arm's mass center B_i is:

$$B_i = \frac{(m_u a_1 + m_l l_1)\left(sin\theta_{1i}^{t_1} - sin\theta_{1i}^{t_0}\right) + m_l a_2\left(sin\theta_{2i}^{t_1} - sin\theta_{2i}^{t_0}\right)}{m_u + m_l} \quad (1\text{-}17)$$

Let $\Delta_{1i} = sin\theta_{1i}^{t_1} - sin\theta_{1i}^{t_0}$ and $\Delta_{2i} = sin\theta_{2i}^{t_1} - sin\theta_{2i}^{t_0}$. Then, B_i can be expressed as function of A_i and Δ_{1i} (Δ_{2i} being eliminated):

$$B_i = \frac{m_u a_1 l_2 + m_l l_1 (l_2 - a_2)}{(m_u + m_l) l_2} \Delta_{1i} + \frac{m_l a_2}{(m_u + m_l) l_2} A_i \quad (1\text{-}18)$$

The relation between A_i and B_i implies that the rotation angle of upper arm θ_{1i} in **ZOX** plane at the starting and ending point of the trajectory of the ith component has to be measured. From eq. (1-18)), h_{aiu} can be expressed as:

$$h_{aiu} = \left| \frac{m_u a_1 l_2 + m_l l_1 (l_2 - a_2)}{(m_u + m_l) l_2} \Delta_{1i} + \frac{m_l a_2}{(m_u + m_l) l_2} A_i \right| \quad (1\text{-}19)$$

Finally, A_i is calculated from the disassembly path of the ith component knowing the position of start and end points.

1.4.2.4 Mechanical energy expenditure for fasteners' disassembling

We suppose that for fasteners' disassembling special disassembly tools will be required. Consequently, these tools are considered as ordinary disassembly components moved by the operator during the disassembly process. Hence, calculating the energy expenditure for disassembling fasteners is performed by using the same model as for the disassembly components.

Thus, with the proposed model, the mechanical energy expenditure for performing all the possible disassembly sequences (including moving the disassembly components, fasteners and tools) can be estimated by eq. (1-13) and (1-19). Note, that the different disassembly sequences are potentially different disassembly tasks which will induce different levels of fatigue in the patient muscles.

1.4.3 Example of calculation

In order to illustrate the analytical model for evaluating the fatigue induced during disassembly sequence simulation, an example of a simple disassembly manufacturing process is presented here below. It consists in disassembling a five-component mechanical assembly. Let the target component be component *3* as presented in Figure 1.3.

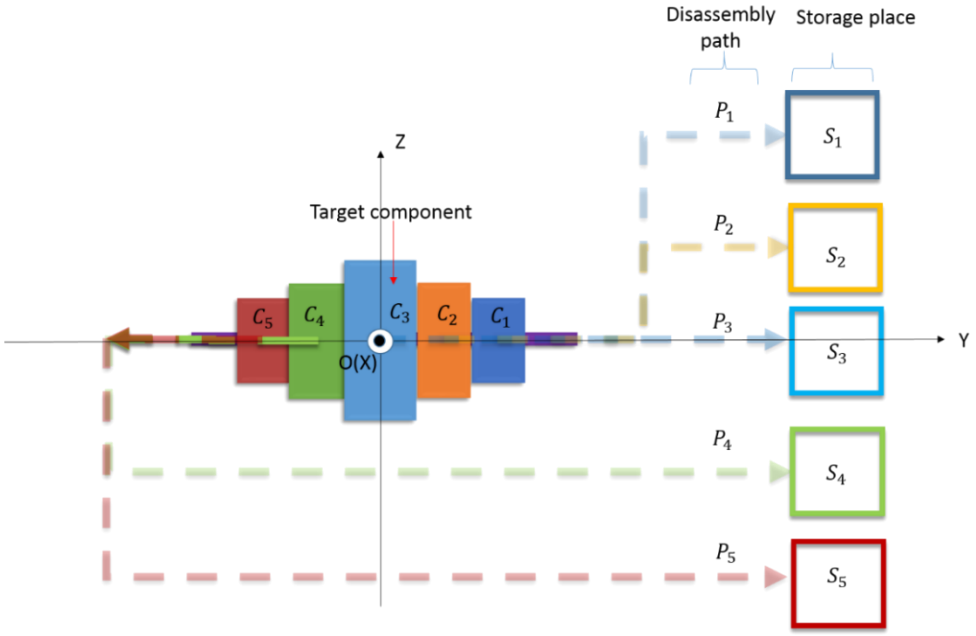

Figure 1.3 Mechanical assembly and parts' trajectories for disassembling target component $\boldsymbol{C_3}$

Legend: Each component ($C_1, C_2 \ldots C_5$) is moved from its initial position to storage place ($S_1, S_2 \ldots S_5$) following the corresponding disassembly path ($P_1, P_2 \ldots P_5$)

There are two possible disassembly sequences for disassembling the target component C_3 : Sequence S1= $\{C_1, C_2, C_3\}$ and Sequence S2= $\{C_5, C_4, C_3\}$. In here, (x_{is}, y_{is}, z_{is}) and (x_{ie}, y_{ie}, z_{ie}) denote respectively the disassembly *starting* point and disassembly *ending* point coordinates of the mass center of *i*th component. The values of the three parameters, namely: *mass* and its *starting* and *ending positions* of each component are presented in Table 1.1.

Table 1.1 Parameters for disassembly sequence evaluation

Mass	Value (kg)	Starting point	Value (mm)	Ending point	Value (mm)
m_1	1	(x_{1s}, y_{1s}, z_{1s})	(0,20,0)	(x_{1e}, y_{1e}, z_{1e})	(0,60,60)
m_2	1.5	(x_{2s}, y_{2s}, z_{2s})	(0,10,0)	(x_{2e}, y_{2e}, z_{2e})	(0,60,30)
m_3	3	(x_{3s}, y_{3s}, z_{3s})	(0,0,0)	(x_{3e}, y_{3e}, z_{3e})	(0,60,0)
m_4	1.8	(x_{4s}, y_{4s}, z_{4s})	(0,-10,0)	(x_{4e}, y_{4e}, z_{4e})	(0,60,-20)
m_5	0.8	(x_{5s}, y_{5s}, z_{5s})	(0,-20,0)	(x_{5e}, y_{5e}, z_{5e})	(0,60,-40)

As previously said, the proposed method for evaluating the disassembly task by mechanical energy expenditure requires to measure angle θ_1 of the arm at the starting and ending point for all the components involved in the disassembly sequences. Kinect 2 was used to capture this angle and the data are as presented in Table 1.2.

Table 1.2 Angle between operator upper arm and horizontal frame line for starting and ending point of the components

Component	1	2	3	4	5
$\theta_{1i}^{t_0}$ (rad)	-0.550	-0.592	-0.627	-0.592	-0.550
$\theta_{1i}^{t_1}$ (rad)	0.500	0.159	-0.387	-0.429	-0.953

Concerning the parameters of the arm, they are the same as in [SYMM97] presented in Table 1.3.

Table 1.3 Parameters of the arm

	m_u(kg)	m_l(kg)	l_1(m)	l_2(m)	a_1(m)	a_2(m)
values	2.537	2.332	0.298	0.419	0.151	0.167

The values of h_{aiu} for each component, calculated according to equation (4-19) are presented in Table 1.4.

Table 1.4 Values of $\boldsymbol{h_{aiu}}$

component	1	2	3	4	5
h_{aiu}(m)	0.223	0.0837	0.025	0.006	0.158

According to the proposed model, the mechanical energy for performing the disassembly Sequence 1 and Sequence 2 are respectively: $\Delta E_{S1} = 41.87J$ and $\Delta E_{S2} = 24.66J$. It is seen that ΔE_{S1} is bigger than ΔE_{S2}. Based on Hypothesis 1, 2, 3 and 4, the results show that performing disassembly Sequence 1 induces more fatigue in the arm's muscles than performing disassembly Sequence 2.

1.5 Experimental disassembly task evaluation by muscle fatigue estimation

1.5.1 Experiments

In order to prove the proposed model, series of experiments were carried out in the Virtual Reality environment GINOVA platform, Grenoble-INP (National Polytechnic Institute). The task consisted in handling a simulated electrical motor (weight of *1kg*) in a restricted vertical space of *0.5m* with repetitive *bottom up* and *up down* movement during *5* minutes with a frequency of *0.42 Hz* (*25* movements for one minute). The distance between subjects' eyes and the display screen is fixed at *2.25 m*.

The visual feedback (displacement of the component in the VR screen) is the same as the displacement of the end of the hand in the real physical environment. That means there is no geometrical coefficient scale between both movements. During the operations, the upper arm of subject is in static position (θ_1 is constant).

1.5.1.1 Participants

Nine subjects (eight male right-handed and one female left-*handed*), aged from *24* to *58*, were involved in the experiments. Unfortunately, the female subject did not endure until the end of the task, so the effect of different sex on fatigue has not been investigated in this stage of the study.

Subjects declared no performed intensive muscle efforts during *24* hours period. All participants reported no history of problem in upper limbs. Since θ_1 is constant, when calculating the mechanical work, the task is performed when only the lower arm is moving.

1.5.1.2 Simulation tests

The environment consists of (Figure 1.4):

- VIRTUOSE 6D35-45 haptic device with force feedback,
- Kinect tracking system,
- stereoscopic display,
- 3D glasses,
- four channels EMG *BIOPAC MP150* system.

The software used to generate the simulation environment is IFC (*Interactive Fitting for CATIA*) which is a CAAV5-based plug-in for CATIA V5TM for interactive simulations. The weight of the component was simulated by the gravity environment in CATIA. Virtual objects

in the software are constrained by gravity field. The force feedback, during collisions, is sent to the subject via the haptic device.

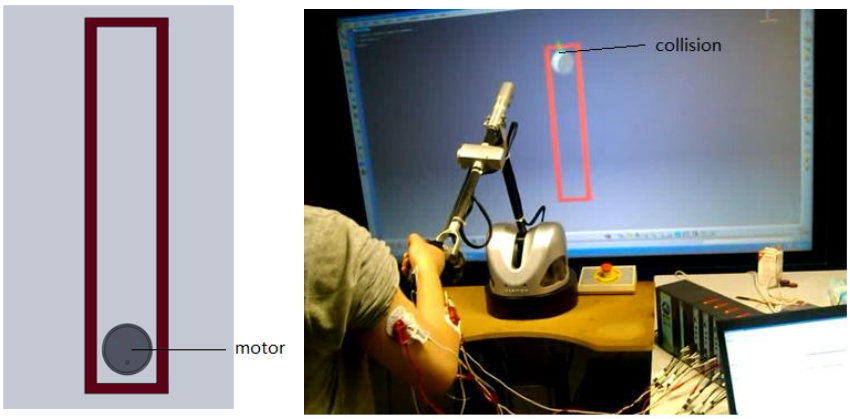

Figure 1.4 Virtual reality experimental environment

The task was divided into two sub tasks in order to discriminate which one induces more muscle fatigue. The first *2.5* minutes period represents the task 1 (*T1*). The total *5* minutes period represents the task 2 (*T2*). The experiment protocol is presented in Appendix 1.

1.5.1.3 EMG processing

During the task (subjects in standing position), the EMG signals on four involved muscles *extensor carpi radialis* (*ECR*), *flexor carpi radialis* (*FCR*), *biceps* and *triceps* were recorded according to SENIAM (surface EMG for non-invasive assessment of muscles) location protocol with four sets of electrodes of EMG *BioPac MP150* system. The signal from the electrode on the *ulnar styloid process* muscle was used as ground signal.

The EMG signals for each subject have been normalized with EMG signals of each muscle detected during the task.

After filtering, Fast Fourier Transfer (FFT) function was used to transfer the raw EMG signal. The power spectrum density of each muscle contraction was estimated by using Hamming window. The median frequency for each muscle contraction was approximated by straight line. Thus, bigger decreasing slope represents faster fatigue process.

1.5.2 Results

Figure 1.5 shows a filtered EMG data which was recorded for a *20* seconds period of *5* minutes task for the four involved muscles.

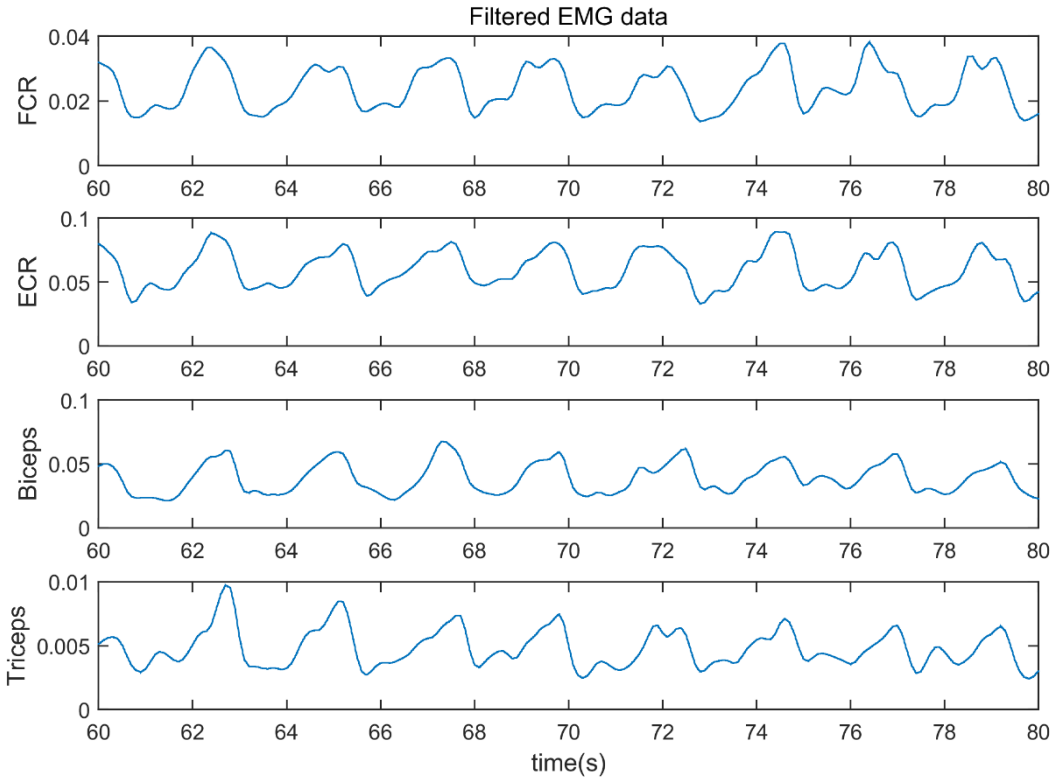

Figure 1.5 Filtered EMG data

The EMG data after *RMS* processing and averaging are presented in Figure 1.6, where:

A – is the Average of the RMS peak values of the first five muscle contractions for the involved muscles in *T2*,

B – is the Average peak value of last five successive muscle contractions of *T1*,

C – the Average peak value of last five successive muscle contractions of *T2*.

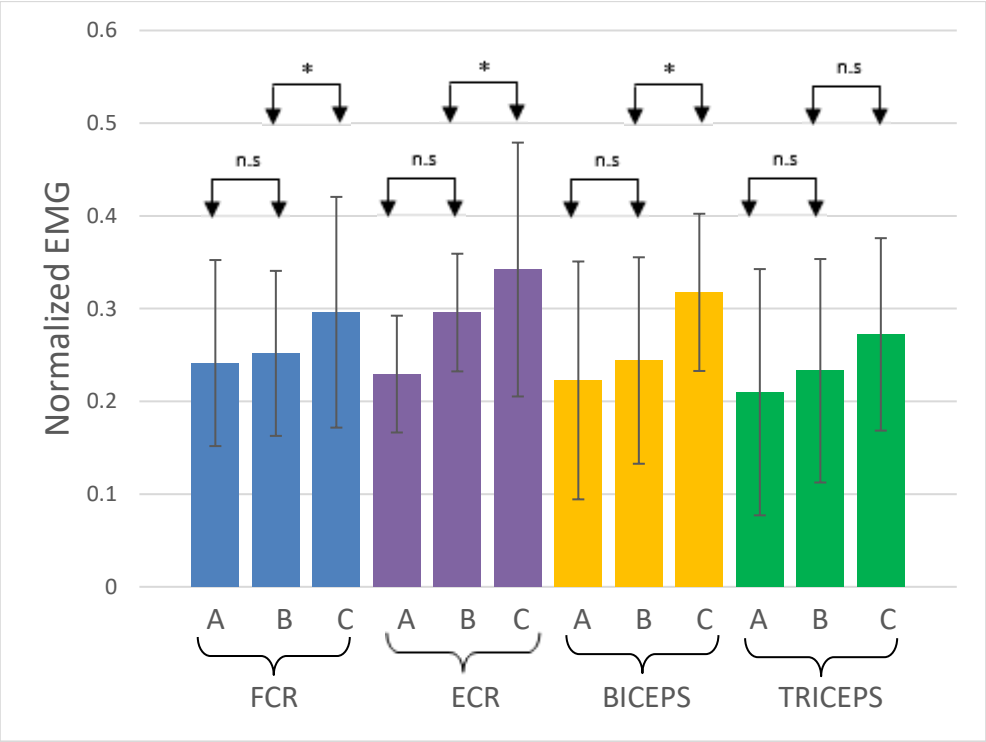

Figure 1.6 Average of peak values of NEMG signal for all subjects at A, B and C for each muscle. (* indicates *significant difference* and *n.s* indicates *no significant difference*)

Student *t* test analysis (unilateral Student *t* test,$\alpha = 0.05$) shown that a significant difference appears between *C* and *B* for *FCR* and *Biceps* muscles only (respectively *t=-1.848, t=-1.775*). No *significant* statistical difference was found between *A* and *B* for all the muscles, neither between *B* and *C* for *ECR* and *Triceps* muscles. The significant difference between *B* and *C* of Biceps and FCR means that EMG signal for performing task 1 (*T1*) is significantly different from task 2 (*T2*). Hence the fatigue induced by *T1* is less than *T2* as the average of *B* is lower than *C* in FCR and Biceps.The results indicated also that *T2* induced more fatigue than *T1*. It means that the task involves greatly flexor muscles (*FCR*, B*iceps*) with greater fatigue in *T2* than *T1* for those two muscles.

Table 1.5 shows the results of median frequency for *FCR* and *Biceps* muscles. It confirms that fatigue appears in both muscles. Moreover, slope values indicate that fatigue increases faster in *T1* than in *T2*.

Table 1.5 Decreasing slope of median frequency of EMG

	T1 (2.5 minutes)	T2 (5 minutes)
FCR	-0,13003878	-0,06598795
BICEPS	-0,03164797	-0,0023069

1.5.3 Discussion

The results of the performed tasks in the VRE show that *Biceps* and *FCR* muscles are the prime movers involved. On the other hand, fatigue develops faster in T1 than in T2. This could be resulted from the fact that the anaerobic exercise of *fast twitch* is the activity mainly involved in the T1 task and the aerobic exercise of *slow twitch* is the principle muscle behavior in *T2* task. The experimental results indicated also greater fatigue in *T2* than in *T1*.

In order to prove the validity of the proposed mechanical model (see Section 1.3.2), it was applied to calculate the mechanical energy expenditure in *T1* and *T2* performed in the VRE. The values of the mechanical energy expenditure are respectively $\Delta E_{T1} = 308\,J$ and $\Delta E_{T2} = 616\,J$. Thus, according to the proposed methodology, the fatigue developed in *T2* is bigger than in *T1*, which is in agreement with the experimental results.

Note that purchasing the fatigue calculation formula and accurate fatigue value associated with specific tasks is not the aim of our research. Instead, the mechanical energy expenditure has been used as an index to compare the induced levels of fatigue while performing different tasks.

In order to compare fatigue for different disassembly tasks, the associated mechanical energy expenditure values are calculated here by the proposed mechanical model (eq. (1-13) and (1-19)).

From the aspect of loading level, since the gravity forces of the components were simulated, it is the same as in the real world. From the aspect of operation method of haptic device, it only allows simulating a single hand operation by holding the handler of the VIRTUOSE haptic device.

The main application field of the results of this chapter is to enable designers to compare the fatigue levels associated with different disassembly tasks simulation performed in VR environment. Note that the difficulties of including physiological parameters and building

complete skeletal-muscle model makes it very difficult to achieve the accurate calculation of fatigue level associated with a specific task. The individual physiological parameters being different may also block the generalization of the model. Instead, the calculation of the mechanical energy expenditure here proposed is relatively simple.

For the calculation of mechanical energy expenditure, the required parameters are:

- *manipulated objects mass*,
- the *starting* and *ending position* of the manipulated objects,
- angle θ_1 between operator upper arm and horizontal frame line for starting and ending position.

For a given task, the first three parameters are easily obtained. If the positions of operator and *manipulated objects* are known, angle θ_1 can be calculated consequently.

As previously said, BMMF models [RoFD04, DNHÅ11] are based on working hours to evaluate both central nervous and peripheral fatigues. They focus more on the relationships among work hours, sleep and performance for a long-time period. Instead, our model focus only on peripheral fatigue for a short time period. Thus, the model proposed here is more suitable to evaluate the relationships among the muscle fatigue levels associated with different disassembly tasks.

There are two reasons for explaining why more real and complex mechanical assembly, which could generate more realistic disassembly sequence, have not been employed here. The first reason is that in order to induce the fatigue in arm muscles, enough exercise should be performed. Pre-tests have shown that if subject is repetitively moving a component between two points with vertical displacement and with a given frequency, he/she will feel fatigue at least after performing the task for a short period time which is equivalent to effectively disassemble lot of components. Instead, a basic task, consisting in manipulating of only one component with sufficiently long trajectory and execution time could be much easier to perform. It also avoids to be effected by the factor of subjects' lacking of experience in haptic device manipulation. Another reason is that this simple task is easy to perform by subjects and allows controlling the velocity of task execution according to Hypothesis 3.

1.6 Conclusion

This chapter introduced a new method for disassembly task evaluation which aims at using the expenditure volume of metabolic energy to quantify fatigue.

The proposed method is more efficient than the method of Bisi et al. [BSHG11] which requires so much data necessary for predicting metabolic energy consumption and consequently fatigue evaluation.

The method is based upon four hypothesizes and proved by experimental tests. Thus, Hypothesis 1 has been proved from the theoretical derivation and experiment results.

The agreement between the theoretical results and experimental ones indicated that the proposed method is pertinent for estimating the level of peripheral fatigue induced while performing a disassembly task in VR environment. The analysis of the median frequency of EMG signals proved the existence of fatigue in the involved muscles. Another interesting result is that subjects fatigue happens faster in *T1* (beginning of the task) than in *T2*.

However, in order to generalize the proposed method, the comparison between the fatigue in real versus virtual environment has to be realized.

Chapter 2
Motor behavior analysis of pseudo-haptic in stiffness discrimination task

Pseudo-haptics is the generation, augmentation or deformation of haptic sensations by information coming from other sensory modalities. This chapter focuses on force applied by subjects when testing pseudo-haptic springs while performing stiffness discriminations. Series of tests for stiffness discrimination between real spring and virtual spring (with pseudo-haptic feedback) were performed. Thus, the materials and the method including measurement items, experiment protocol, participants and data analysis are presented first. Then, the results concerning: the perception under different stiffness, the pressing force, some kinematic parameters, the EMG (Electromyography) signals and the co-activation are presented.

Finally, how subjects applied forces according to the stiffness of pseudo-haptic spring and how does the pseudo-haptics induce different muscle co-activation levels on subjects' forearm are discussed.

2.1 Introduction

Visual feedback plays an important role in different aspect of human behavior and sensation such as: motor control [MoAr13, SMRB09], restoring brain function [RaAl09] and perception of physical properties [SrBB96]. Let us recall that from [LBCC01], "*pseudo-haptics is the generation, augmentation or deformation of haptic sensations by information coming from other sensory modalities* ".

One amongst the first works about pseudo-haptics was reported in [LCKR00] where *Lécuyer et al.* showed that the haptic information can be provided to user by the illusion generated by the pseudo-haptic feedback (here the stiffness). Several physical properties have been simulated by using the pseudo-haptic feedback such as stiffness, friction, shape, weight, force field etc.

As we are aware there is no work focusing on how the pseudo-haptic feedback influences the user's motor behavior in stiffness discrimination task. Thus, this chapter focuses to better understand how the pseudo haptic feedback influences the user's perception and force applied on the spring during stiffness discrimination tasks. Here we proposed to reuse the stiffness discrimination task presented in [LCKR00] consisting in discriminating the stiffness of real springs and virtual (pseudo-haptic) springs[2]. We choose a stiffness discrimination task in order to be able to confirm the existence of the pseudo-haptic effect (by comparing the perception results with the results of previous existing work) before performing our experiments.

In the stiffness discrimination task performed in here, the real springs have different stiffness levels and the stiffness of the virtual spring varies in 11 different percentages from the stiffness of the compared real spring (see details in Section 2.4.1). Subjects had to distinguish the stiffer between a real and a virtual spring. For this purpose, the subjects' discrimination answers, force applied on springs and EMG signals of the involved muscles on subjects' forearms were recorded and analyzed for investigating the trend of change in force following the change of springs' stiffness.

[2] In the remaining of thesis, virtual spring is used to represent the pseudo-haptic spring.

2.2 Previous work

2.2.1 Pseudo-haptics

2.2.1.1 Definition of pseudo-haptics

As previously said, the first work related with pseudo-haptics was presented in [LCKR00] where an isometric device, the Spacetec Spaceball™ 2003C model (Figure 2.1.a), together with visual feedback were used to provide a stiffness information during pressing on a virtual spring (Figure 2.1.b). The Spaceball was used as a force sensor which reacted to user's applied force. The combination of displacement of virtual spring and the internal isometric device resistance is called *pseudo-haptic feedback* since it can provide a stiffness information perceived by user which is similar with haptic sensation. The definition of pseudo-haptics as proposed by *Lécuyer et al*. in [LBCC01] is: *"the generation, augmentation or deformation of haptic sensations by information coming from other sensory modalities"*. Pseudo-haptic feedback uses vision to distort the user's haptic perception and verges on haptic illusions.

(a) (b)

Figure 2.1 Pseudo-haptic device in [LCKR00]: a). Isometric input device called Spaceball; b). virtual display of a 'virtual spring'.

2.2.1.2 Vision dominance

Simulating the spatial properties (distance, position, size, displacement amplitude, etc.) by using pseudo-haptic feedback probably relies on the sensory dominance of vision over touch [Lécu09]. Srinivasan et al. [SrBB96] pointed out the visual dominance over the kinesthetic of hand position in a proposed stiffness discrimination task. In the experiment, subjects were asked to compared the stiffness of two virtual springs. Through pressing the springs, they can feel the

displacement and the pressing force by the hand and see the deformation of spring displayed on computer screen. The results indicated that the subject's perception of stiffness were greatly influenced by the visual information.

Vision dominance is not always existence during perceiving the physical properties. *Ernst* and *Banks* proposed in [ErBa02] an experiment asking subjects to estimate the height of a bar in three situations with:

- visual feedback,
- haptic feedback,
- and both visual and haptic feedback.

Through measuring and analyzing the variance associated with visual and haptic estimation, it is indicated that the vision dominant occurs when the variance of the visual estimation is lower than the variance associated with haptic estimation [ErBa02]..

2.2.1.3 Physical properties simulated by pseudo-haptics

Since Lécuyer brought in the concept of pseudo-haptic feedback in 2000, different types of physical properties have been simulated based on pseudo-haptic feedback.

a.) Friction simulation

The first work contributing to the pseudo-haptics effect was to simulate the friction [LéCC01]. In the performed experiments, subjects had to manipulate a virtual cube, either by a 2D mouse or by Spaceball, to pass through the grey area (see Figure 2.2). The speed of the virtual cube was accelerated or deaccelerated comparing with subjects' actual movement. This acceleration/deceleration is done by controlling the ratio between the subjects' actual movement displacement and the displacement of the virtual cube with using 2D mouse while controlling the ratio between the subjects' finger force and displacement of the virtual cube with using Spaceball. All subjects feel a light friction when the speed of virtual cube was accelerated and a heavy friction when the speed was decelerated. The results also indicated that subjects thought using the Spaceball, which is an isometric device, can conduct to better feel of the friction than the use of the 2D mouse, which is an isotonic device.

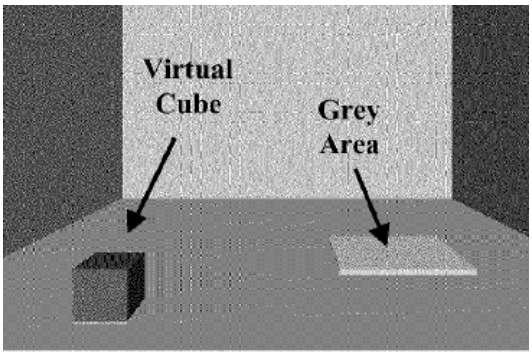

Figure 2.2 Lécuyer's swap experiment display [LéCC01].

Three year later, *Crison et al*. [CLSM04] applied pseudo-haptic feedback to simulate the friction of milling. Through changing the ration between the users' actual motion and the motion of the virtual cutting tools, subjects can feel their resistance according to different simulation parameter.

b.) Stiffness simulation

Before the appearance of the pseudo-haptics concept, *Srinivasan et al.* [SrBB96] has controlled the visual feedback of spring to confuse subjects' haptic sensation in stiffness discrimination task. The haptic stimulus was provided by virtual spring composed by a three degree of freedom haptic interface called *Planer Grasper* (see Figure 2.3.a). Three years later, through using PHANToM haptic interface (see Figure 2.3.b) *Wu et al.* [WuBS99] also changed subject's perception of stiffness by manipulating the visual feedback in different levels.

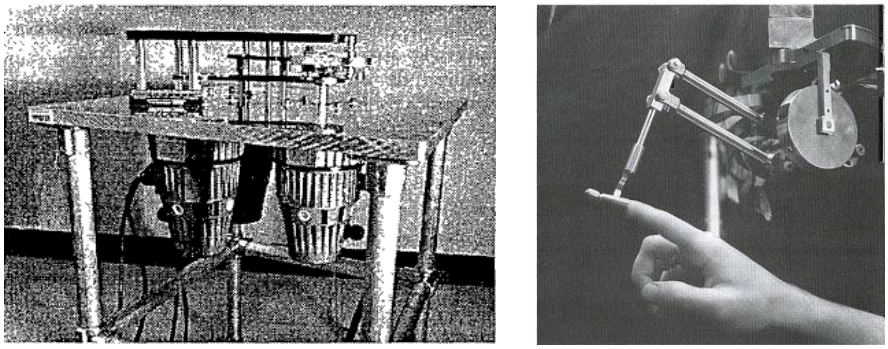

(a) (b)

Figure 2.3 (a). Planar Grasper [SrBB96]; (b). PHANToM haptic interface [MaSa94];

One year after, *Lecuyér et al.* [LCKR00] proposed a stiffness discrimination task which consists in comparing a real spring and a virtual one. They define the real spring as *a*

physically existing spring in reality with a known stiffness value while the virtual spring was graphically displayed on a computer screen and was dynamically animated when pushing the Spaceball^{TM}. Pseudo-haptic was utilized to provide the stiffness information of virtual spring to subject and change the value of simulated stiffness. Virtual spring was simulated from the subject's finger force applied on an isometric device (SpaceBall, which is used as a force sensor). By applying different ratios between the actual finger force and the displacement of the virtual spring

$$K_{Virtual} = \frac{F_{user}}{D_{virtual}} \quad (2\text{-}1)$$

the stiffness of virtual spring varies in different percentages from the stiffness of the compared real spring. The subjects' perception results indicated that changing the virtual feedback in pseudo-haptic changes subjects' perception on stiffness of virtual spring. From the results of this experiment, different PSE (Point of subjective equal) were found when the different real springs were compared with the virtual spring. There are three real springs (249, 363 and 544*N/m*) used in this experiment. The PSE value decrease when the stiffness of the compared real spring increases. That means that softer the compared real spring is, more underestimated the stiffness of the virtual spring is. *Lécuyer et al*. performed another experiment [LBCC01] where subjects were asked to participate in a stiffness task involving two virtual springs simulated by a system based on PHANToM. The displacements of one realistic spring and pseudo-haptic spring being displayed on computer screen subjects had to answer which one was stiffer. One spring has a realistic behavior since it had identical virtual and real displacements. The pseudo-haptic spring is either stiffer or softer than the first one. Different from the [LCKR00], the PSE point in this experiment are negative.

Li et al. [LLLS12] introduced a low-cost haptic simulation systems for tissue stiffness simulation based on pseudo-haptic feedback. They created a softness map which can change the ration between the speed of cursor movement and the speed of finger movement when the subject touches different point in the softness map. The user will then experience a higher resistance when the cursor speed is slower.

c.) Torque simulation

Inspired from using a pseudo-haptic spring in stiffness discrimination, *Paljic et al*. [PaBC04] conducted an experiment which consisted in torsion discrimination between

a real torsion spring (Figure 2.4.a) and a virtual (or pseudo-haptic) one . Two types of virtual torsion springs were used in the experiment: the first one is an isometric torsion spring with infinite physical stiffness (Figure 2.4.b) the other one is an elastic torsion spring with finite physical stiffness (Figure 2.4.c). When subject rotates the plastic cap of the real torsion spring, the pulley rotates synchronously and consequently pulls the torsion spring at two sides to create a torque which is opposite to the rotation direction of user's hand. There are two types of stiffness discrimination:

- real torsion spring vs. isometric virtual torsion spring,
- and real torsion spring vs. elastic virtual torsion spring.

Each type of stiffness discrimination task had one group of subjects participated. Torques applied on the virtual torsion spring, answer time and subjects' answer were recorded and analyzed. The results indicate that the subjects' group who compared elastic virtual torsion spring with real torsion spring had a higher resolution in stiffness perception, but with higher distortion of perception.

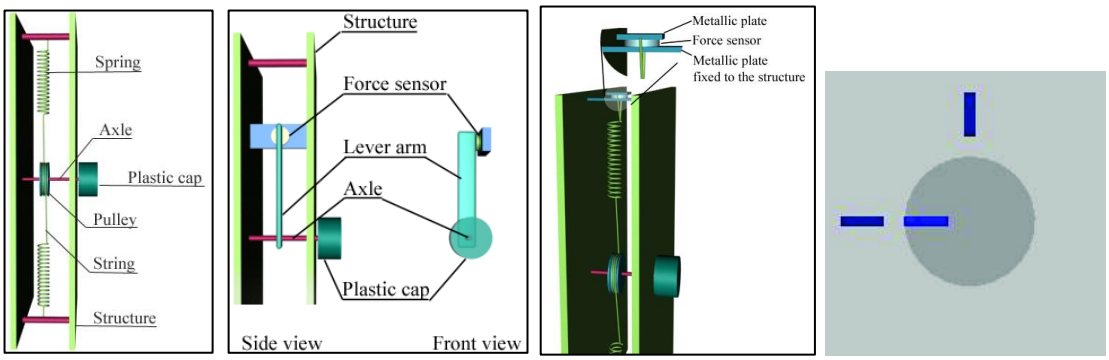

(a) (b) (c) (d)

Figure 2.4 Two compared torsion springs [PaBC04]: a). Real torsion spring; b). Isometric virtual torsion spring; c). Elastic virtual torsion spring; d). Visual feedback of pseudo-haptic torsion spring.

d.) Texture and shape simulations

By changing the cursor speed, texture and shape can also be simulated by pseudo-haptic feedback. *Lécuyer et al.* [LéBE04] introduced a techniques of simulating textures in desktop applications without haptic interface. What the subject sees is the top view of texture, which is the white disk in Figure 2.5. Subject manipulates the Green cursor to pass through the White disk in order to perceive the texture. The ratio between the hand motion and the cursor motion on the computer screen give subject a feeling of passing

different textures by using the green cursor. The acceleration or the deceleration of motion of the cursor indicates a negative or positive slope.

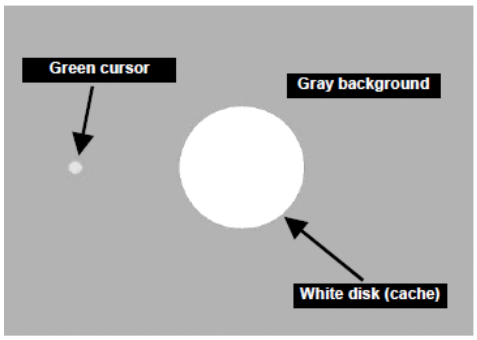

Figure 2.5 The scenario of texture simulation by using pseudo-haptic feedback [LéBE04].

e.) Weight and mass simulation

Dominjon et al. [DLBR05] conducted an experiment discriminating the heavier ball between two. The force feedback was provided by PHANToM device (Figure 2.6.a). In order to feel the force subject had to grasp a foam ball while observing its motion on the computer screen (Figure 2.6.b). Through manipulating the ratio between the amplitudes of movements of the user's real hand and the virtual ball, subjects had different perceptions on ball mass. The discrimination results indicate that decreasing or amplifying the motions of users' hand modified their perception of object's mass.

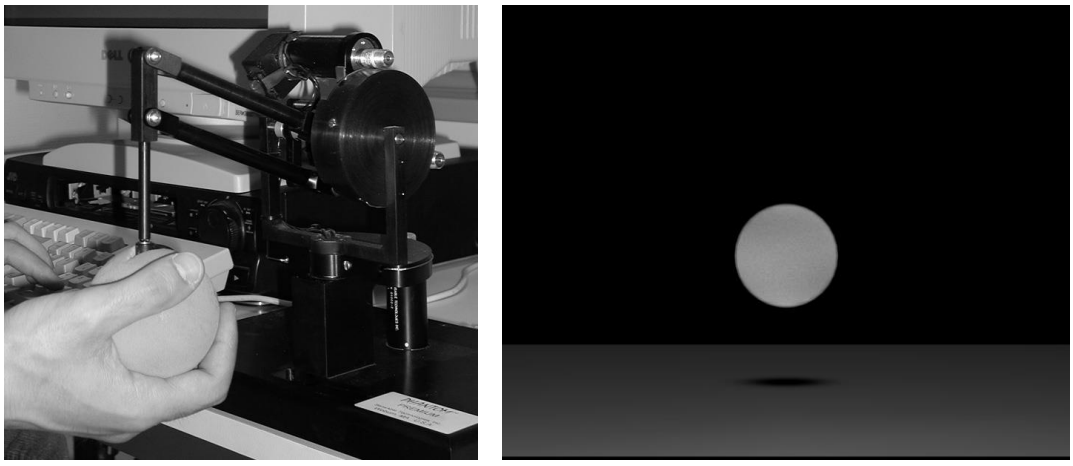

(a) (b)

Figure 2.6 Mass discrimination task in [DLBR05]: a). Experiment setup; b). Virtual ball displayed on computer screen.

Palmerius et al. [PJHS14] investigate pseudo-haptic feedback effect in human weight perception through a series of experiments using Desktop PHANToM as haptic device. The subject wear shutter glasses for stereo vision. The user interface is fully 3D (Figure 2.7.a). The experimental task consisted in selecting the heaviest box among three arranged horizontally (Figure 2.7.b). The results proofed that the pseudo-haptic feedback changed their weight perceptions.

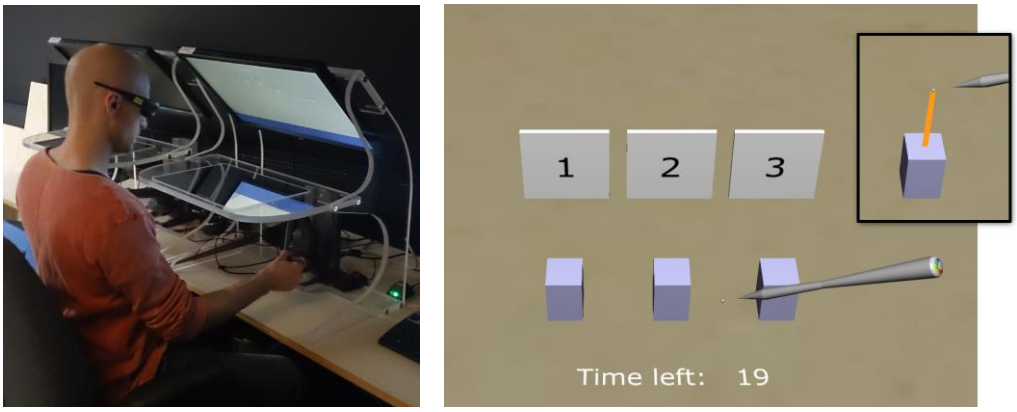

(a) (b)

Figure 2.7 Simulation of weight based on pseudo-haptic feedback [PJHS14]: a). Experiment setup; b). Experiment task scenario.

Recently, *Jauregui et al*. [JAOM14] used the pseudo-haptic feedback to make subjects successfully discriminate the weight of four objects. Subjects had to order the weights of four visual dumbbells according to the perceived virtual weight. During the weight lifting task, motions captured by subjects were reconstructed on a self-animated avatar which can be synchronously observed in computer screen (Figure 2.8)). There are three methods for modifying the visual animation of the self-avatar:

- Control/Display (C/D) ratio,
- Angle of inclination
- and motion profiles (speed and acceleration).

The C/D ration, amplifies /decreases the detected gesture of subject's hand in order to generate of feeling of holding objects with different weights. For the angle of inclination (upper-body inclination), different angles were associated with different weights. The motion profile simulates this angle during the motion of lifting different objects.

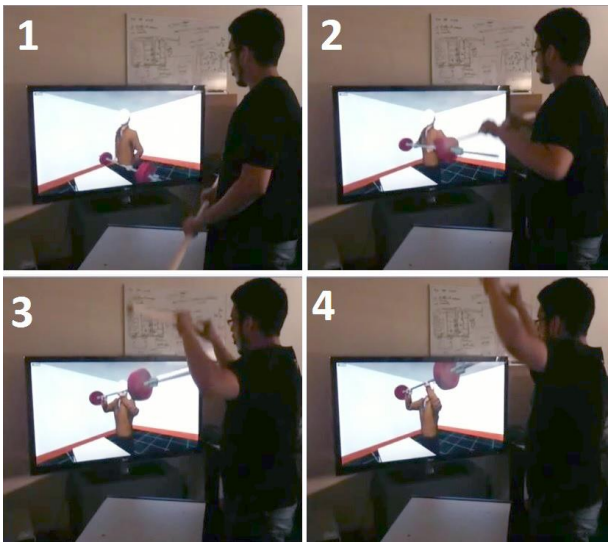

Figure 2.8 Avatar's animation corresponding to different motions during the lifting of the subject [JAOM14].

f.) Force fields simulation

Pusch et al. [PuMC08] proposed an augmented virtual reality system using pseudo-haptic feedback to simulate force fields. The positon of subjects' head and the moving hand are tracking by a position sensory system (see Figure 2.9.a) while subjects are watching avatar hands movement though the head-mounted display (HMD) (Figure 2.9.b). Subjects were asked to move their hands to control the avatar hand and put it in the force field which is limited inside a purple tube. The control of the strength simulated force field was realized by controlling the ration between subjects' actual hand movement displacement and the avatar hand movement displacement. When subjects' hands move against the force field direction, they feel strong force field if the avatar hand movement was slow down comparing with subjects' actual hand movement, and less strong force field if the avatar hand movement was less slow down. In this way, subjects felt the resistance as when they put the hand in a wind stream.

(a) (b)

Figure 2.9 HEMP (Hand-displacEMent-based Pseudo-haptics) systems [PuMC08]: a). Subject wear a head-mounted display while the head and hand positions were tracked; b). The scenario of feeling the force field.

2.2.1.4 Analysis of previous pseudo-haptic works

Previous works, a part of which was presented here above, has shown that pseudo-haptic feedback can influence subject's perception. Such as in [LCKR00], through analyzing the PSE point, Lécuyer et al. concluded that there exists an underestimation of virtual spring stiffness. Just noticeable different and Weber fraction were used to provide the discrimination compliance. Palijic et al. analyzed in [PaBC04] the influence of pseudo-haptic feedback on subjects' answer time in torque discrimination task. A year later, Dominjon et al. analyzed in [DLBR05] how subjects' answer in weigh discrimination changed following the change of pseudo-haptic feedback.

Besides influencing the perception of stiffness and weight, pseudo-haptic feedback can also influence subject's motor behavior, corresponding to the muscle involvement and limb coordination. Recently *Ban et al.* [YTFS13] proved that the brightness of object can change the perception of weight, and in turn of muscle involvement. The more brightness the object is, the more underestimated perception of weight is and less the produced muscle fatigue is. The fatigue generated by holding object for a long time can be also reduced by this illusion. *Tomohiro et al.* [TaHi08] proposed an experiment which asked subject to horizontally move a virtual ball into the target position on the computer screen. Once the virtual ball arrives at the target position, it starts vertically vibrating with a certain level of amplitude which provides a pseudo-vibration sense. It is reported that changing the vibration amplitude of the ball, changes

also the muscle involvement. But how the pseudo-haptic influences the subject's motor behavior in stiffness discrimination has not been investigated.

Although Lécuyer et al. [LCKR00] and Paljic et al. [PaBC04] have analyzed the subject answer in stiffness discrimination task, how does pseudo haptic feedback influence pressing force and involved muscle activity is not known. In their experiments, although the pseudo-haptic feedback has been utilized to simulate the stiffness of torque, the visual feedback of the real spring and virtual spring were not uniformed. In [LBCC01], this drawback has been overcome by using PHANToM force feedback device to simulate virtual springs compared in stiffness discrimination task. The PSE value found in [LBCC01] (*-24%*) is different from the *+9%* found in [LCKR00]. Although Paljic et al. recorded the torque applied on the virtual spring, the force on real spring had not been recorded, so the comparison between the forces applied on both real and virtual springs cannot be achieved. In this context, we propose to put force sensors on both real and virtual springs, so the force applied on the springs can be recorded, analyzed and compared. Secondly, in order to reduce the difference between the visual feedback of real and virtual springs, their displacements are displayed on the computer screen. Consequently, the forms of the visual stimulus for both real and virtual springs can be uniformed.

2.2.2 Motor behavior during stiffness discrimination

2.2.2.1 Force behavior in real stiffness discrimination

Karadogon et al. [KWHC10] analyzed the force in the stiffness discrimination task where the spring is simulated by PHANToM haptic device. It is proved that the force and pressing speed are increasing following the increase of the stiffness of the simulated spring. However, this experiment does not involve pseudo-haptic feedback, because subjects' actual hand motions were the same as the motion they saw in the computer screen.

There are also many works investigating finger forces applied during stiffness discrimination with real springs. *Fujita et al.* [Fuji04], investigated pinch movements. In their experiment two elastic objects have nonlinear stiffness while the other three have a linear stiffness. The objective was to study the applied pinch forces during stiffness discrimination task. The results shown that no matter the stiffness of object, the pinch force increases with the increase of object stiffness. In this optic, *Endo* [Endo16] investigated a stiffness discrimination task and the applied forces for springs within the stiffness range between *59 N/m* and *2360 N/m*. During the discrimination task, two specimens that differed by one or two levels of stiffness

were paired. In total nineteen pairs were used in the experiment (pair IDs: P1–P19). The results showed that the force applied on the springs increased with the stiffness of specimens until to reach a stabilization for the higher stiffness values (Figure 2.10).

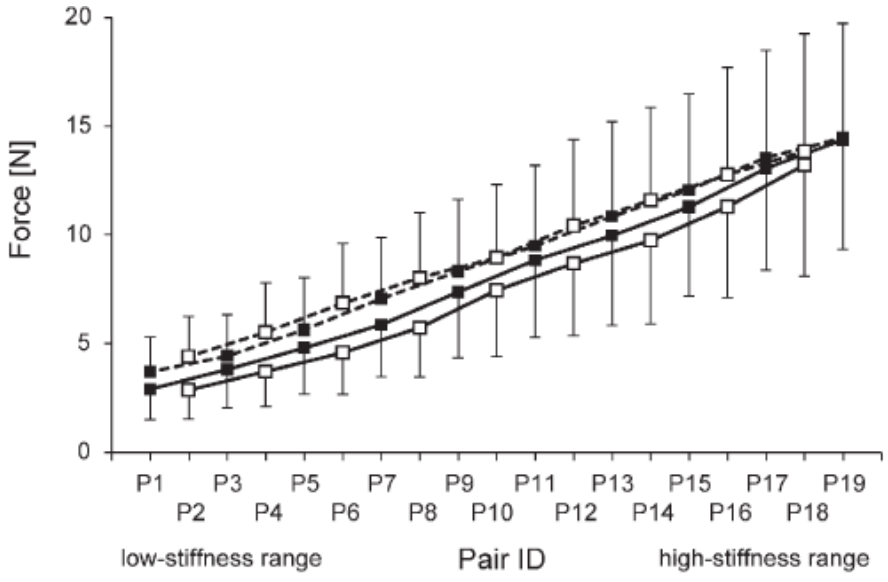

Figure 2.10 Force applied on different compared specimens [Endo16].

2.2.2.2 Muscle co-activation

For stabilizing the joint movement and improving the control of the limb movement, the muscle has a coordinate mechanism for co-activation which means that both agonist and antagonist muscles will be activated. The muscle co-activation which is normal during performing fine task has been widely studies [FrAv13].

In biomechanics, different results about co-activation were reported in static versus dynamic tasks. According to [GrOs98, SSGO01], muscle co-activation increases following the increase of maximal joint velocity in dynamic task. Conversely, in static conditions, antagonistic co-activation appears to increase with agonist activation which is proportionally greater during maximal voluntary contraction (MVC) [HéDA91, YaWi83]. With the increasing of MVC level, the net force exerting by the muscles, crossing the joint, increases also. This means that during performing the static task, the co-activation increases following the increase of the net force exerting by the muscles crossing the joint.

For dynamic task (pressing the real spring for instance) the muscle co-activation should increase following the different maximal pressing velocity on real spring.

For static task when pressing the virtual spring (a pseudo-haptic spring), it is not clear what would be the co-activation pattern. In fact, the subject applies a static force on the spring but receives dynamic visual feedback as the spring length changes. Thus, the question whether the muscle co-activation will change following the change of visual feedback in pseudo-haptics as user press on a static real spring is open.

2.3 Materials and Method

2.3.1 Real Springs and Virtual Springs

The purpose of the performed experiments is to discriminate the stiffness of two compared springs: one real and one virtual. The experimental protocol in [LCKR00] was replicated. However, in order to uniform the stiffness stimuli of two compared springs (real spring and virtual ones) their displacements were displayed on the computer screen. Note that this method is different from the method of Lecuyér et al. [LCKR00] which only displayed the displacement of virtual spring.

Figure 2.11 shows the realized test bench for the experiment. Inside a box (Figure 2.11.a), there are four springs, labeled as 1, 2, 3 and 4 with stiffness of *202N/m*, 304 *N/m*, *608 N/m* and *2500 N/m* respectively. Each spring, situated in metallic tube, is loaded by the force via a bottom. Under each spring, a force sensor (KISTLER 9017B) allows to record the vertical force applied on the spring with *2000 Hz* sampling frequency during each trial.

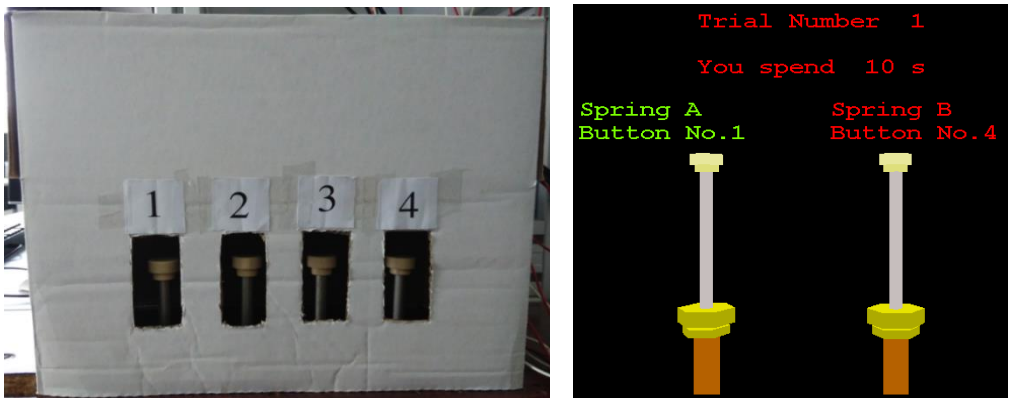

(a) (b)

Figure 2.11 Experimental setup: a). four springs inside the box; b). two simulated springs presented on computer screen for each trial.

The real spring is one amongst springs 1, 2 and 3. The stiffness of a spring is defined by the ratio between the applied force and its visual displacement. For the real spring, no mismatch

existed between the visual feedback and the real spring displacement. The force applied in spring 4 coupled with change in visual feedback displayed on computer screen generates different stiffness of virtual spring. For the virtual spring a difference existed according to compared real spring. Previous tests in [LCKR00] shown that below -40% and above *+60*% of real spring stiffness the subjects' perception results were not influenced by the visual feedback anymore. Therefore, as proposed in [LCKR00] the stiffness of virtual springs vary *-40%, -30%, -20%, -10%, 0%, +10%, +20%, +30%, +40%, +50*% and *+60*% from the stiffness of compared real spring. The displacement *D* of each spring, visualized on the computer screen, is calculated based on the applied force and its stiffness, as:

$$D=F/k \qquad (2\text{-}2)$$

where: *F* is the detected force that subject apply on spring

k is the stiffness.

In order to prevent the contact between the button and the top of the tube, the message "*Stop pressing*" is displayed on the screen when the distance between the button and the top of tube is smaller than *1 mm*.

2.3.2 Measurement items

Four force sensors (KISTLER 9017B) were installed in the bottom of each tube of the springs. While pressing the springs, the forces were recorded with 2000 Hz sampling frequency during each trial. The visual displacement of each spring, movement of the button, on the computer screen is calculated based on the applied force and the simulated stiffness.

According to SENIAM (Surface ElectroMyoGraphy for the Non-Invasive Assessment of Muscles) [HFMS99] and Leouffre thesis [Leou14] recommendations, a total of six sets of electrodes respectively located in two flexors and two extensors on the forearm of subject were used to record the EMG[3] (electromyography) signal. Both flexor digitorum superficials and flexor carpi radialis muscles, have two set of electrodes located on. Two set of electrodes were separately located in extensor digitroum muscle and extensor carpi radialis longus muscle. The EMG signals were recorded with *2000 Hz* sampling frequency during the experiment. Figure 2.12 shows the electrodes' placement on the forearm.

[3] All the EMG mentioned in this chapter means surface electromyography

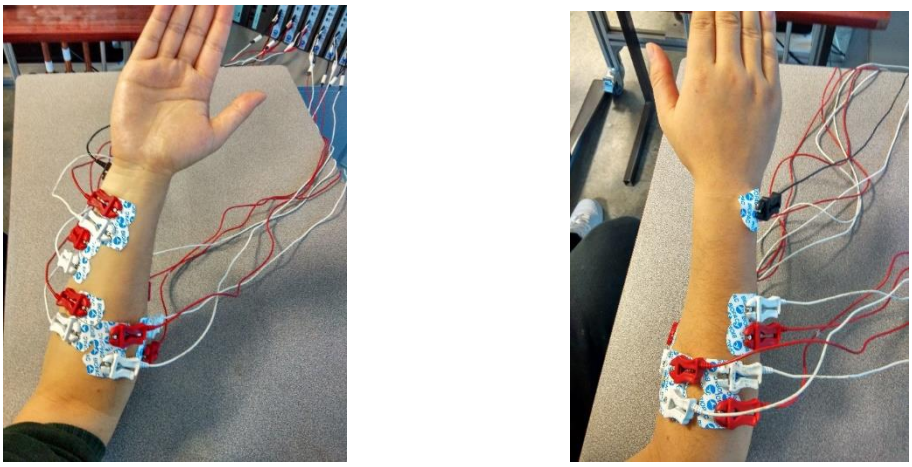

a) b)

Figure 2.12 The placement of electrodes on forearm: a). Four sets of electrodes for flexors; b). Two sets of electrodes on extensors (the black electrode is for the ground).

2.3.3 Experimental test

The experiment includes two parts:

- maximal voluntary contraction (MVC) measurement in order to calibrate force and EMG data, at the beginning of each test,
- stiffness discrimination task.

During the tests, subjects have to use their predominant index finger while applying the forces. The forearm is in horizontal position and rests on two identical mats situated under the subject's wrist and elbow. During the experiment, the subject is in sitting position (Figure 2.13).

Figure 2.13 Subject performing the task in sitting position with using dominant hand to test the spring and non-dominant hand to manipulate the keyboard.

2.3.3.1 MVC Measurement

As previously said measurement of MVC take place before stiffness discrimination task. For this purpose, subjects are asked to perform three items:

- maximal flexion force,
- maximal extension force,
- maximal co-contraction (without contact with the button).

Each item is performed consecutively three times and consists in: performing the action (force/co-contraction) during *3* seconds followed by *5* seconds break. After performing each item, subject had *5* minutes to rest before starting the stiffness discrimination task. For the maximal flexion and extension forces, subject had to continuously apply the maximum force (as Figure 2.14.a) by vertically pulling and pushing a ring attached with the force sensor towards down and towards up (as Figure 2.14.b). The maximal co-contraction consists in keeping the palm and forearm horizontally and co-contracting all the forearm muscles (as Figure 2.14.c). During performing each item, the force and EMG signal were recorded.

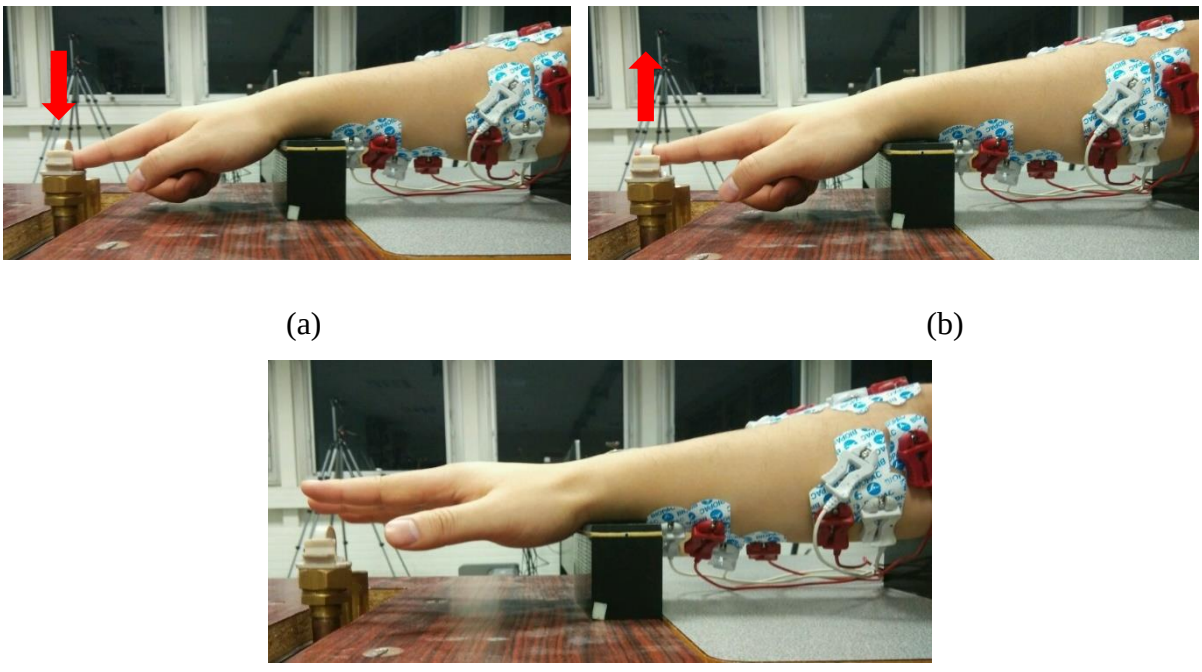

(a) (b)

(c)

Figure 2.14 Three MVC items: a). MVC flexion; b). MVC extension; c). MVC co-contraction.

2.3.3.2 Stiffness discrimination task

There are three stiffness comparing pairs: real spring 1-%virtual spring1, real spring 2-%virtual spring 2 and real spring 3-%virtual spring 3 which gives *33* (=*3x11*) compared pairs in the

experiment. For each pair, as previously said, 11 virtual springs were compared to one real spring, and there are 6 trails for virtual spring of each pairs. Thus, each subject has to perform *6x33=198* trails which takes about 45 minutes.

As previously said, for each trial, subjects were asked to perform a stiffness discrimination task between a real spring and a virtual one. The button's displacements of two compared springs were displayed on the screen libeled "*Spring A*" and "*Spring B*". For each piston, the ID of the corresponding button was indicated just below "*Spring A/B*" (Figure 2.11 b.).

Each trial starts by pressing spring B (i.e. virtual spring) first. After, the subject can switch back and forth between the two springs as he/she wishes. For subject information, on the top of the screen were indicated the trails' number and the time spent for this trail. During the pressing, subjects had to focus on the computer screens and were not allowed to observer the movements of their finger on the spring. For each trail, after testing the springs, the subjects had to push *S* button on the keyboard, with the non-dominant hand, in order to *Stop* the trail. Then the question: *Which spring is stiffer* was displayed on the computer screen. The subjects had to push key *A* or *B* in order to respond the question. The answer was automatically recorded. As previously said, in order to avoid the contact between the bottom and the tube, the message "*Stop pressing"* was displayed on the screen *1 mm* before the contact.

2.3.4 Participants

Fifteen subjects (12 males and 3 females), aged from 20 to 33 participated in the experiments. All subjects have declared not having:

- corrected visual impairments,
- impairments of haptic sensitivity (sensitivity of touch, numbness of the fingers and loss of finger location perception),
- diseases or symptoms which induce hand movement disorders.

All subjects declared also being naive to the purpose of the experiment (Appendix 2).

2.3.5 Experimental data analysis

2.3.5.1 Perception results

As there are 6 trails for each stiffness change percentage of each pairs the mean value of number of response "*Spring B is stiffer*" is calculated. The function, which express the

relationship between the proportion of "*Spring B is stiffer*" response and the stiffness change percentage, is called *psychometric function* [Gesc97]. In order to fit a mathematical function to the psychometric function, *z* score was used to convert the proportion values into *z* score based on the normal distribution table in [Gesc97].

In order to compare the discrimination performance of our experiment with other works, especially [LCKR00], the Just Noticeable Difference (JND) has been calculated.

$$JND=DLu-PSE \qquad (2\text{-}3)$$

where: - *PSE* is the Point of Subjective Equal,

-*DLu* the Differentiation Line upper).

Both of them are corresponding to the simulated stiffness which subject have a z score of 0 (probability of *50*%) and *0.67* (probability of *75*%). The Weber fraction *W*:

$$W=(DLu-PSE)/PSE \qquad (2\text{-}4)$$

provides the size of the observer's difference threshold during the discrimination task [TDBS95].

2.3.5.2 Pressing force

Figure 2.15 shows the raw data of force and EMG signal on each muscle during a trail of stiffness discrimination. The forces raw signals are filtered with using *2-nd* order *12.5 Hz* Butterworth low pass filter [SMRB09]. For each test, the maximal peak of each pressing force is automatically detected (Figure. 2.16). The average value of force peak on both real and virtual springs are then calculated.

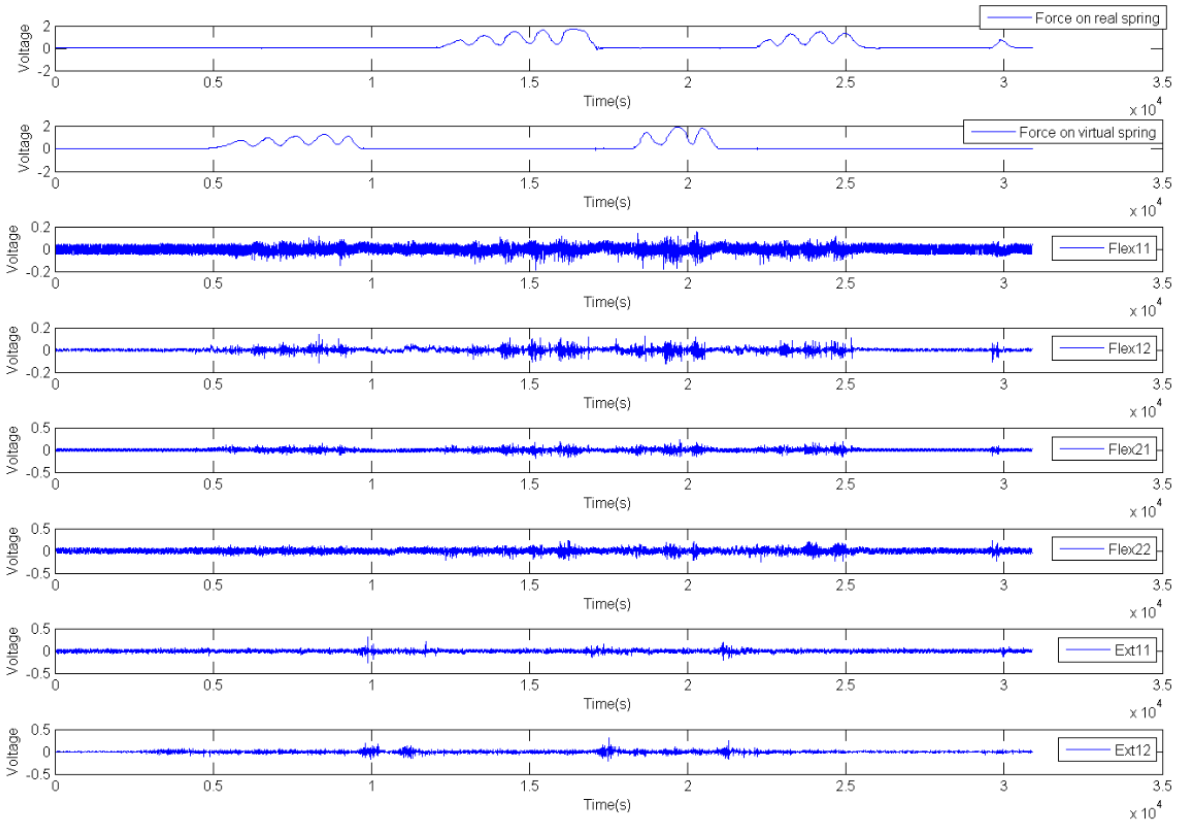

Figure 2.15 Raw data of force and EMG on flexors and extensors during a trial of stiffness discrimination task.

The force data recorded during the stiffness discrimination task is firstly filtered with the same filter in the process of maximal flexion force data. Then the realized MATLAB program finds the start and end point of each press, and also the peak of force of each press on both real spring (RS) and virtual spring (VS) as shown in Figure. 2.16. The average value of force peak on real spring and virtual spring in each trial are then calculated. The normalized force peak is also calculated by dividing the maximal flexion force of each subject per force peak detected.

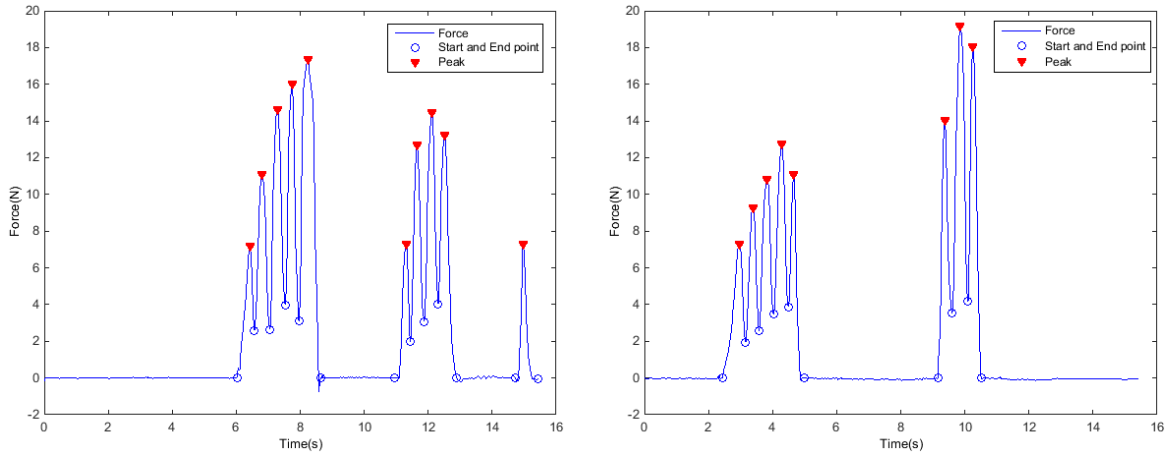

(a) (b)

Figure. 2.16 Start and end point of force on each press and the peak of the force of each press. (a) Force on real spring; (b) Force on virtual spring.

2.3.5.3 Kinematic parameters

In order to investigate the kinematic performance of index finger when the subject is pushing on real and virtual springs three kinematic parameters are proposed and consequently calculated:

- the *number of pressing*, defined by the number of detected peak on the force,
- the *pressing duration* on real and virtual spring, defined by the time difference between the start and end point of each press,
- and *pressing frequency* defined by the ratio between the number of pressing and pressing duration.

Concerning the number of pressing, it is supposed that the pressing frequency of the finger is lower than *4Hz*, then *500* data point (sampling frequency is *2000Hz*) will be the minimal data length between two peak of force. *Findpeaks* function of MATLAB was used to detect the peak. This function can find the local maxima based on a customer defined requirement. A local peak is a data sample that is either larger than its two neighboring samples or is equal to infinitive number. If a peak is flat, the function returns only the first point. The press duration is calculated by recording the time at start and end point of each press. The start and end points for pressing phase were automatically detected. A threshold was given to horizontally cross the force signal and guarantee that the cross point between the threshold line and the curve of force signal was even number which promises that each peak has a start and end point. The start and end point are respectively the first point of a peak in force beyond the threshold and the first point lower than the threshold.

According to [SSGO01], both agonist and antagonist muscles are involved during the task. This sharing pattern, labelled *muscle co-activation*, is described to vary with the joint velocity. One explanation for the variation of muscle co-activation is that it enables the subject to better control the joint stability and the movement accuracy. Then it is meaningful to analyze the maximal pressing velocity depending of the joint angle velocity. The pressing velocity is:

$$v = \frac{dx}{dt} = \frac{d(\frac{F}{k})}{dt} \tag{2-5}$$

where: F is the detected force signal and k is the stiffness of the spring.

Figure 2.17 shows the force value and the calculated velocity based on eq. (2-5). Note, that for the real spring, v is the velocity of the fingertip in vertical direction which is proportional to the angle velocity of the wrist joint. The physical stiffness of virtual springs being too high (*2500 N/m*), the angle velocity of the wrist joint is almost zero. Thus, v is the velocity of the virtual spring button without movement of the finger joint.

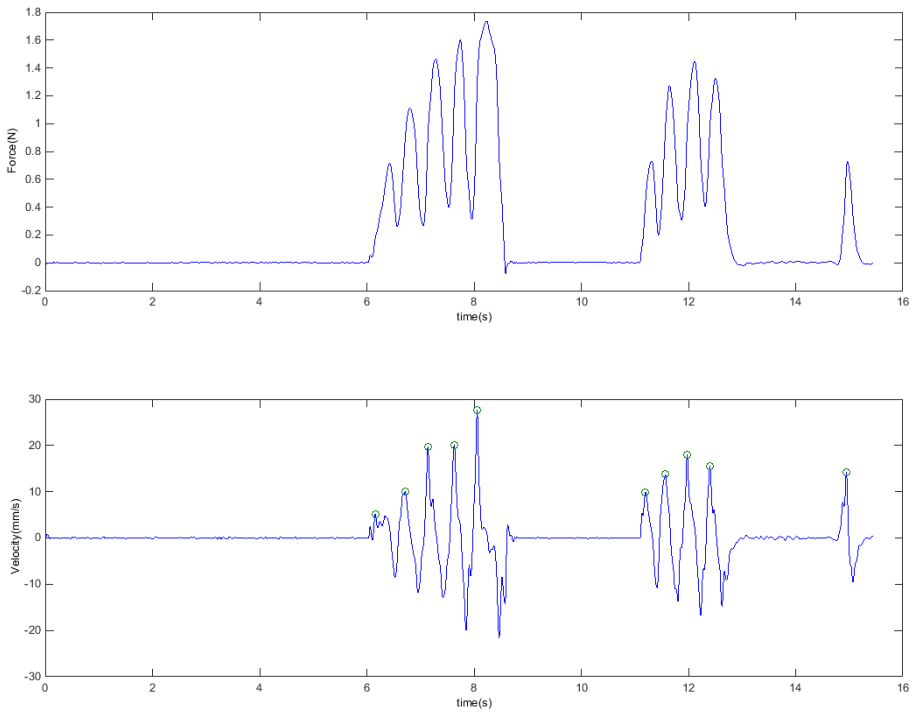

Figure 2.17 Subject force applied on real spring (figure up), and velocity and the detected positive peak value on pressing velocity (figure down).

2.3.5.4 EMG signal and co-activation

The raw EMG were filtered with a *200* order of bandpass FIR filter between *20Hz* and *500Hz* which is the main frequency domain of EMG signal [DGKR10]. All EMG signals have been

processed by using RMS (root mean square). The epoch for the RMS processing is *500*. Figure 2.18 shows the raw data of EMG and the RMS EMG signals after filtering on two extensors during performing the MVC.

For the EMG signals of six involved muscles during the MVC, two parameters were calculated.

The first one is the average of the integrated EMG (*IEMG*) calculated as:

$$IEMG = \frac{1}{\Delta t}\int_{t_1}^{t_2} EMG dt \tag{2-6}$$

where: - *EMG* are the signals after RMS processing,

- t_1 and t_2 are respectively the start moment and the end moment of performing MVC,
- and $\Delta t = t_2 - t_1$.

For the flexors, t_1 and t2 correspond the start and end points detected on EMG signals during performing the maximal flexion force. For the extensors, t1 and t2 correspond to the start and end point detected on EMG signals during performing the maximal extension force. The flexor which has the biggest IEMG value during performing the maximal flexion force is the most involved flexor. The most involved extensor is the extensor which has the biggest IEMG signal during performing the maximal extension force. For both flexors and extensors muscles, the averages of the integrated EMG were calculated during performing the MVC flexion and MVC extension.

The second parameter is the average peak value calculated as:

$$\overline{P_{EMG}} = \frac{1}{3}\sum_{i=1}^{3} p_i \tag{2-7}$$

where: p_i is the detected peak value during each muscle contraction.

For flexors and extensors $\overline{P_{EMG}}$ were calculated respectively based on their EMG signal recorded during performing the MVC flexion and MVC extension. The calculated $\overline{P_{EMG}}$ value for each muscle were used in the EMG normalization process.

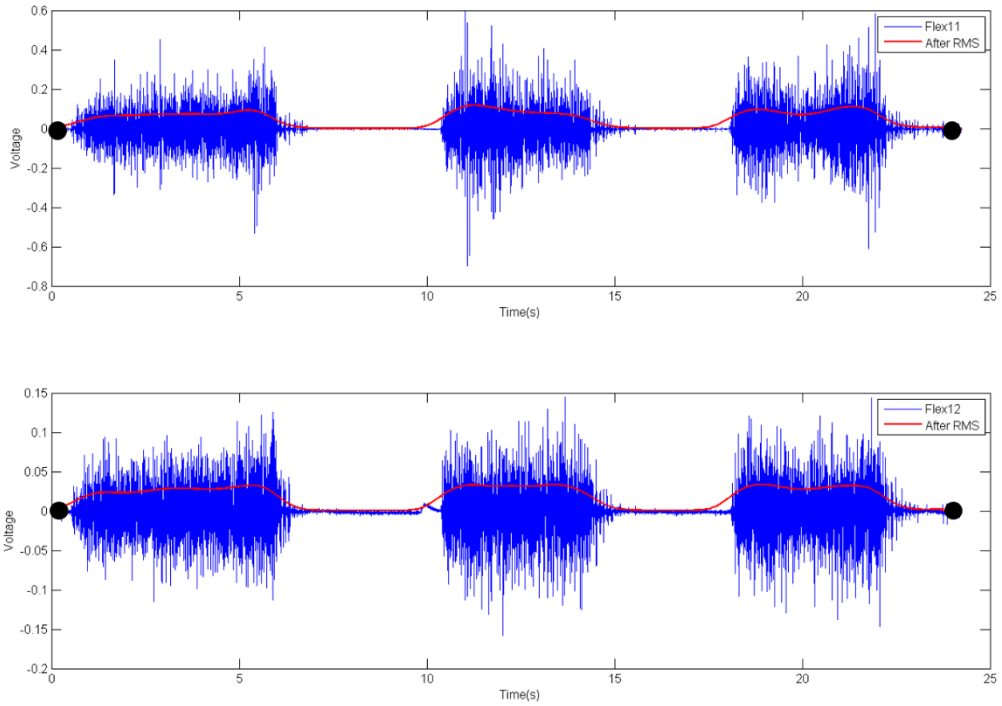

Figure 2.18 Raw EMG and RMS EMG on two flexors during MVC flexion. The black dots represent the start and end point of the performing MVC.

Then, all the EMG signals have been normalized by $\overline{P_{EMG}}$. The peaks of EMG on most power flexor were detected and the average of all detected peaks were calculated for each trial during the stiffness discrimination task. All the EMG values after RMS processing on most involved extensor at the moment of peaks in EMG on most involved flexor were taken and their average values were calculated for each trial as well. Figure 2.19 presents the peaks detected in the EMG RMS values in one trial during the stiffness discrimination task. The circles represent the detected start and end point of each peak of flexor EMG signals. The triangles represent the detected peaks.

According to [FaWi85, OHLR86, UDFV96, KeAP03], there are two different types of methods for calculating the co-activation index (*CI*). Those two method are shown respectively as (2-8) and (2-9).

$$CI = \frac{2 \times EMG_{Ant}}{EMG_{Ago} + EMG_{Ant}} \times 100\% \tag{2-8}$$

$$CI = \frac{EMG_{Ant}}{EMG_{Ago}} \times 100\% \tag{2-9}$$

where: EMG_{Ant} and EMG_{Ago} represent respectively the peak values of the most involved antagonist muscle (extensors) and agonist muscle (flexors). Ervilha et al. [ErGD12] point out that the muscle co-activation is more reliably estimated with using (2-8).

The most involved antagonist muscle is defined as the extensor who has the highest *IEMG* value while performing the maximal extension force. The most involved agonist muscle is defined as the flexor who has the highest *IEMG* value while performing the maximal flexion force. The $\overline{CI}$ while pressing real spring and virtual spring for each trial is the average of *CI*s at detected peaks in the EMG signal on most involved flexor.

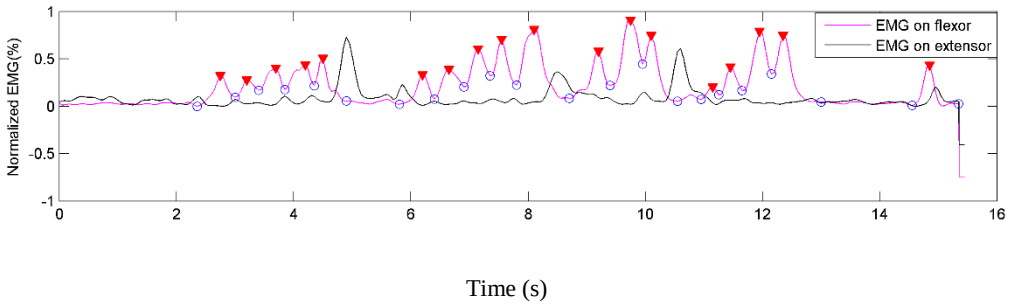

Figure 2.19 EMG signal on the most involved flexor and extensor with the peak detected.

2.3.5.5 Statistical analysis

Analysis of variance (ANOVA) was performed to test the force changes (i.e. dependent variable) applied either on the real or the virtual springs. The Shapiro-Wilk method [ShWi65] has been previously applied to verify the normality of the force data. Two-way ANOVA tests with repeated measures were used to ascertain the significance of the results. The task consisted to discriminate the stiffness of a simulated spring versus the stiffness of its corresponding real spring. The independent variables were:

- the changes in virtual stiffness labeled *'virtual stiffness'* (11 levels: from *-40*%, to *+60*% with a step of *10*%),
- the real stiffness values labeled *'stiffness scale'* (3 levels: *202 N/m*, *304 N/m* and *608 N/m*),
- and the type of spring labeled '*spring'* : 2 levels: real and virtual (simulated).

The first test consisted in characterizing the effect of change in 'virtual stiffness' versus the 'stiffness scale' for the following nine dependent variables separately on virtual and real springs:

- pressing force,
- normalized pressing force,
- pressing duration,
- number of pressing,
- pressing frequency,
- maximal pressing velocity,
- peak of EMG signal on flexor,
- peak of EMG signal on extensor,
- co-activation at the peak of EMG on flexor.

A second test was performed to compare the effect of change in 'stiffness scale' versus 'spring' on force at *0*% stiffness percentage (i.e. exactly for the same real and simulated stiffness).

A third test was performed to compare the effect of change in 'stiffness scale' versus 'spring' on variables:

- pressing duration,
- number of pressing,
- and pressing frequency.

The chosen level of significance was $p<0.01$. All the statistical analyses above were performed under MATLAB Software (MATLAB 2014a, MathWorks).

In order to test whether the slopes in the linear model are significantly different, a test of nested model has been performed in *R* software (version 3.2.5). Recall that the slopes express the relationship between the force and logarithm of stiffness for real and virtual springs.

2.4 Results

2.4.1 Perception under different stiffness

Figure 2.20.a shows the Subjects' perception of the stiffer spring for three different pairs (real spring 1-virtual spring, real spring 2-virtual spring and real spring 3-virtual spring) with element different stiffness change percentages of virtual spring. The RS and VS respectively represent the real and virtual spring.

Figure 2.20.b presents the results of transferring the subjects' answer into *z* score. With the *z* score, subjects' answers are presented in a linear model. The equation of linear regression for each comparison pair are also presented in Figure 2.20.b.

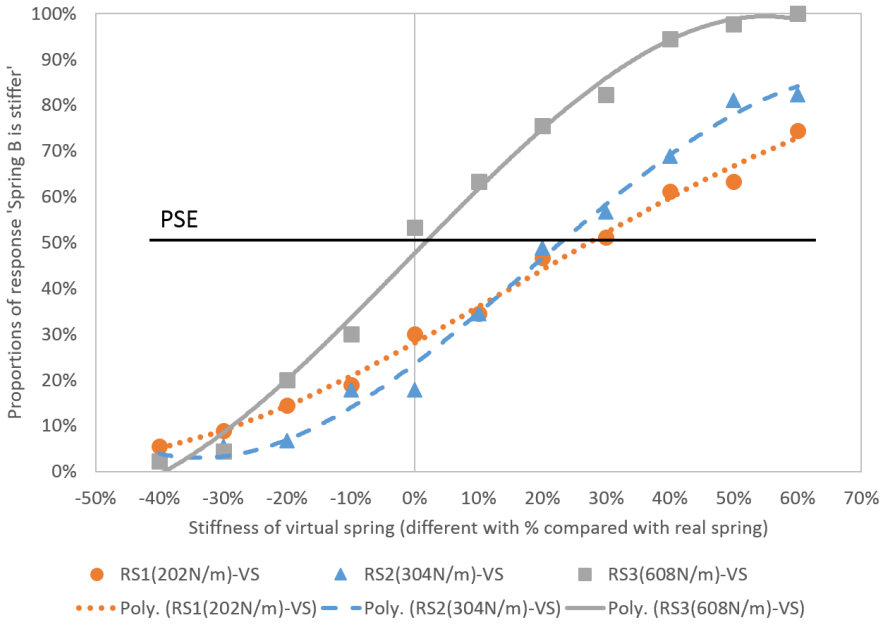

(a)

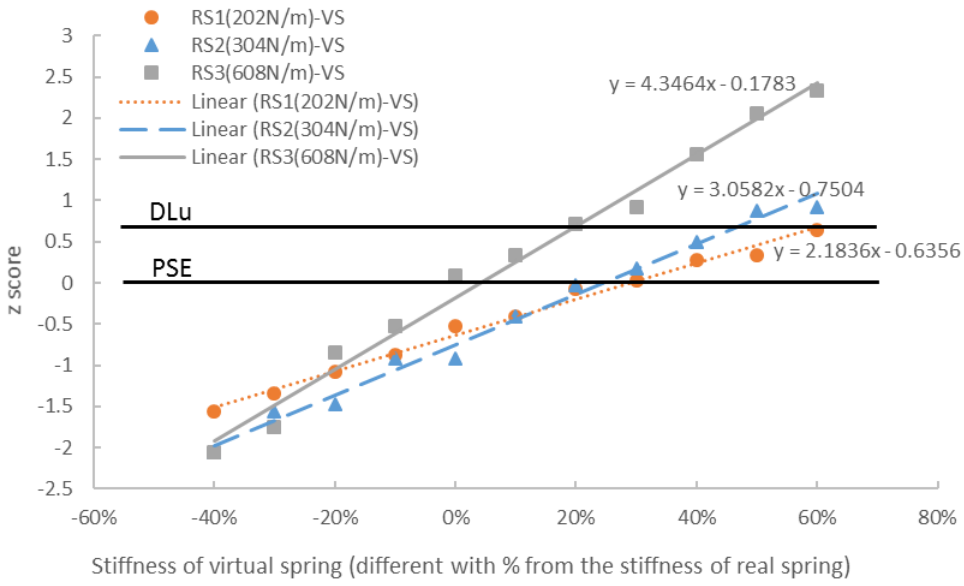

(b)

Figure 2.20 Subjects' stiffness discrimination results: a). Proportion of response "Spring B is stiffer"; b). *z* score of subjects' perception.

The PSE point in Figure 2.21.a, confirms the conclusion of Lécuyer et al. in [LCKR00] that less stiffer the compared real spring is, more underestimated the stiffness of the virtual spring is. The JND for three curves had been calculated. The average JND is *19.3*% (see Figure

2.21.b) which is bigger than the *13.4%* reported in [LCKR00]. Based on the *z* score of subjects' answers, the *PSE*, *DLu* and Weber fractions are calculated. The results are presented in Figure 2.21.c. The Weber fractions obtained in here are above *1*. Their average value for the three compared pairs is 1.24.

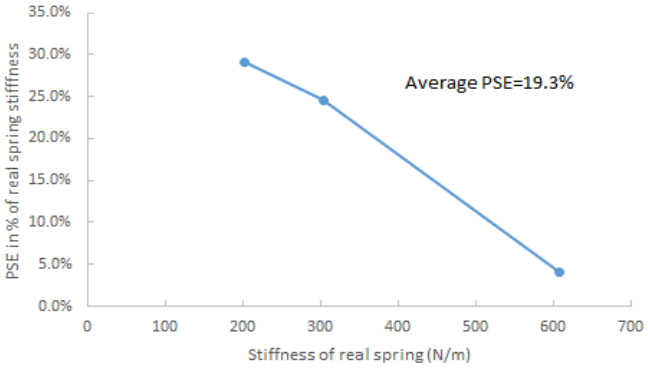

(a)

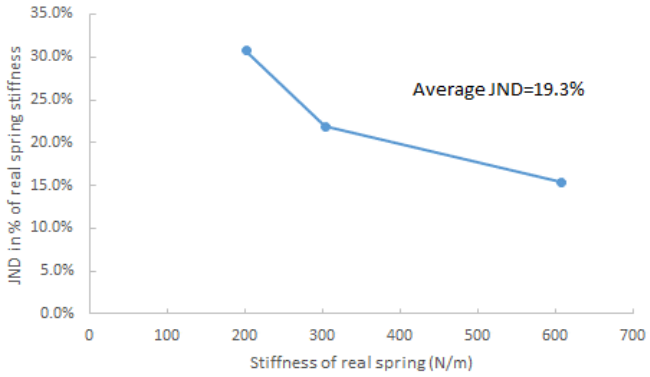

(b)

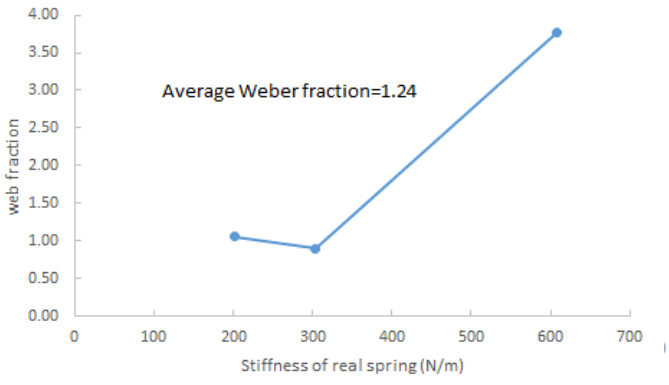

(c)

Figure 2.21 Subjects' answers *t*-score results (a). PSE; (b). JND (c). Weber fractions.

2.4.2 Force

2.4.2.1 Force applied on real springs

The results presented in Figure 2.22.a. show a main effect for 'stiffness scale' (*F=9.9012*, *p*-value<*0.001*). The force increases significantly from *5.88N* to *11.31N* for the stiffer spring. No significant effect was noted for the 'virtual stiffness' as indicated in Figure 2.22.b (*F=0.84234*, *p*-value=*0.58762*), meaning that the forces applied on the real spring were not changed according to the stiffness of virtual spring. No significant interaction between 'stiffness scale' of real spring and 'virtual stiffness' was observed either (*F=0.96235*, *p*-value=*0.47438*).

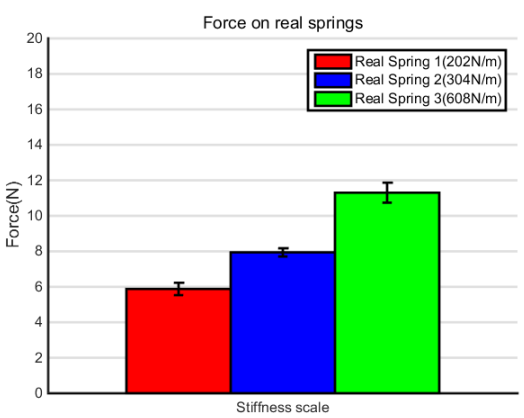

(a)

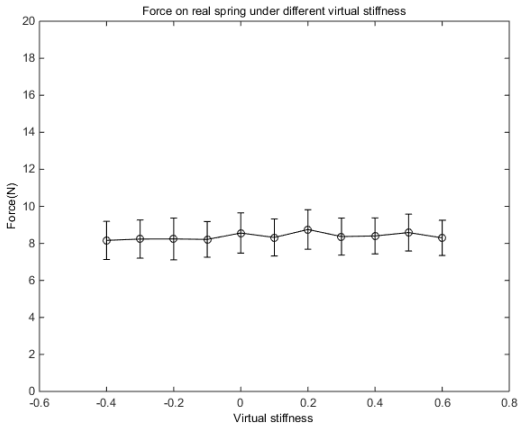

(b)

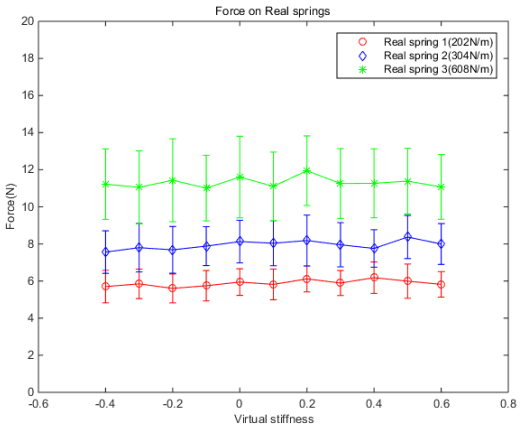

(c)

Figure 2.22 Average of force with standard error of mean (SEM[4]) applied on real spring without normalization: a). no matter what is the 'virtual stiffness' of compared virtual spring; b). under different 'virtual stiffness' of compared virtual spring, no matter which stiffness scale is; c). under different 'virtual stiffness'.

[4] All the average values presented in this chapter are with SEM

The statistical analysis of normalized force on real spring reveals the same information as found in force without normalization applied on real spring (Figure 2.23). The results indicate that:

- The 'stiffness scale' of real spring has a significant effect on force applied on virtual spring ($F=33.181$, p-value<0.001);

- The 'virtual stiffness' has no significant effect on force applied on different real spring ($F=0.51883$, p-value$=0.87806$);

- There is no significant interaction between the 'stiffness scale' of real spring and 'virtual stiffness' for all the force applied on real spring ($F=0.62614$, p-value$=0.79267$).

This means that the task requirement is quite low since it requires force intensity between *20*% and *40*% of maximal capacity. One interesting conclusion is that the different force capacities of the subject does not influence the way he/she tests the springs. In other words, the force applied on a real spring depends solely on its stiffness and not on the force capabilities of the subject.

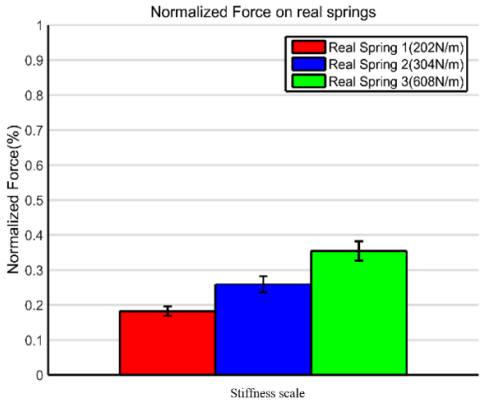

(a)

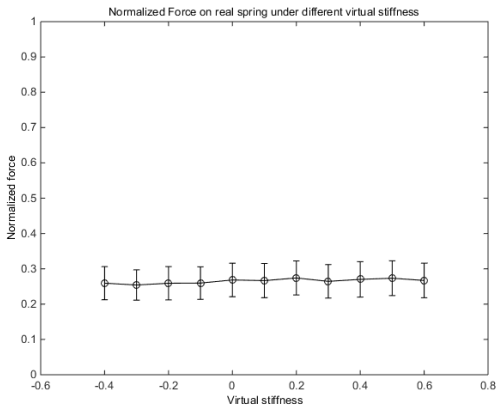

(b)

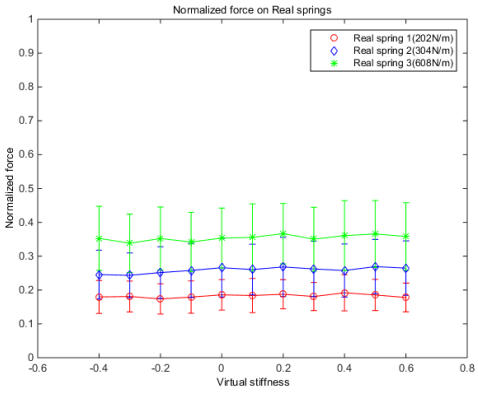

(c)

Figure 2.23 Average of normalized force applied on real spring without normalization: a). no matter what is the 'virtual stiffness' of compared virtual spring; b). under different 'virtual stiffness' of compared virtual spring, no matter which 'stiffness scale'; c). under different 'virtual stiffness'.

2.4.2.2 Force applied on virtual spring

The results presented in Figure 2.24 show that:

- 'Stiffness scale' has a significant effect on force applied on virtual spring (*F=31.495*, *p*-value<*0.001*. This means that the force applied on virtual spring increases with the real stiffness used for comparison, from *9.59N* to *12.45N* (Figure 2.24.a).
- A significant effect was observed for the 'virtual stiffness' (*F=8.6101*, *p*-value<*0.001*). It means that the applied force significantly increases, whatever the stiffness of real spring is (Figure 2.24.b).
- A significant interaction between 'stiffness scale' and 'virtual stiffness' was noted (*F=3.3764*, *p*-value<*0.001*). This indicates that different changes were noted between the change percentage and the real stiffness of real spring (Figure 2.24.c).

Post-hoc analysis performed with the slopes of each curves (Figure 2.24.d) showed that the slopes were significantly different. They significantly decreased when the real stiffness increased.

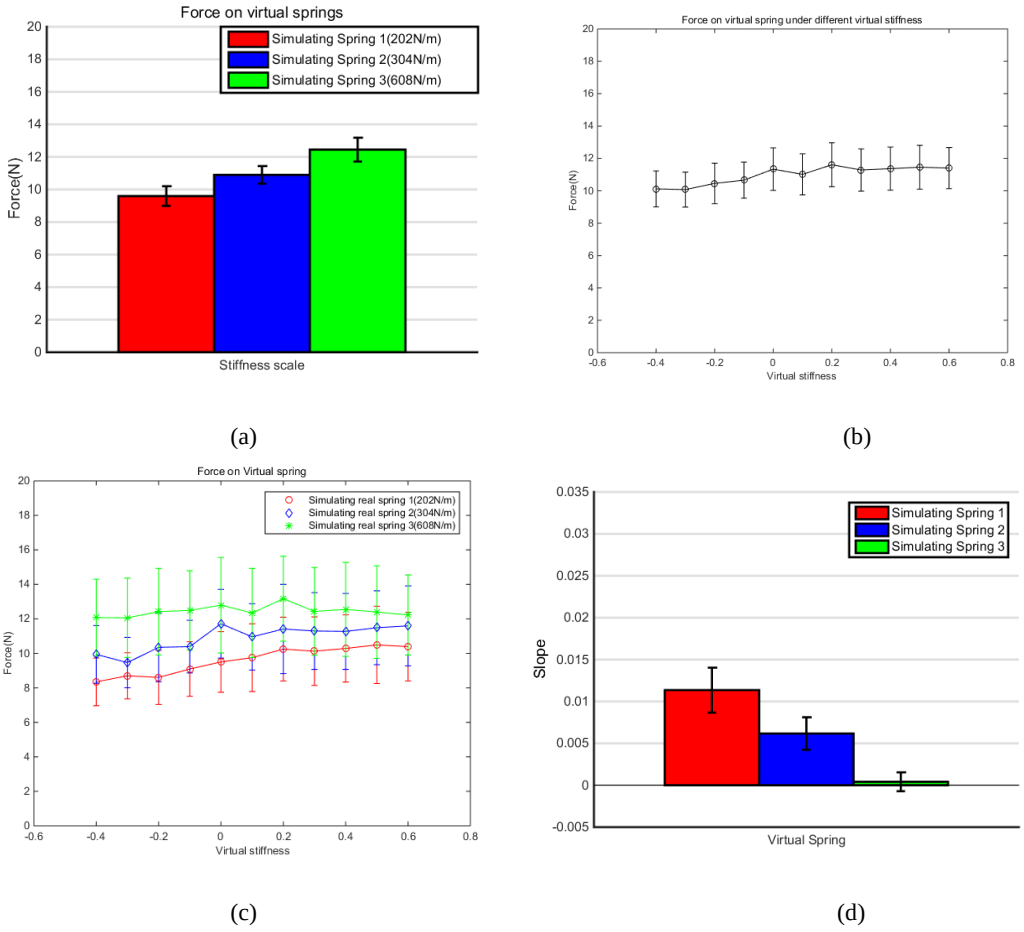

Figure 2.24 Average of force without normalization applied on virtual spring: a). compared with different real springs, no matter what is the 'virtual stiffness'; b). under different 'virtual stiffness', no matter which the compared real spring was; c). under different 'virtual stiffness' for simulating different real springs; d). The average of slope for force without normalization under different 'virtual stiffness' on virtual spring (*p*-value<*0.001*).

The normalized force applied on virtual spring has the same tendency as in force without normalization (Figure 2.25). The results indicate also that 'stiffness scale' has a significant effect on force applied on virtual spring (*F= 9.9012*, *p*-value<*0.001*). The value increases from *32.27%* to *40.27%* when the 'stiffness scale' change from *202 N/m* to *608 N/m*. The 'virtual stiffness' has a significant effect on force applied on virtual spring (*F=7.6978*, *p*-value<*0.001*). The normalized force increases from *33.63%* to *37.52%* under minimal and maximal 'virtual stiffness'. There is a significant interaction between 'stiffness scale' and 'virtual stiffness' for all the normalized forces applied on virtual spring (*F=2.8725*, *p*-value<*0.005*). Figure 2.25.d indicates the result of post-hoc analysis. The slope of force for each simulated real spring in Figure 2.25.c are different. Following the increase of stiffness of simulated real spring, the slope decreases from *0.01135* to *0.000412*.

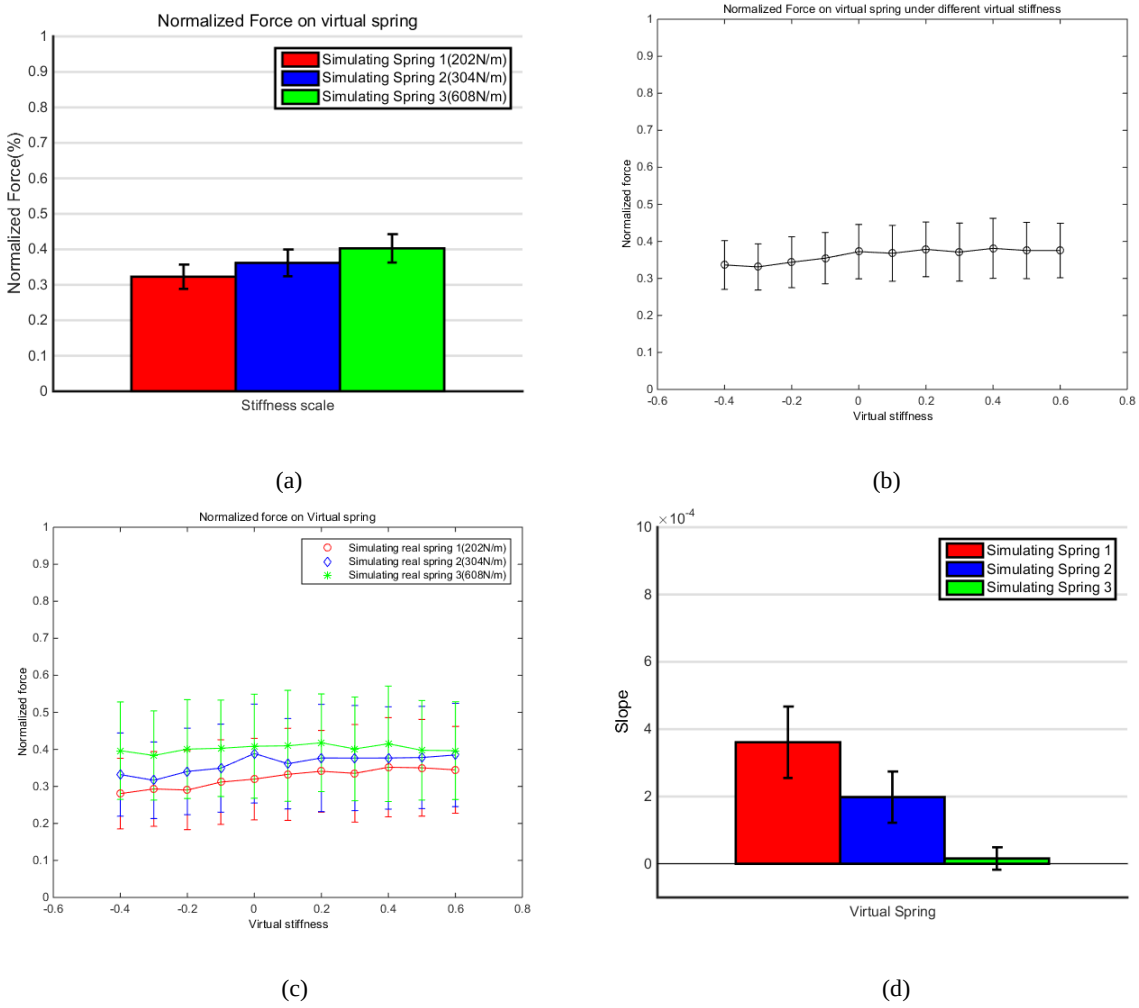

Figure 2.25 Average of normalized force applied on virtual spring: a). compared with different real springs, no matter what is the 'virtual stiffness' of virtual spring; b). different 'virtual stiffness' of virtual spring, no matter which the compared real spring was; c). under different 'virtual stiffness' for simulating different real springs. d). Average of slope for force with normalization under different 'virtual stiffness' on virtual spring (*p*-value<*0.001*).

2.4.2.3 Comparison between the force on real spring and virtual spring under identical stiffness

Figure 2.26 shows the comparison between the forces applied on real and virtual spring under identical stiffness (0% of change). A significant effect was noted for the spring type (*F=118.32*, *p*-value<*0.0001*) and for the stiffness (*F=94.034*, *p*-value<*0.0001*) meaning that the force applied on the real spring is lower than this applied on the virtual one, while the force increases from low to higher stiffness values. A significant interaction between the spring type and 'stiffness scale' (*F=8.907*, *p*-value<*0.001*) was also observed. The force applied on real spring increases from *5.946N* to *11.6N* and from *9.5N* to *12.79N* on virtual spring. This means that the forces applied on the real spring were statistically lower than those applied on the virtual spring when the stiffness of real and virtual springs are the same. But the difference in the forces decreases for the stiffer spring.

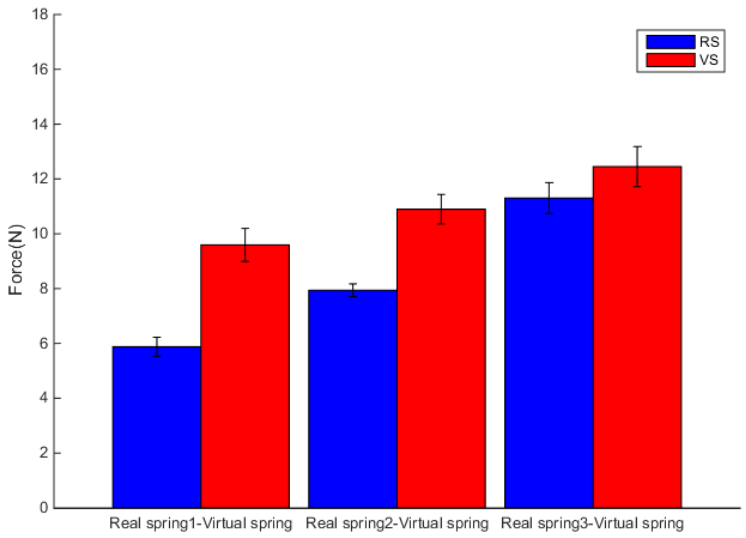

Figure 2.26 Comparison between the force on virtual spring and corresponding real spring during identical simulation. All the compared pairs have significant differences between force on virtual spring and real spring (*p*-value<*0.0001*).

2.4.3 Kinematic parameters

2.4.3.1 Pressing duration

The pressing durations for different real springs were recorded and are presented in Figure 2.27. The results indicate that:

- The stiffness of real spring has no significant effect on pressing duration (*F=2.703*, *p*-value=*0.067251*). That means the pressing duration on each real spring are not significantly different.
- The 'virtual stiffness' has a significant effect on pressing duration (*F=3.2489*, *p*-value<*0.001*). From Figure 2.27.b, it seems that when the 'virtual stiffness' of virtual spring is+*10*% higher than the stiffness of virtual spring, the pressing duration on real spring are higher than the other conditions.
- There is no significant interaction between the stiffness of real spring and 'virtual stiffness' (*F=0.84841*, *p*-value=*0.58173*). This means that comparing the stiffness for close values is more difficult for the subjects and requires more time to test the springs.

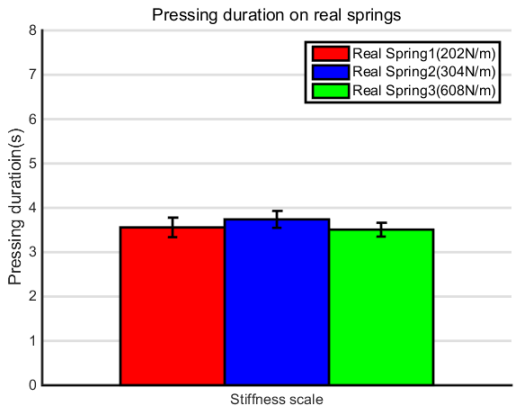

(a)

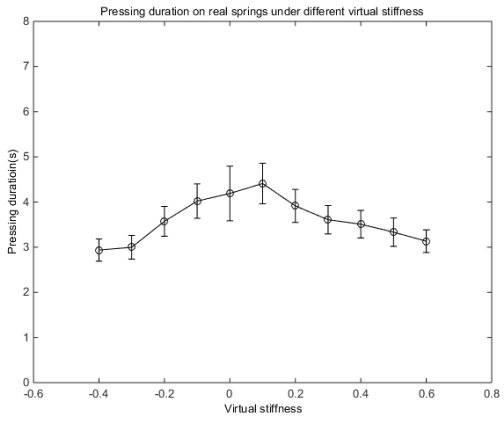

(b)

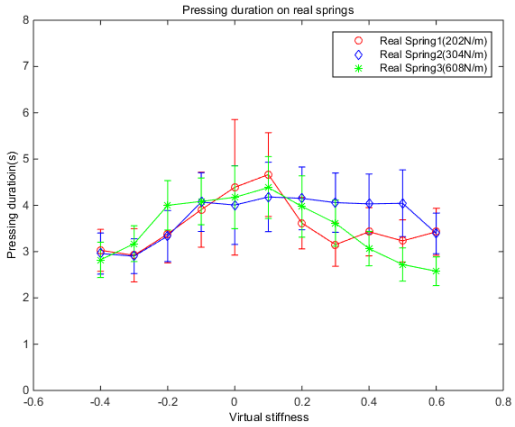

(c)

Figure 2.27 Average of pressing duration on different real springs: a). no matter what is the 'virtual stiffness' of the compared virtual spring; b). under different 'virtual stiffness' of virtual spring; c). pressing duration under different 'virtual stiffness'.

The relationship among pressing duration on virtual spring, ‘stiffness scale’ and ‘virtual stiffness’ are presented in the Figure 2.28. The statistical results indicate that:

- The ‘stiffness scale’ has no significant effect on pressing duration (*F=1.8122*, *p*-value=*0.16357*). That means the pressing duration on virtual spring when simulates different real springs are not significantly different.
- The ‘virtual stiffness’ has a significant effect on pressing duration (*F=2.3786*, *p*-value<*0.01*). Figure 2.28.b shows that there is a peak when the stiffness of virtual spring is 10% higher than the stiffness of compared real spring.
- There is no significant interaction between the ‘stiffness scale’ and ‘virtual stiffness’ (*F=0.88655*, *p*-value= *0.54505*). These results corroborate previous ones, thus confirming that discriminating close stiffness values requires more time because the subjects are more confused.

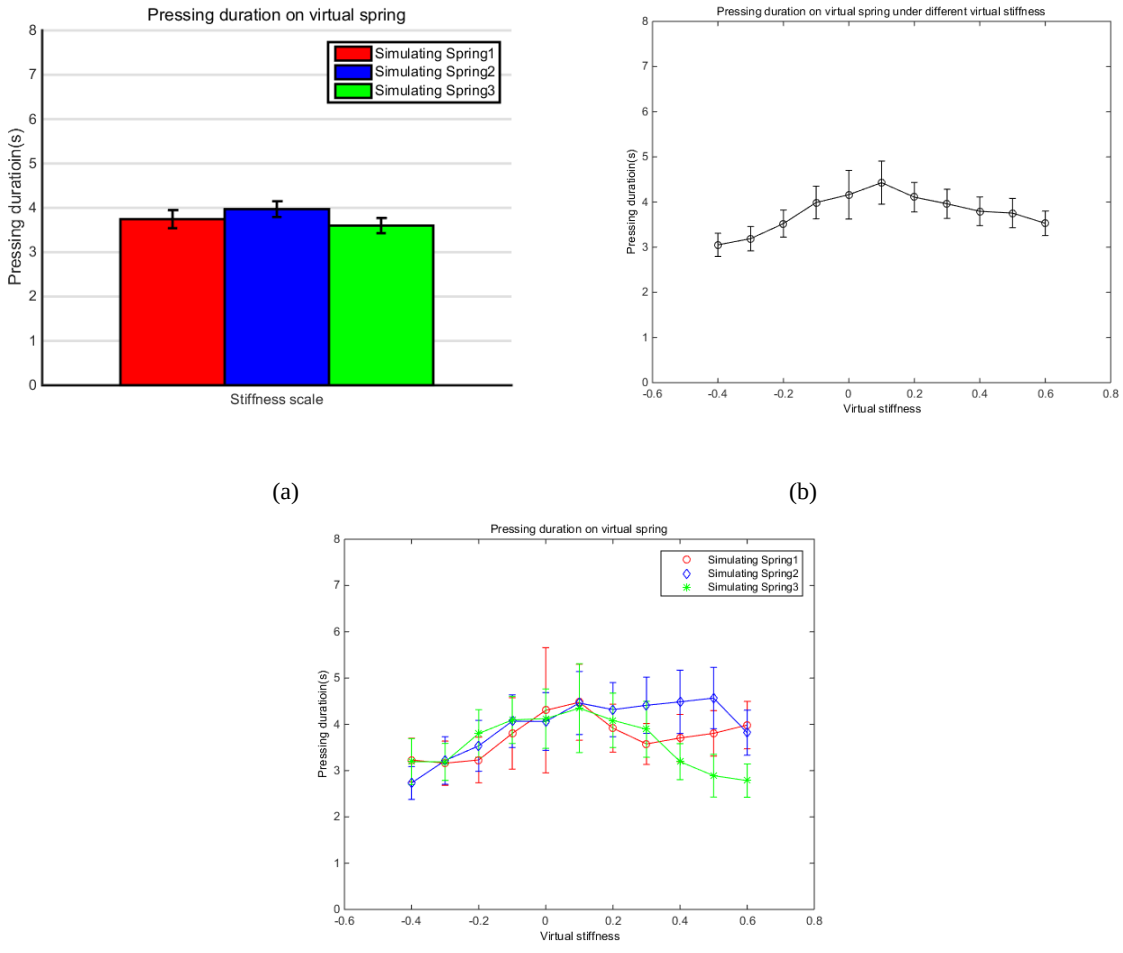

Figure 2.28 Average of pressing duration on virtual spring: a). compared with different real springs, no matter what is the ‘virtual stiffness’ of virtual spring; b). under different ‘virtual stiffness’ of virtual spring, no matter which the compared real spring was; c). under different ‘virtual stiffness’ for different simulated real springs.

In order to compare the pressing duration on virtual spring and corresponding real spring, the two-way repeated measures ANOVA comparing spring type (real spring or virtual spring) vs. stiffness scale (*202 N/m*, *304 N*/m and *608 N/m*) have been performed and gave the following results:

- The spring type has a significant effect on pressing duration ($F= 9.516$, p-value<0.01),
- The stiffness scale has a significant effect on pressing duration ($F= 8.6786$, p-value<0.001),
- There is no significant interaction between the spring type and stiffness scale ($F= 0.46635$, p-value$= 0.62732$).

The *t*-test analysis indicates that the pressing duration on virtual spring of compared pair real spring 1-virtual spring and real spring 2-virtual spring are significantly different from corresponding real spring (shown in Figure 2.29). This means that the test durations for virtual spring are higher than for the real spring. However, for higher stiffness values, the testing time is not differing between real and simulated springs. One probable explanation may be that for stiffer virtual and real springs, the discrimination depends more on the visual feedback which is more accurate than the proprioceptive feedback.

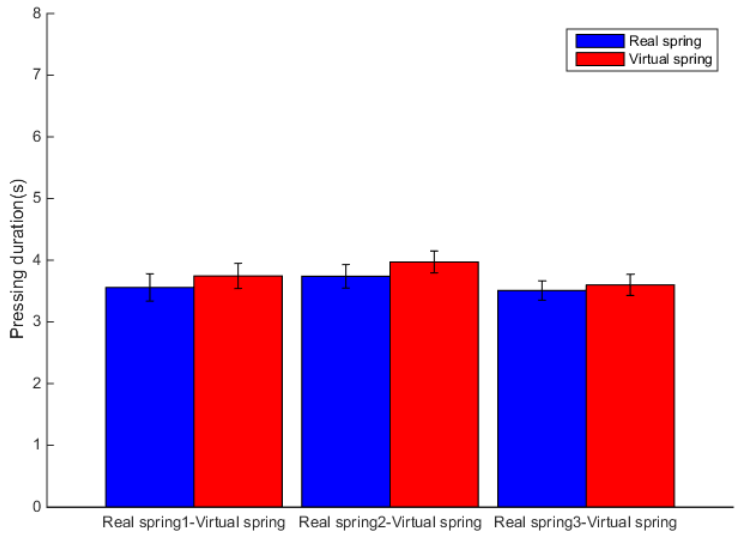

Figure 2.29 Comparison between the pressing duration on virtual spring and the corresponding real spring. The compared pairs: Real spring1-Virtual spring and Real spring2-Virtual spring have significant differences inside the pressing duration on virtual spring and real spring (p-value<0.01).

2.4.3.2 Number of pressing

Figure 2.30 presents the number of pressing applied by the subjects on different real springs. The statistical results show that:

- The stiffness of real spring has no significant effect on number of pressing (*F=2.703*, *p*-value= *0.067251*) which reveals that subjects almost press the same times on each real spring,
- The 'virtual stiffness' has a significant effect on number of pressing (*F=3.2489*, *p*-value<*0.001*). Figure 2.30.b shows that there is a peak when the stiffness of virtual spring is *10*% higher than the stiffness of the real one. That means subjects need to press more time at condition of *+10*%.
- There is no significant interaction between the stiffness of real spring and 'virtual stiffness' (*F= 0.84841*, *p*-value= *0.58173*) which means that changes are the same whatever the stiffness are.

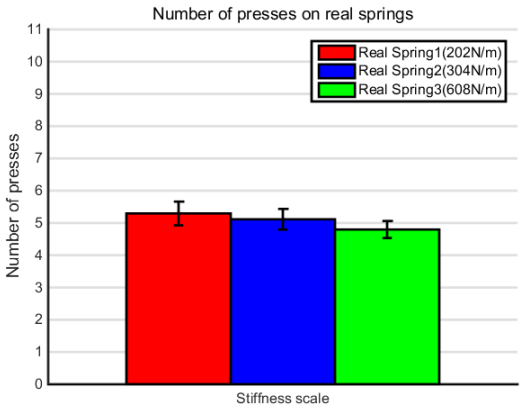

(a)

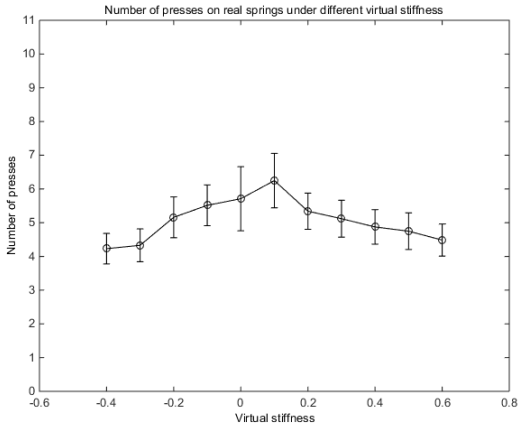

(b)

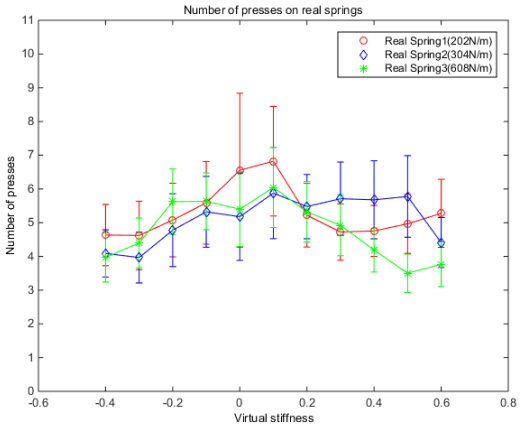

(c)

Figure 2.30 Average of number of pressing on different real springs: a). no matter what is the 'virtual stiffness' of the compared virtual spring; b). under different 'virtual stiffness' of virtual spring; c). under different 'virtual stiffness'.

The number of pressings on virtual spring are shown in Figure 2.31. The statistical results indicate that:

-The 'stiffness scale' has no significant effect on number of pressing (*F=0.21081*, *p*-value=*0.80995*) which means no matter which real spring is simulated by the virtual spring, the number of pressing does not significantly change.

- The 'virtual stiffness' has a significant effect on number of pressing (*F=3.3227*, *p*-value<*0.001*). As the pressing duration, there is also a peak when the stiffness of virtual spring is *10*% higher than the stiffness of real spring (Figure 2.31.b).

- There is no significant interaction between the 'stiffness scale' and 'virtual stiffness' (*F=1.0151*, *p*-value= *0.42766*), meaning that the number of pressing increases in the same way whatever the virtual springs.

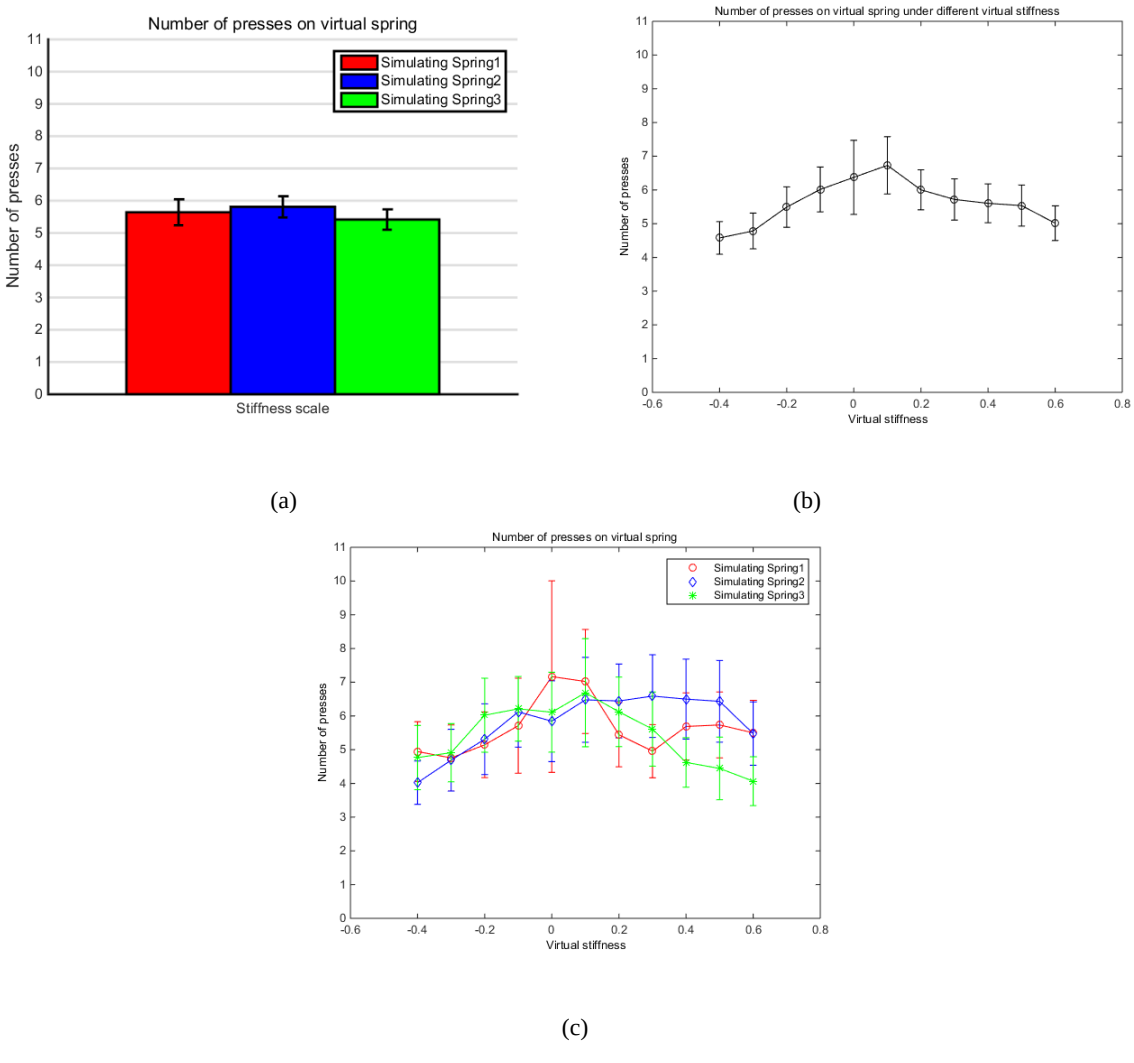

Figure 2.31 Average of number of pressing on virtual spring: a). compared with different real springs, no matter what is the 'virtual stiffness' of the virtual spring; b). under different 'virtual stiffness' of virtual spring, no matter with which real spring it is compared; c). under different 'virtual stiffness' for different simulated real springs.

Comparing the number of pressing on virtual spring and the corresponding real spring, gives the following results:

- The spring type has a significant effect on number of pressing (*F= 8.8493*, *p*-value<*0.01*). This indicates that the number of pressing on real spring is significantly lower than on virtual spring.
- The 'stiffness scale' has a significant effect on number of pressing (*F= 5.5828*, *p*-value<*0.01*). This means that both number of pressing on real and virtual springs vary following the change of the stiffness.
- There is no significant interaction between the spring type and 'stiffness scale' (*F=1.0838*, *p*-value= *0.3384*) meaning that the number of pressing on virtual spring are significantly higher than on the corresponding real spring.

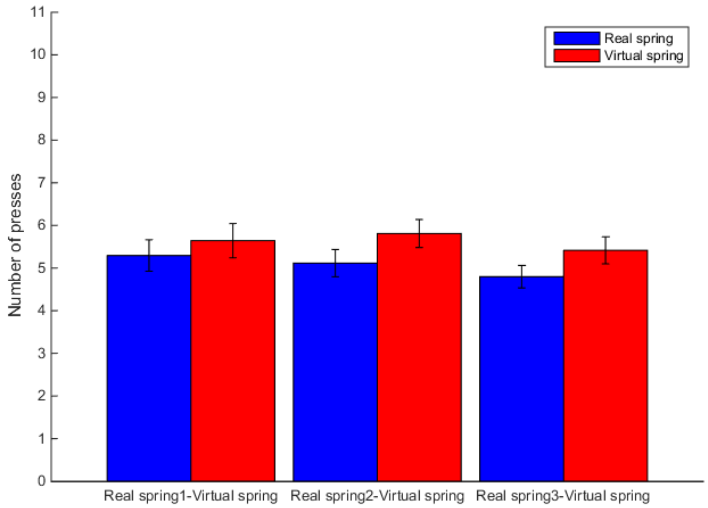

Figure 2.32 Comparison between the number of pressing on virtual spring and the corresponding real spring. All the compared pairs have significant differences between the number of pressing on virtual spring and real spring (*p*-value<*0.01*).

2.4.3.3 Pressing frequency

The subjects' pressing frequencies while pushing the different real springs are presented in Figure 2.33. The results indicate that;

- The stiffness of real spring has a significant effect on pressing frequency (*F=13.926*, *p*-value<*0.001*) and the pressing frequency on real spring 1 seems higher than the other two real springs.

- The ‘virtual stiffness’ has no significant effect on pressing frequency (*F=1.1897*, *p*-value= *0.29256*) which means that the pressing frequency were not influenced by the different ‘virtual stiffness’ whatever the real spring.
- There is no significant interaction between the stiffness of real spring and ‘virtual stiffness’ (*F= 0.62489*, *p*-value=*0.79376*), meaning that the changes in pressing frequency is the same for each virtual stiffness, whatever the stiffness scale is.

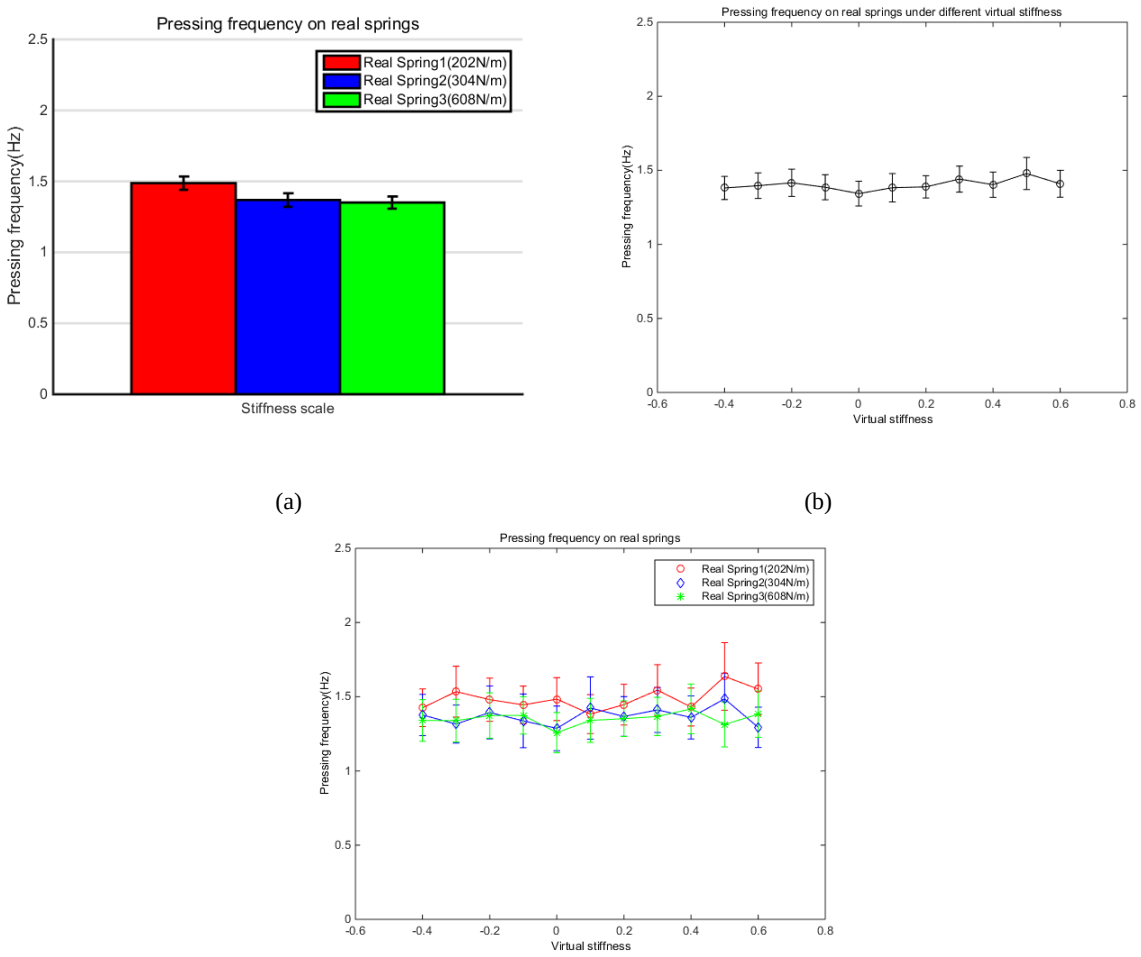

Figure 2.33 Pressing frequency on different real springs: a). no matter what is the ‘virtual stiffness’ of the compared virtual spring; b). under different ‘virtual stiffness’ of virtual spring; c). under different ‘virtual stiffness’.

Figure 2.34 presents the pressing frequency on virtual spring. The results indicate that:

- The ‘stiffness scale’ has no significant effect on pressing frequency (*F=0.17619*, *p*-value=*0.83847*). The pressing frequency on virtual spring varies around 1.5*Hz* no matter which real spring it simulates.

- The ‘virtual stiffness’ has no significant effect on pressing frequency (*F=1.4241*, *p*-value=*0.163*).
- There is no significant interaction between the ‘stiffness scale’ and ‘virtual stiffness’ (*F=1.1651*, *p*-value=*0.30966*) either.
- The pressing frequencies on virtual spring when simulating different real springs are the same.

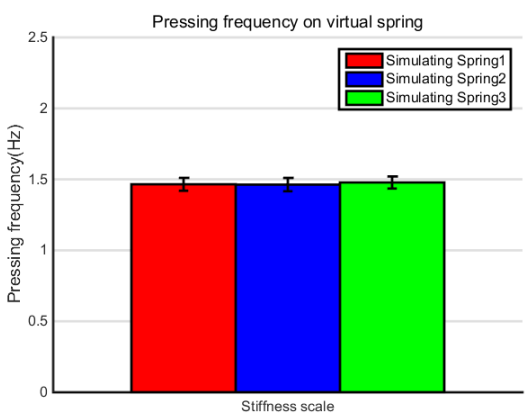

(a)

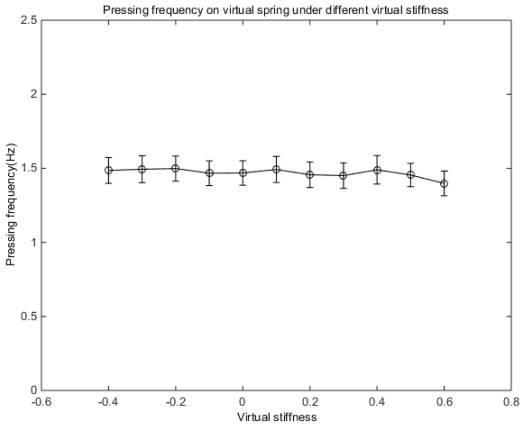

(b)

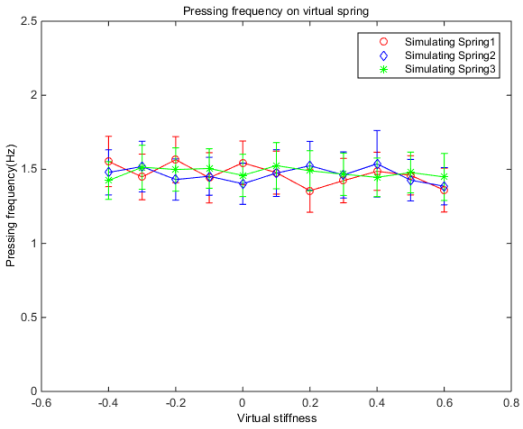

(c)

Figure 2.34 Average of pressing frequency on virtual spring: a). compared with different real springs, no matter what is the ‘virtual stiffness’ of virtual spring; b). under different ‘virtual stiffness’ of virtual spring, no matter with which real spring it is compared; c). under different ‘virtual stiffness’ for simulating different real springs.

The statistical results comparing the pressing frequency on virtual spring and corresponding real spring shown that:

- The spring type has no significant effect on pressing frequency (*F= 1.7002*, *p*-value= *0.19237*);
- the 'stiffness scale' has a significant effect on pressing frequency (*F= 8.4596*, *p*-value<*0.001*);
- there is a significant interaction between the spring type and stiffness scale (*F=10.464*, *p*-value<*0.001*).

The *t*-test of post-hoc analysis indicates that all forces on virtual spring are significantly different from the forces on corresponding real spring. From Figure 2.35, is seen that the pressing frequency on virtual spring of compared pairs real spring 1-virtual spring and real spring 2-virtual spring are significantly higher than the corresponding real spring.

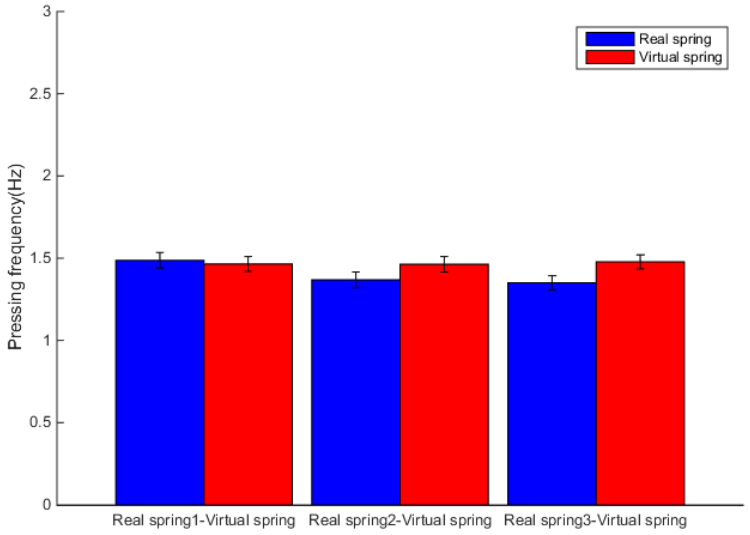

Figure 2.35 Comparison between the pressing frequency on virtual spring and corresponding real spring. The compared pairs: Real spring2-Virtual spring and Real spring3-Virtual spring have significant differences between the pressing frequency on virtual spring and real spring (p-value<0.01).

2.4.3.4 Pressing velocity

The results presented in Figure 2.36.a. show

- The main effect of stiffness on pressing velocity (*F=440.62*, p-value<*0.001*). The velocity decreased from *15.82 mm/s* to *9.60 mm/s* for the stiffer spring. That means

the maximal pressing velocity decreases following the increase of the stiffness of real spring.

- No significant effect was noted for the 'virtual stiffness' as indicated in Figure 2.36.b (*F=2.2269*, *p*-value=*0.0141*), meaning that the subject pressing velocity on the real spring were not changed according to the stiffness of the simulated spring.
- No significant interaction between stiffness of real spring and 'virtual stiffness' was observed (*F=1.1417*, *p*-value=*0.32653*).

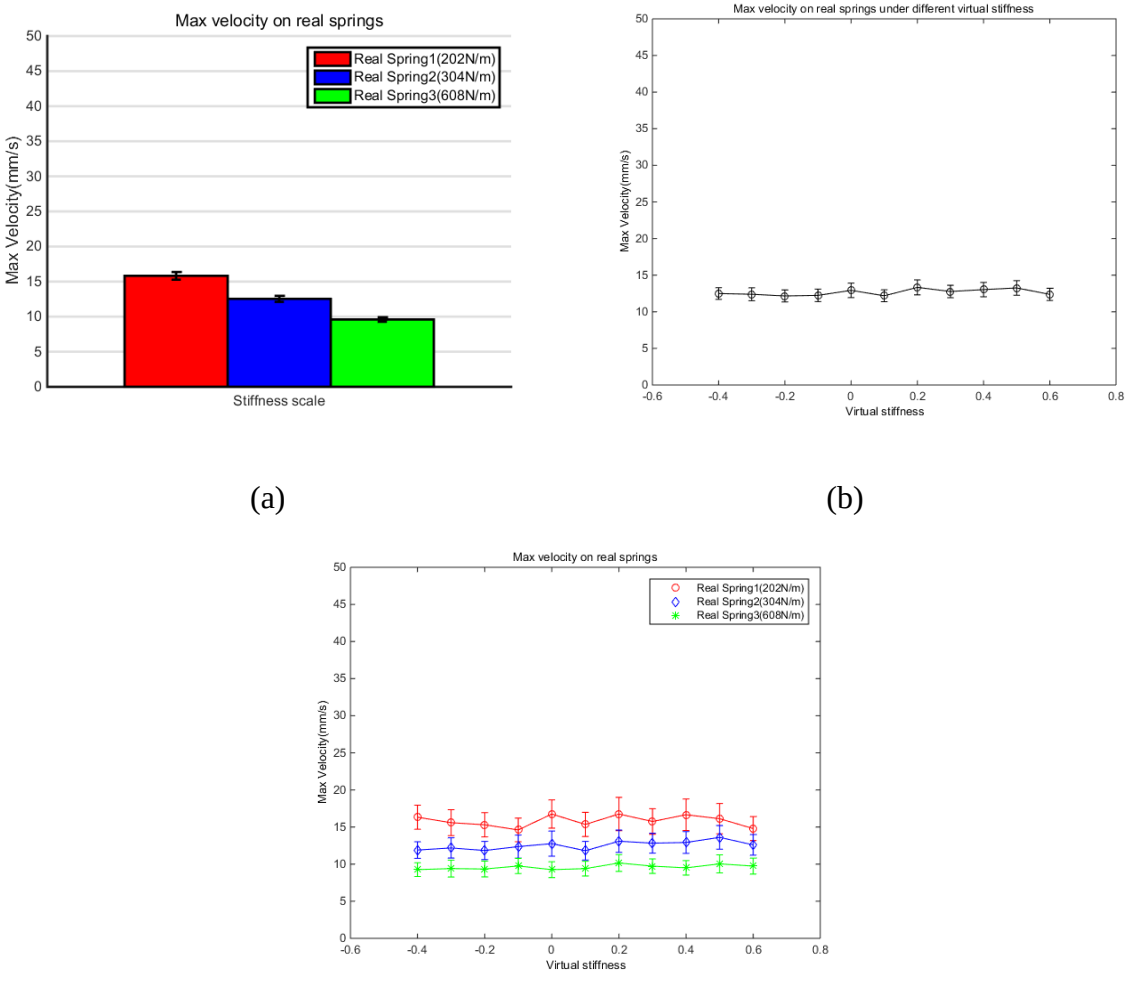

Figure 2.36 Average maximal pressing velocity on real springs: a). no matter what is the 'virtual stiffness' of compared virtual spring; b). with SEM on real springs under different 'virtual stiffness' of compared virtual spring, no matter which real spring; c). with SEM on each real spring under different 'virtual stiffness'.

The results in Figure 2.37.a show that:

- There is a significant effect of the 'stiffness scale' on the maximal pressing velocity (*F= 950.81*, *p*-value<*0.001*). The velocity decreased from *23.54 mm/s* to *10.85 mm/s*.

This indicates that the maximal pressing velocity decreases with the increase of the 'stiffness scale'.

- Significant effect of the 'virtual stiffness' had been observed on the maximal pressing velocity (*F= 40.489*, *p*-value<*0.001*) Figure 2.37.b. This means that the velocity on virtual spring decreases in the same way from lower virtual stiffness to the higher one, whatever the stiffness scale.
- A significant interaction between 'stiffness scale' and 'virtual stiffness' was observed in Figure 2.37.c (*F= 3.5302*, *p*-value<*0.001*). This reveals that when the stiffness changes from *-40%* to *+60%*, the maximal pressing velocity decrease more as the virtual stiffness increases. Comparing with results on real springs, the maximal pressing velocity on virtual springs changed when the 'virtual stiffness' changed.

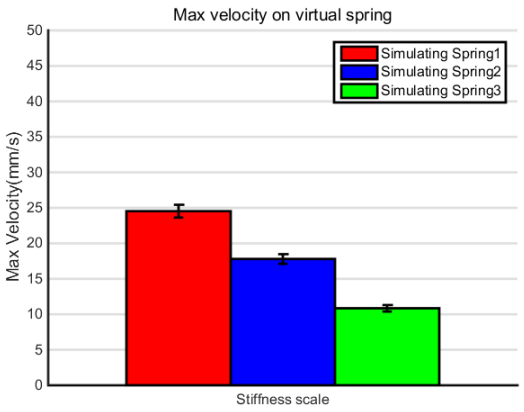

(a)

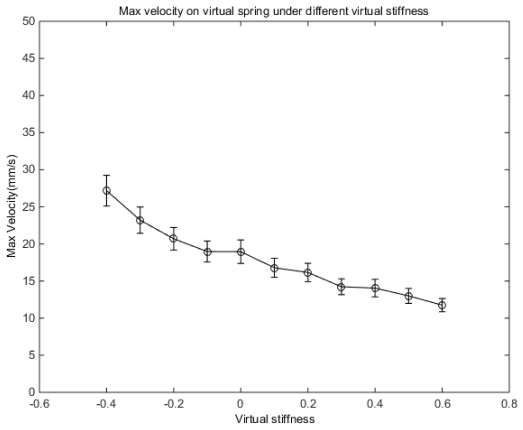

(b)

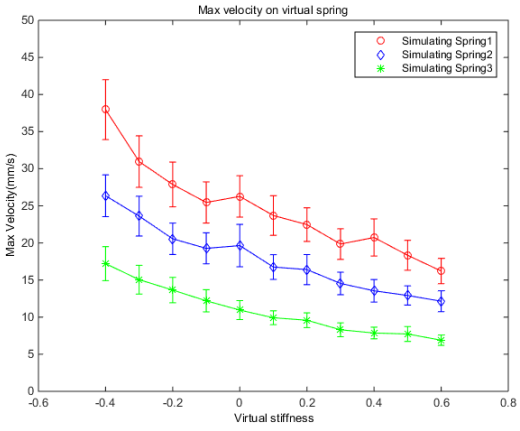

(c)

Figure 2.37 Average maximal pressing velocity on virtual spring: a). no matter what is the 'virtual stiffness' of compared real spring; b). under different 'virtual stiffness', no matter which real spring it is compared with; c). under different 'virtual stiffness'.

2.4.4 EMG signal and muscle co-activation

2.4.4.1 EMG signal on flexor

From the EMG signals on most involved flexor during pressing on real springs, the results presented in Figure 2.38.a. showed:

- A significant effect for stiffness (*F= 49.351*, *p*-value<*0.001*). The EMG on flexor increased from *0.2898* to *0.4678* for the stiffer spring. No significant effect was noted for the 'virtual stiffness' as indicated in Figure 2.38.b (*F=0.95322*, *p*-value=*0.48269*), meaning that the subject's EMG when pressing on the real spring were not changed according to the stiffness of virtual springs
- No significant interaction between stiffness of real spring and 'virtual stiffness' (*F=1.1698*, *p*-value=*0.30634*).

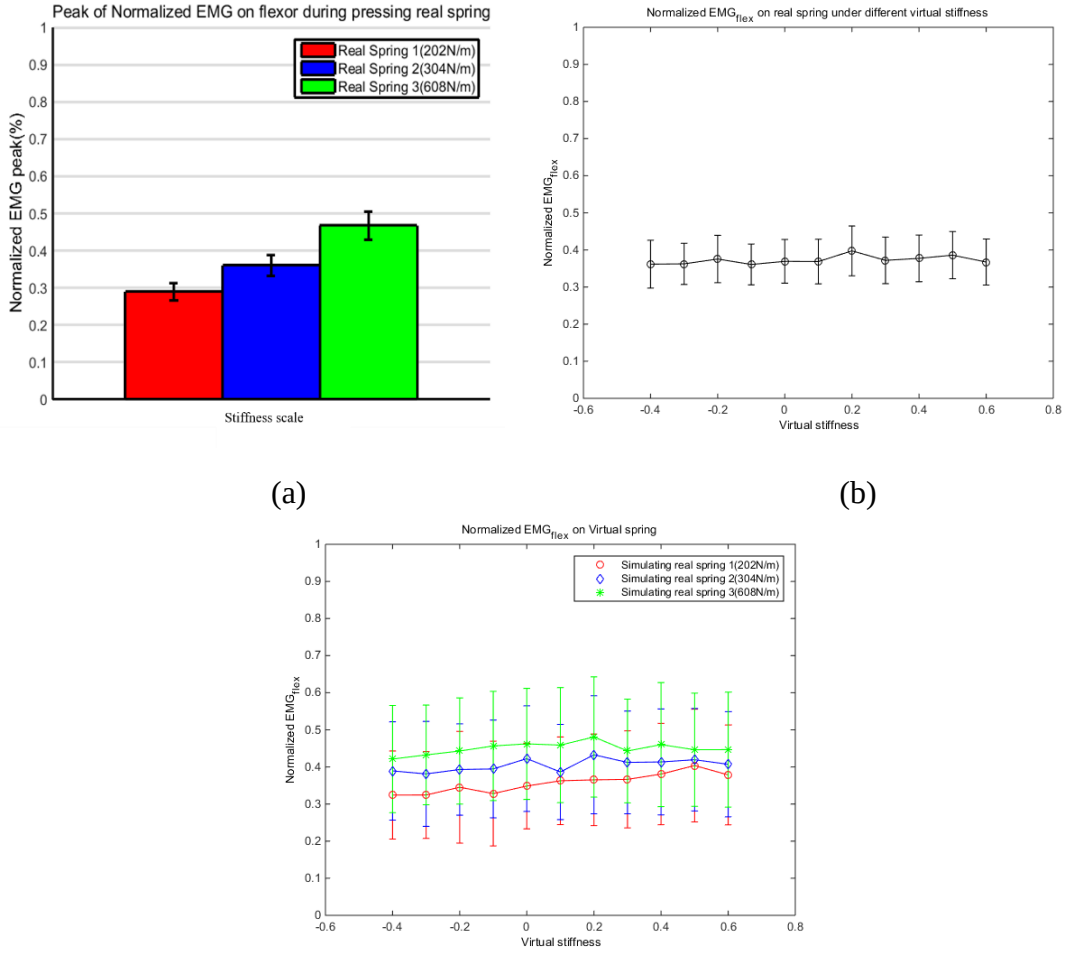

Figure 2.38 Average peak of normalized EMG signals on most involved flexor during pressing on real springs: a). no matter what is the 'virtual stiffness' of compared virtual spring; b). under different 'virtual stiffness' of compared virtual spring, no matter which real spring; c). under different 'virtual stiffness'.

Figure 2.39 shows the EMG signals on most involved flexor during pressing the virtual spring. As shown in Figure 2.39.a, the 'stiffness scale' has a significant effect on EMG of flexor (*F= 27.54*, *p*-value*<0.001*). The EMG signals on flexor increase from *0.3571* to *0.4501* indicate that the EMG on flexor increases when the stiffness is higher. The significant effect of 'virtual stiffness' has been also found on the EMG signals on flexor (*F= 2.9796*, *p*-value*<0.001*) (Figure 2.39.b). The values varied from *0.3783* to *0.4018* when 'virtual stiffness' changed from *-40%* to *+60%*. There is no significant interaction observed between the 'stiffness scale' and 'virtual stiffness' (*F= 1.5552*, *p*-value=*0.11388*) (Figure 2.39.c). This means that when the stiffness scale and the virtual stiffness are increasing, the EMG signals in flexor are also increasing.

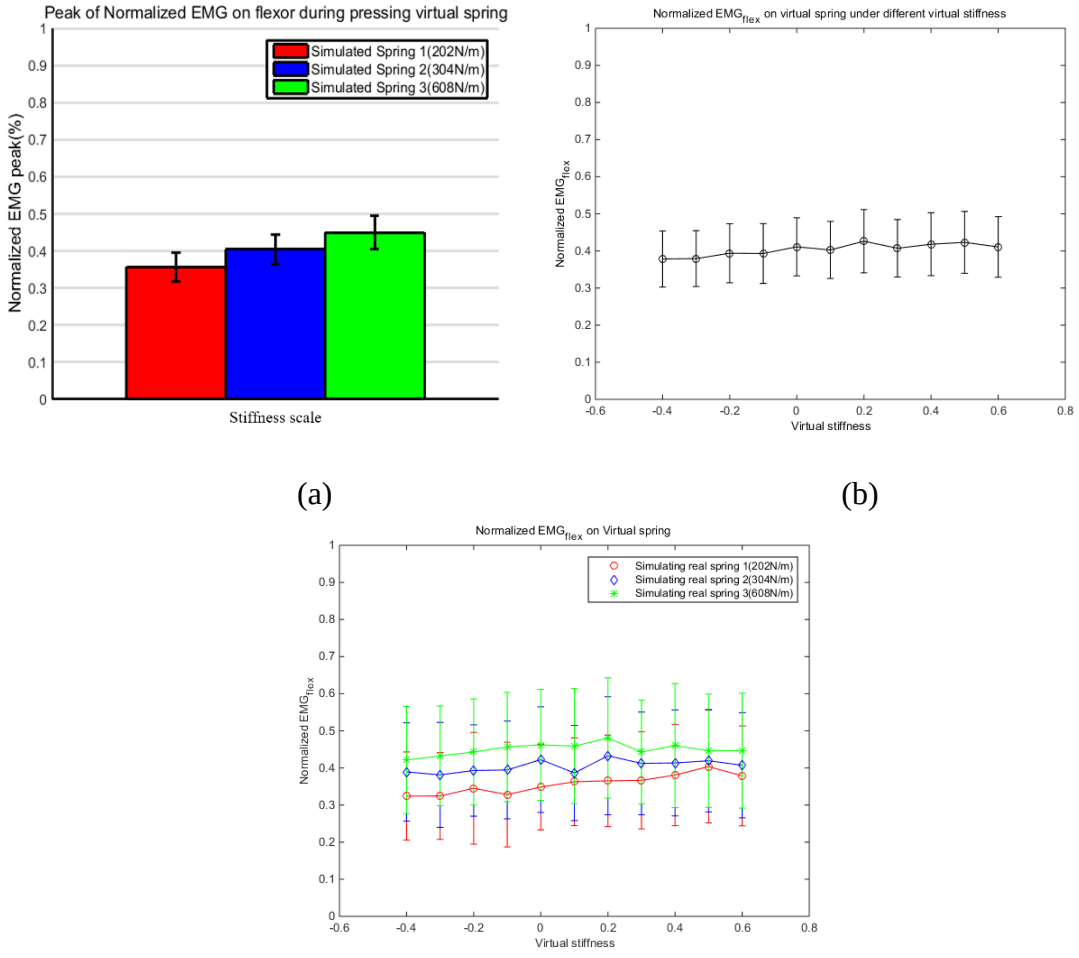

Figure 2.39 Average peaks of normalized EMG signals on most involved flexor during pressing on virtual spring: a). with different 'stiffness scale'; b). under different 'virtual stiffness' of compared real spring; c). with SEM on virtual spring under different 'virtual stiffness'.

2.4.4.2 EMG signal on extensor

The EMG signals on most involved extensor during pressing on real springs, Figure 2.40.a shown that:

- Stiffness had a significant effect on EMG of extensor (*F=87.488*, *p*-value<*0.001*).
- No significant effect was noted for the 'virtual stiffness' as indicated in Figure 2.40.b (*F=0.75626*, *p*-value=*0.67141*), meaning that the EMG on extensor were not changed according to the spring stiffness. This means that the extensor muscle remains at the same state, whatever the "stiffness scale" and "virtual stiffness".
- There was no significant interaction between them (*F=0.88967*, *p*-value=*0.54208*).

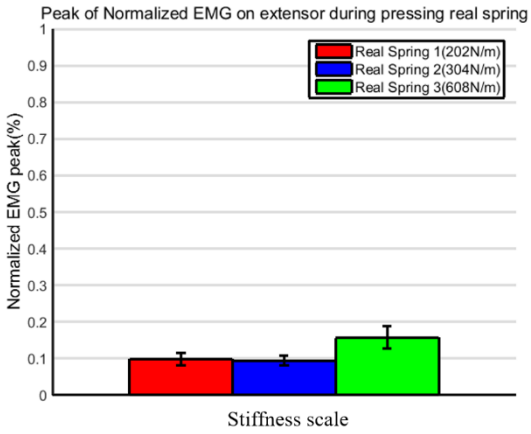

(a)

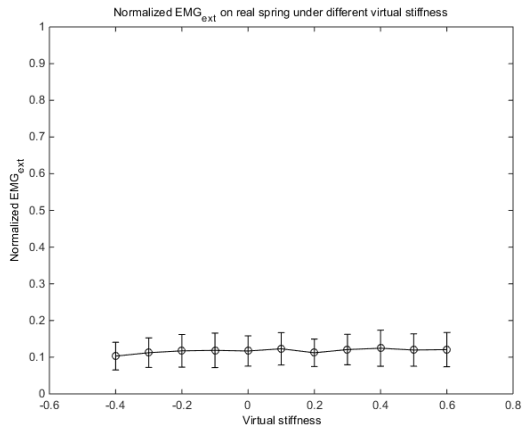

(b)

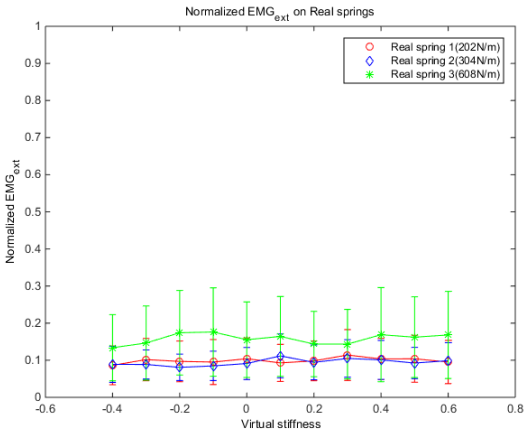

(c)

Figure 2.40 Peaks of normalized EMG signal on most involved extensor for real springs: a). no matter what is the 'virtual stiffness' of compared virtual spring; b). under different 'virtual stiffness' of compared virtual spring, no matter which real spring; c). under different 'virtual stiffness'.

From EMG signals of extensor during pressing on virtual spring, Figure 2.41.a shown that:

-The stiffness had a significant effect on EMG of extensor (*F=4.7122*, *p*-value<*0.01*).

-No significant effect was noted for the 'virtual stiffness' as indicated in Figure 2.41.b (*F=1.0389*, *p*-value=*0.40745*), meaning that the EMG on extensor during pressing the virtual spring did not change, whatever the stiffness scale.

- No significant interaction between 'stiffness scale' and 'virtual stiffness' was observed (*F= 0.69752*, *p*-value=*0.72766*) (Figure 2.41.c).

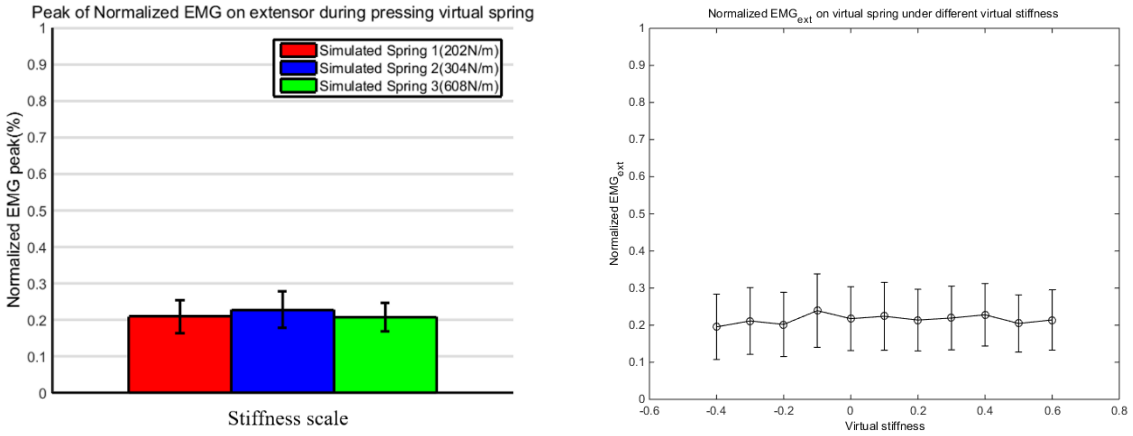

(a) (b)

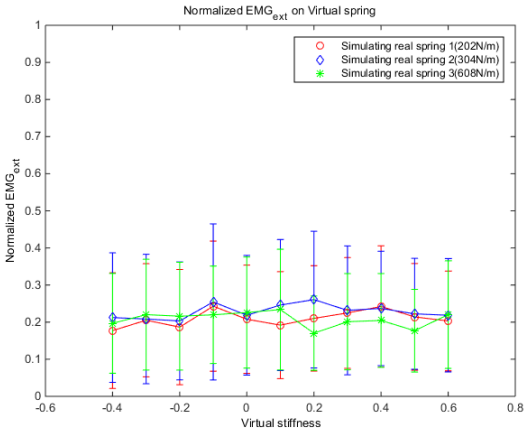

(c)

Figure 2.41 Average peaks of normalized EMG signal on most involved extensor during pressing on virtual spring: a). with different 'stiffness scale'; b). under different 'virtual stiffness' of compared real spring; c). under different 'virtual stiffness'.

2.4.4.3 Muscle co-activation

Figure 2.42.a shows that:

- The stiffness has a significant effect on muscle co-activation of wrist joint (*F=16.007*, *p*-value<*0.001*).
- No significant effect was noted for the 'virtual stiffness' as indicated in Figure 2.42.b (*F=1.2415*, *p*-value=0.2589), meaning that the muscle co-activation during pressing the real spring were not changed according to the virtual spring stiffness.
- There is no significant interaction between stiffness of real spring and 'virtual stiffness' observed (*F=1.0182*, *p*-value=*0.425*) Figure 2.42.c.

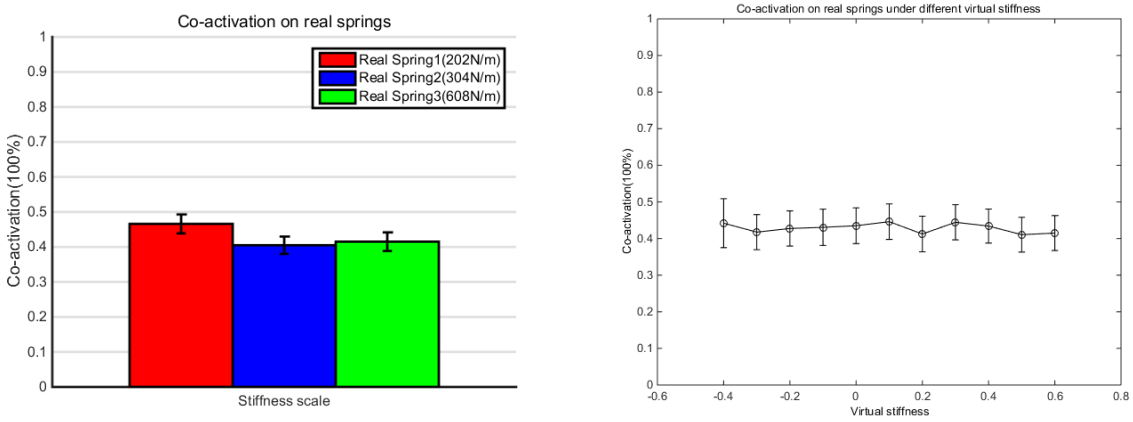

(a) (b)

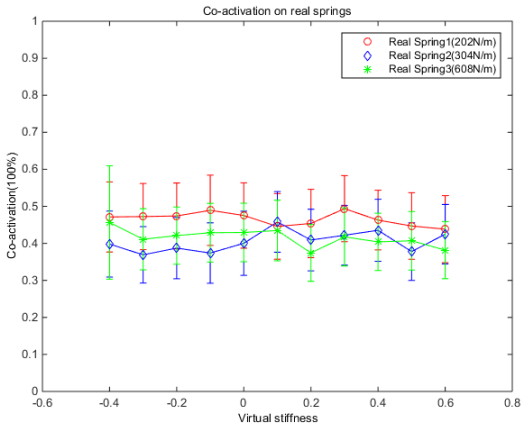

(c)

Figure 2.42 Muscle co-activation of wrist joints during pressing on real springs: a). no matter what is the 'virtual stiffness' of compared virtual spring; b). under different 'virtual stiffness' of compared virtual spring, no matter which real spring; c). under different 'virtual stiffness'.

Figure 2.43.a shown that:

- The stiffness had a significant effect on muscle co-activation (*F=29.93*, *p*-value<*0.0001*).
- No Significant effect was noted for the 'virtual stiffness' as indicated in Figure 2.41.b (*F=0.89*, *p*-value=*0.543*), meaning that the EMG on extensor during pressing the virtual spring did not change according to the spring stiffness.
- No significant interaction between 'stiffness scale' and 'virtual stiffness' was observed (*F=0.65*, *p*-value=*0.775*) (Figure 2.41.c). This means that when the stiffness changes from *-40%* to *+60%*, the EMG signals on extensor are different based on the different stiffnesses.

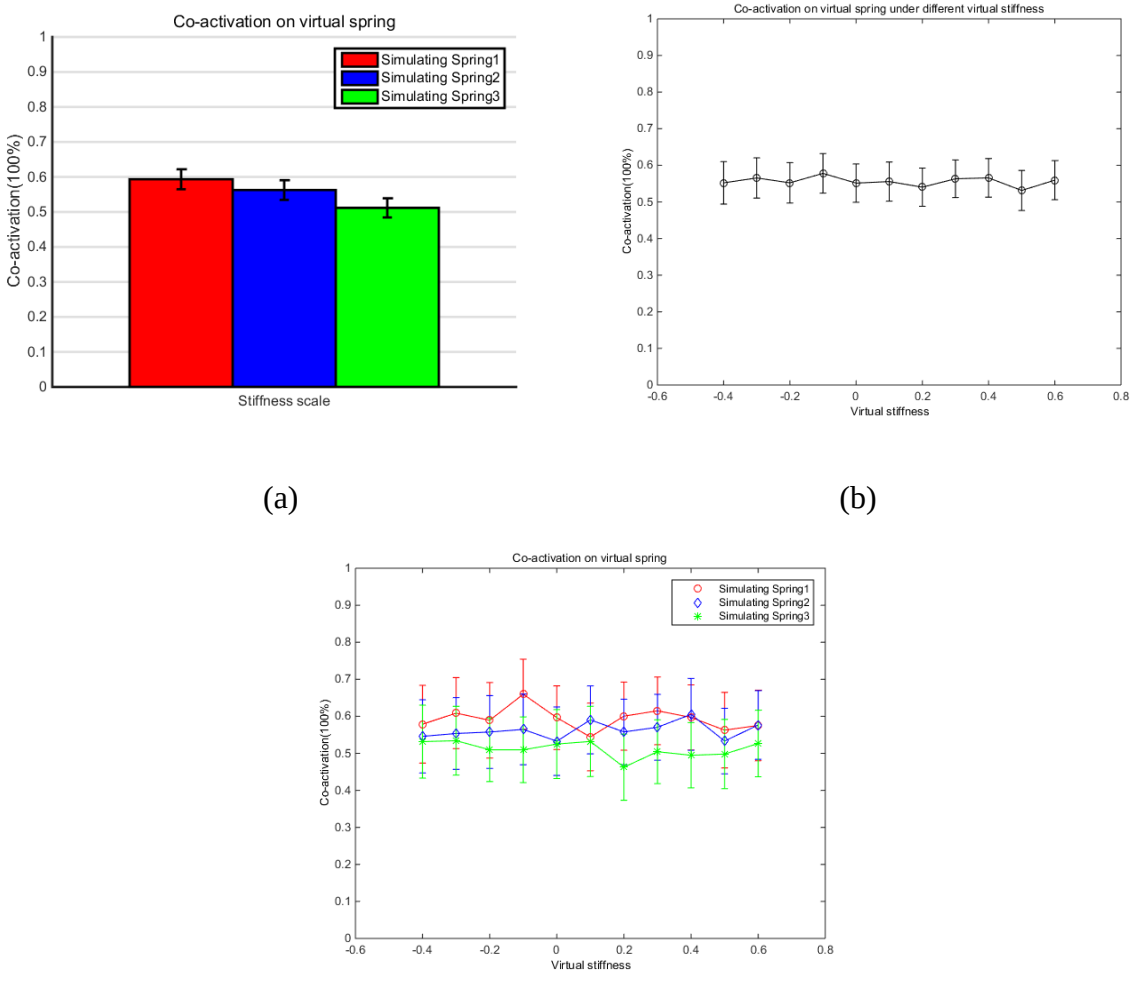

Figure 2.43 Muscle co-activation of wrist joints during pressing on virtual spring: a). no matter what is the 'virtual stiffness' of the compared virtual spring; b). under different 'virtual stiffness' of compared virtual spring, no matter which real spring; c). under different 'virtual stiffness'.

2.4.5 Summary

In this section, we presented the statistical results in the aim to know whether the independent variables have a significant influence on the dependent variables or not. We also wanted to know whether there is interaction between two independent variables. Table 2.1 provides a summary of the two-way ANOVA with repeated measures where 'stiffness scale' and 'virtual stiffness' are independent variables.

Table 2.1 ANOVA test result summary. EMG_{flex}=Normalized EMG signal on most involved flexor; EMG_{ext}= Normalized EMG signal on most involved extensor; CA=Muscle co-activation for wrist joints. ("*" indicates that there is a significant effect of the independent variable on the corresponding dependent variable, and "n.s" indicate the opposite).

Dependent variable / **Independent variable**		Force without normalization	Normalized force	Pressing duration	Number of pressing	Pressing frequency	Pressing velocity	EMG_{flex}	EMG_{ext}	CA
Real spring	Stiffness scale	*	*	n.s	n.s	*	*	*	*	*
	Virtual stiffness	n.s	n.s	*	*	n.s	n.s	n.s	n.s	n.s
	Interaction	n.s	n.s	n.s	n.s	n.s	n.s	n.s	n.s	n.s
Virtual spring	Stiffness scale	*	*	n.s	n.s	n.s	*	*	*	*
	Virtual stiffness	*	*	*	*	n.s	*	*	n.s	n.s
	Interaction	*	*	n.s	n.s	n.s	*	n.s	n.s	n.s

Among all the statistical results presented above, force without normalization, pressing velocity and muscle co-activation provide some important information. For the force applied on real springs, it is only influenced by 'stiffness scale'. However, the force applied on virtual springs were not only influenced by 'stiffness scale', but also the 'virtual stiffness'. The effect of two independent variables on maximal pressing velocity are the same as in force. The 'stiffness scale' has significant effect on subjects' muscle co-activations during pressing on both real and virtual springs.

2.5 Discussion

Figure 2.20.a shows how subjects' answers change when the stiffness of virtual spring increases for each comparison pair. Thus, for comparison pairs: real spring 1-virtual spring and real spring 2-virtual spring an underestimation of stiffness of virtual spring appears. When the proportion of response "Spring B is stiffer" is *50*%, subjects consider that the two compared springs have the same stiffness. From Figure 2.20.a, is seen that less stiff the real spring is, bigger the difference between perceived stiffness of virtual spring and the compared real spring is. It seems that the subject's answer varies with the stiffness of virtual spring. The bigger the difference

between the stiffness of real spring and virtual spring is, the closer to the correct answer the subject answer is.

2.5.1 Confirmation of stiffness underestimation

As demonstrated in [LCKR00], less stiff the compared real spring is, more the stiffness of the virtual spring is underestimated. The subjects consider that the stiffness of real spring 1 is the same as this of virtual spring when the stiffness of virtual spring is *+30*% higher than the stiffness of the real one. This value is bigger than the 'virtual stiffness' value of compared pair real spring 2-virtual spring (*+20*%) and compared pair real spring 3-virtual spring (*0*%). This confirms the conclusions reported in [LBCC01, LCKR00] that if the difference between the stiffnesses of real and virtual springs increases, bigger visual displacement is necessary in order to compensate this difference. Although in [LCKR00], the stiffness discrimination was performed by pinching, it is reported in [PCDS14] that differential sensitivity for stiffness discrimination task is not significantly affected by the exploration method (pressing or pinching). This conclusion allows us to compare our results with those in [LCKR00].

Lécuyer et al. proposed two explanations for the underestimation of the virtual spring stiffness in [LCKR00]:

a) As both real and virtual springs in the experiment have different locations and the graphic representor is a bilateral transition between these two springs, it may have a psychological effect on the stiffness perception;
b) While pushing the virtual spring, subject's thumb is almost static. This results in the confliction between *the proprioceptive feeling of motion of the thumb and the visual feedback of the displacement of the spring*. Consequently, "visual feedback replaces proprioceptive sense in some extent".

In his Ph.D. thesis Lécuyer [Lécu01], complemented some reasons to explain the underestimation:

c) *The subject always pressed the real spring first which might influence their perception of the stiffness of the virtual spring*;
d) As the subject needs to switch between the real spring (in real environment) and virtual spring (virtual environment) the monoscopic view may influence the results;
e) On the computer screen the virtual spring moves in left and right direction while subjects' fingers are pressing in up and down direction.

We are not concerned by explanations a) and d) because in our experiment both real and virtual springs have uniform graphic representors on computer screen (up and down direction). In our experiment, subjects were asked to press on the virtual spring first, hence we are not concerned by explanation c) either. As in our experiment both physical and simulated springs on computer screen move up and down, then the explanation e) is also excluded. At the end, the explanation b) concerns both Lécuyer's and our experiment which might explain the underestimation.

Based on the explanations given by Lécuyer concerning this underestimation, we propose here below our reflection.

While pressing the virtual spring, the subject's finger is almost static (Lecuyer et al.'s explanation b)). According to [ErBa02], in the task involving visual and proprioceptive (perception) feedbacks, the most dominant is the perception. As the finger is almost static, subject's perception error of his/her finger displacement is smaller than the perception error of virtual spring displacement rendered on the screen. Let us assume that the perceived displacement D_P of the virtual spring is:

$$D_P = w_1 \times D_V + w_2 \times D_F \tag{2-10}$$

where:

- D_V is the displacement of virtual spring on the computer screen,
- D_F is the subject's finger displacement,
- w_1 and w_2 are respectively the weight of D_V and D_F.

Then the difference between the perceived stiffness k_P and the simulated stiffness k_S can be expressed as:

$$\Delta k = k_S - k_P = F_V(D_V - D_P)/D_P D_V \tag{2-11}$$

where F_V is the subject's force applied on virtual spring.

As D_F is very small comparing with D_V, then $D_F \approx 0$. Hence, the relative perception error $\Delta k/k_S$ is:

$$\Delta k/k_S = (1 - w_1)/w_1 \tag{2-12}$$

The derivation of $\Delta k/k_S$ to w_1 is:

$$\frac{d(\Delta k/k_S)}{dw_1} = \frac{-1}{w_1^2} < 0 \qquad (2\text{-}13)$$

Consequently, $\Delta k/k_S$ is a monotonically decreasing function of w_1.

Following the decrease of the simulated stiffness of the virtual spring, D_V becomes bigger, hence the difference between the perception error of D_V and D_F becomes bigger. In our opinion this is the reason why w_1 decreases following the decrease of k_S. This means that the coefficient weight of the virtual spring displacement decreases when the simulated stiffness of virtual spring decreases. Assuming w_1 is function of k_S, thus $dw_1/dk_S>0$. Then the derivation of $\Delta k/k_S$ to k_S is:

$$\frac{d(\Delta k/k_S)}{dk_S} = \frac{d(\Delta k/k_S)}{dw_1} \cdot \frac{dw_1}{k_S} < 0 \qquad (2\text{-}14)$$

where: $\Delta k/k_S$ is the 'virtual stiffness' corresponding to the PSE point in the subjects' discrimination results.

If $\Delta k/k_S=0$, the perceived stiffness is equal with the simulated stiffness.

If $\Delta k/k_S<0$, the virtual spring stiffness is underestimated

Hence, $\Delta k/k_S$ increases following the decrease of k_S, according to eq. (2-14), the smaller the simulated stiffness of the virtual spring is, the bigger its underestimation is.

The reflection presented here above is a possible explanation for conclusion presented in [LCKR00] that the bigger subject's underestimation of the virtual spring stiffness is accompanied with less stiffness of virtual spring.

After transferring the subjects' answers into *z* score, the linear regression analysis results for the data of three comparison pairs indicated that they have different slope values. The PSE point, JND and Weber fraction reported in here are higher than those reported in [LCKR00].

One explanation may be that work cue in our experiment is different from this in Lécuyer [LCKR00]. In Lécuyer's experiment] there is a red line in the pole (see Figure 2.1.b) while our experiment shows a cue, "Stop pressing" when the distance between the pressing button and the top of tube is smaller than *1mm*. In this way, the work cue in our experiment is limited comparing with [LCKR00]. As mentioned in [TDBS95] the compliance JND is poor when the work cues and terminal force cues are eliminated or reduced.

2.5.2 Kinematic parameters

When virtual spring's stiffness is *10*% higher than the stiffness of the real spring, both pressing duration and number of pressing values are bigger than the other ten conditions no matter for real or virtual spring. This means that subjects need more information for performing discrimination at *+10*% than at *0*%. Based on the results in Figure 2.20.a, the discrimination answers '*Spring B is stiffer*' for pairs: real spring 1-virtual spring, real spring 2-virtual spring and real spring 3-virtual spring, arrived at *50*% when the 'virtual stiffness' of virtual spring are respectively *30*%, *20*% and *0*% which have an average of *16*%. In addition, *10*% is closer to *16*% which is the average value of 'virtual stiffness' corresponding to the case when subjects have *50*% correct answers. This indicates that averagely when the stiffness of virtual spring is *10*% higher than this of the real spring, it is more difficult to perceive the difference of stiffness.

The number of pressing reflects similar problems/difficulties as the pressing duration in the stiffness discrimination task. Both number of pressing on real spring and virtual spring does not change following the change of the 'stiffness scale'. However, there is a peak when the stiffness of the virtual spring is *10*% higher than the stiffness of the real spring. That allows to say that averagely, the stiffness discrimination task was most difficult at the condition of *+10*%.

The pressing frequency difference decreases following the increase of real spring's stiffness. Note that this difference does not exist on virtual spring when it simulates different real springs. The average value of pressing frequencies on the different real springs (Figure 2.33.a and Figure 2.34.a), and the statistical results about the effect of real spring stiffness and the 'stiffness scale' of virtual spring on pressing frequency clearly indicate that: real spring 1 (*202 N/m*) has higher pressing frequency than real spring 2 (*304N/m*) and real spring 3 (*608N/m*) while there is no significant difference between the pressing frequency on real spring 2 and real spring 3. The boundary between high and low spring pressing-frequency should be between *202 N/m* and *304 N/m*. However, this phenomenon does not symmetrically exist on virtual spring. That means that concerning the pressing frequency, pseudo-haptic feedback does not induce different pressing frequency levels as the real spring do.

In the pressing velocity aspect, both real and virtual springs show a decreasing tendency following the increase of the stiffness. Figure 2.36.a and Figure 2.37.a have clearly shown this tendency. The results shown in Figure 2.36.c revel that for a real spring, the pressing velocity is not influenced by the stiffness of the compared virtual spring while for the virtual spring, the

increase slopes following the increase of ‘virtual stiffness’ with different stiffness scales are significantly different.

The pressing frequency reflects a complementary information about the manner of pressing: fast press (tapping) or slow press. However, it (the pressing frequency) cannot reflect the maximal pressing velocity. That means two pressing movements with the same pressing frequency may have different average pressing velocity. From this aspect, the pressing velocity reflects more information than the pressing frequency.

2.5.3 Force behavior

The statistical results, shown that the forces with or without normalization provided quite the same information. For the real spring, for instance, higher stiffness induces higher force which is in agreement with the conclusions in [Endo16, KWHC10, PCDS14].

Note that virtual stiffness does not have significant effect on the force applied on the real spring. That means whatever the virtual stiffness of the virtual spring is, it does not influence the force applied on the real spring.

When the real stiffness of the compared real spring increases, the finger force applied on virtual spring increases. Following the increase of the virtual stiffness, the force applied on virtual spring also increases. It indicates that changing the stiffness simulated by the pseudo-haptic can induce subjects to change their force applied on the virtual spring as in real spring. According to the statistical results, the significant interaction between the ‘virtual stiffness’ and ‘real stiffness’ on the force applied on the virtual spring indicates that the relationship between the stiffnesses of the virtual spring and the force applied on it is not linear and the slope of force changes following the increase the stiffness of the virtual spring.

When the virtual spring has the same stiffness as the real one, the force applied on real spring increases with *95.1*% while on virtual spring, the force increases only with *34.63*%. Comparing the augmentation of force applied on real and virtual springs, reveals that both forces induced by the real spring and the pseudo-haptic increase following the increase of the stiffness, but their increasing slopes are different.

Following the change of stiffness of virtual spring, the force applied on it also increases. This means that the pseudo-haptic feedback can induce subject’s forces to increase or decrease as in the real spring in stiffness discrimination in reality. This conclusion is important for

potential medical applications requiring pseudo-haptic feedback such as: training or rehabilitation.

However, the increase of force in both real spring and virtual spring have an upper limit. For instance, a stiffness discrimination task was performed in [Endo16]. The forces without normalization applied on different compared specimens with different stiffness were evaluated. According to Weber-Fechner law, the relationship between the perception and stimulus should obey the following equation [Rich94, Vand10]:

$$p = k.ln(\frac{S}{S_0}) \quad (2\text{-}15)$$

where: - p is the volume of perception,

- S is the volume of stimulus,
- S_0 is the threshold of stimulus below which it is not perceived at all,
- k is the parameter to be estimated using the experimental data.

We contacted Hiroshi Endo and he generously provided us the raw data used in [Endo16]. According to Weber-Fechner law, the force data in [Endo16] (Figure 2.44.a) may be expressed as a linear function of the springs' stiffness. Based on the original data provided by Endo, we found significant first order linear regression equation ($F(1, 36) = 2.32e+03$, $p<0.001$), with an R^2 of *0.985*. This means that the predicted force is equal to *-11.134+3.318 ln* (stiffness) *ln* (N/m) where force is measured in *N*. Force increased with *3.318* for each *ln* (*N/m*) of stiffness.

For the second order linear regression, the coefficient of term stiffness-square is not significantly different from *0* (*p*-value=*0.69911*). Then, the relationship between the force F_R applied on real spring and its stiffness S_R is expressed as:

$$F_R = -11.175 + 3.345.ln(k_R) \quad (2\text{-}16)$$

Figure 2.44.b presents the results of the first order linear fitting. According to eq. (2-16), the derivation of F_R to k_R is $F_R'=3.345/k_R$. That means that increase rate will slow down following the increase of the stiffness. As the finger's force is limited, there should exist an upper limit in its increasing.

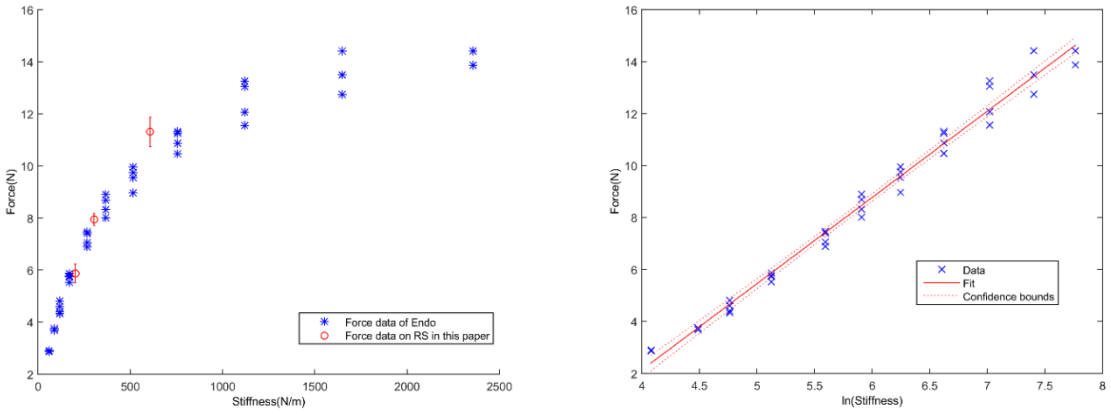

(a) (b)

Figure 2.44 Force applied on real springs: a). Force according the data of Endo's paper; b). linear regression for Endo's force data.

The force on virtual spring (pseudo-haptic) behaves in a similar way as the force on real spring. A first order equation of linear regression was performed for the force without normalization on virtual spring. A significant regression equation was found (F (1, 31) *=208, p<0.001*), with an R^2 of *0.87*. Predicted force on virtual spring is equal to *-2.222+2.2522 .ln* ($stiffness_{virtual}$).

For the second order linear regression, the coefficient of term stiffness-square is not significantly different from 0 (*p*-value=*0.0017646*). Thus, the relationship between the force on virtual spring and the stiffness S_V, it expressed as:

$$F_V = -2.148 + 2.232.\,ln(k_V) \tag{2-17}$$

where: F_V is the force on virtual spring and k_V its stiffness.

From equations (2-16) and (2-17), there are:

$$\frac{dF_R}{dk_R} = \frac{3.345}{k_R} \tag{2-18}$$

$$\frac{dF_v}{dk_v} = \frac{2.232}{k_v} \tag{2-19}$$

Both $d(F_R)/d(k_R)$ and $d(F_V)/d(k_V)$ are negative and consequently F_R and F_V are monotonically decreasing functions. This means that following the increase of the stiffness, the speed with which the force increases both in real and virtual springs decreases.

Equations (2-16) and (2-17) also give that $d(F_R)/d(k_R) > d(F_V)/d(k_V)$. It is seen that the slope of F_V is always lower than of F_R corresponding to the same stiffness. In order to verify

this statement, we proposed the nested model to express the linear relationship between the force and stiffness as:

$$Force_{ij} = \alpha_j + \beta \log(Stiffness)_{ij} + \varepsilon_{ij} \quad (2\text{-}20)$$

where:

- α_j represents the ordinate at the origin for the modality *j* (real spring or virtual spring),
- β_j represents the slope of the regression line for the modality *j*,
- ε_{ij} represents the residual error.

The aim of testing the proposed nested model is to determine whether point clouds should be adjusted by different regression lines from the point of view of their regression coefficients (slopes, ordinates at the origin). To do this, the *anova* function of software *R* was used. The results of test of nested models indicates that it is preferable to keep the model (2-20) and to adjust the two points clouds (data of force on real spring and virtual spring) by two different regression lines (F = *40.76*, *p*-value *<0.0001*). Table 2.2 below gives the estimated values of the regression coefficients of the model.

Table 2.2 Regression coefficient of the nested model

α_R	α_V	β_R	β_V
-11.175	-2.148	3.345	2.232

Figure 2.45 presents the relationship between the pressing force and the stiffness for real and virtual springs. The two solid lines are the regression lines defined by the method of the least squares. The dotted lines are the prediction intervals. Points represent the data used to construct the regression models.

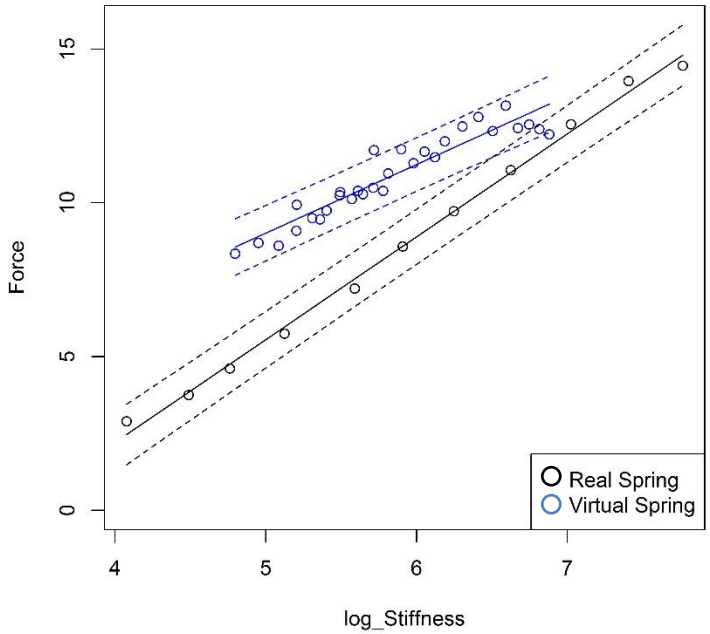

Figure 2.45 Force-Log_Stiffness relations for real and virtual springs.

Given the residual analysis (homoscedasticity, normality) and the adjusted coefficient of determination ($R^2 = 0.973$), the linear adjustment for both point clouds is appropriate. If the form of the link is the same between the force and the logarithm of stiffness for real and virtual springs, the point clouds should be adjusted by two different regression lines, the values of the regression coefficients being significantly different (p-value < 0.0001). This means that two slopes in Figure 2.45 are significantly different.

Figure 2.46 presents the curve of force on virtual spring and real spring calculated according to eq. (2-16) and (2-17). At this aspect, regarding the force, the subject's behavior in computer-based environment involving pseudo-haptic feedback has the same behavior tendency as in reality, although the forces on real and virtual springs have different slopes for equal stiffnesses.

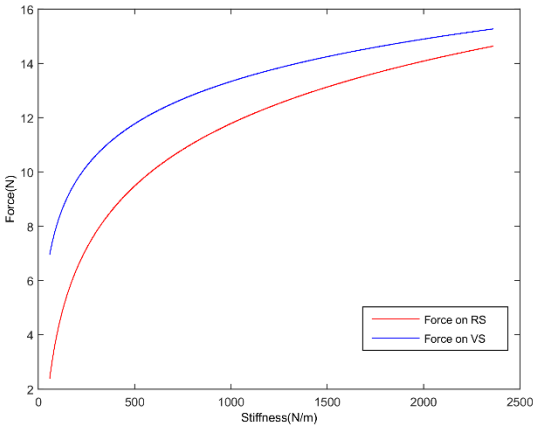

Figure 2.46 Force on real and virtual springs plotted based on eq. (2-16) and eq. (2-17).

Whether it is the force on real or virtual spring, the curves arrive at a tray with a decreasing gap between them when the stiffness increases. The derivation of the difference between F_V and F_R to stiffness k is:

$$(F_v - F_R)' = \frac{-1.113}{k} \tag{2-21}$$

where: k is the stiffness of the spring.

The negative slope of the difference between F_V and F_R indicates that this difference decreases with the increase of the stiffness. In another saying if the simulated stiffness of the pseudo-haptic feedback is higher, less difference exists in the force between pseudo-haptic spring and real spring. This also theoretically explain the conclusion reported in [Endo16] that the forces reach the same magnitude when the stiffness increases.

For the same force magnitude, the stiffness of virtual spring is lower than the stiffness of real spring. This conclusion is also seen from Figure 2.46. It indicates that for inducing the same force as in real spring, the simulated stiffness of virtual spring is lower than the stiffness of real spring. The reason may be the physical stiffness of the virtual spring which is higher than the stiffness of the real springs.

From Figure 2.46 is also seen that for same stiffness, the force applied on the virtual spring is higher than the force on real spring. According to Weber-Fechner law, the bigger force is associated with the bigger perceived stiffness. As the physical stiffness of virtual spring is bigger than the stiffness of real springs, naturally subjects applied bigger force on virtual spring comparing with the real one.

2.5.4 EMG signal on flexor and extensor

During the pressing phase, the agonist muscle is the flexor. Then the tendency of EMG signal's changes on flexor muscle should be in agreement with the force. For the real spring, only the 'stiffness scale' has significant effect both on force applied on real spring and EMG signal on flexor. No significant effect was observed of 'virtual stiffness' and interaction between the 'stiffness scale' and 'virtual stiffness' on both force applied on real spring and EMG signal on flexor. For the virtual spring, 'stiffness scale' and 'virtual stiffness' have significant effect on both the force applied on virtual spring and EMG signal on flexor. Then from the aspect of evaluating the significant effect of 'stiffness scale' and 'virtual stiffness' brought by the pseudo-haptic feedback, EMG on flexor provides similar information as the pressing force.

The extensors being the antagonist muscle during the stiffness discrimination task, comparing with the flexor, its EMG signals have no significant change tendency following the change of the 'stiffness scale' and the 'virtual stiffness' no matter for real or virtual spring.

2.5.5 Muscle co-activation

For the real spring, the maximal joint velocity decreases following the increase of its stiffness (Figure 2.36.a). As pressing the real spring is a dynamic task, this observation confirms the conclusion in [SSGO01]. The stiffness of real spring also has a significant effect on co-activation. Although there is no significant different between the co-activation on real spring 2 and real spring 3, the co-activation in real spring 1 is higher than the other two real springs. Then, we can conclude that for the real springs the muscle co-activation decreases following the increase of its stiffness.

For the virtual spring, following the increase of its stiffness, the maximal pressing velocity decreases, the pressing force increases and the muscle co-activation decreases. From this aspect, the relationship between the force and muscle co-activation during pressing virtual spring is not the same as in static task as reported in [HéDA91, YaWi83]. Conversely, the relationship between the maximal pressing velocity and muscle co-activation, are the same as in dynamic task despite the finger applies a static fingertip force.

Note, that the maximal pressing velocity, while pressing the real spring, depends on maximal joint's velocity (relative velocity). While pressing the virtual spring this maximal pressing velocity represents the maximal velocity of the virtual spring displacement on computer screen. Our results indicate that the maximal pressing velocity is significantly

influence by the simulated stiffness. That means the pseudo haptics can induce different levels of muscle co-activation by changing the simulated stiffness of the virtual spring.

Another interesting point is that co-activation does not depend solely on mechanical constraints associated with the task as it is classically reported. It may depend on a component associated with the cognitive and/or central nervous system for muscle involvement planning of individual. With pseudo-haptic feedback, the relationship between the static force and the muscle co-activation is inverse as in static task. This phenomenon probably exists only in case of pseudo-haptic feedback.

2.6 Conclusion

Here the aim was to study the difference of hand force between the real spring and pseudo-haptic (virtual) spring, and how the force is changing following the change of visual feedback. Through an experiment which involved real spring and pseudo-haptic feedback in a stiffness discrimination task, subjects' pressing force of index finger on both real and virtual springs were recorded and analyzed. The Weber-Fechner law was used to analyze the relationship between the force and stiffness of real and virtual springs.

In the force behavior aspect, both real spring and pseudo-haptic feedback have increased the subjects' pressing force with the increase of stiffness. It was found that the relationships between stiffness and force are not linear, but adapted to Weber-Fechner law.

Corresponding to the same stiffness, the force on virtual spring is higher than on the real spring, but the gap between them decreases following the increase of stiffness.

The slope of force on both real and virtual springs (with pseudo-haptic feedback) decreases following the increase of the spring stiffness. Although the slope of the force on virtual spring is always lower than in the real spring corresponding to the same stiffness, the force change tendency induced by the pseudo-haptic feedback is similar with this induced by the real spring.

An underestimation of the stiffness of virtual spring was found in the stiffness discrimination results which is in agreement with the results reported in [LCKR00]. An assumption about the relationship among the perceived displacement, virtual spring displacement and finger displacement was proposed and applied to explain the underestimation of the stiffness of the virtual spring.

In real spring, both the maximal pressing velocity and the muscle co-activation decrease following the increase of the stiffness. This phenomenon was also observed during pressing the virtual spring. As the subject's index finger was almost static, the change of the muscle co-activation is associated with the stiffness of the virtual spring simulated by the pseudo-haptic feedback.

In summary, the pseudo-haptic feedback can induce the similar force behavior as in real spring. But pseudo-haptic feedback causes a different level of stiffness underestimation of virtual spring which increases with the decrease of simulated stiffness scale. The pseudo-haptic can also induce different muscle co-activation levels as in the real spring.

The meaning of this conclusion is that the pseudo-haptic feedback can be utilized to induce different levels of muscle co-activation without providing different virtual-haptic feedback in reality. Hence, the hand force changing between the real spring and the pseudo-haptic spring, following the change of the visual feedback, may be used as potential application for rehabilitation of motor disorder patients. In our opinion this will considerably decrease the cost of some existing rehabilitation therapies thus providing more possibilities for customized rehabilitation applications.

Part II

Application in CRPS rehabilitation

In this part a new application which manipulate the relationship between the actual motion and rendered motion in virtual reality is developed and its potential application for Complex Regional Pain Syndrome (CRPS) rehabilitation tested in CHU Grenoble is presented. It consists of one chapter (Chapter 3).

Chapter 3
Virtual reality and CRPS rehabilitation

First this chapter, introduces the basic notions and characteristics of Complex Regional Pain Syndrome (CRPS), called also Reflex Sympathetic Dystrophy (RSD), including its symptoms and the traditional physical therapy for rehabilitation. As one of the effective methods, mirror therapy with its mechanism of back mirror therapy and the mirror neuron system are presented. Secondly, comparing with the traditional method for physical therapy, some virtual reality environments and platforms for CRPS rehabilitation applications in general, and for hand movement reconstruction in particular are presented. In order to overcome some drawbacks of traditional physical therapy as mirror therapy, we need an application which allows to manipulate the relationship between the user's physical hand motion and rendered avatar hand motion. For this purpose, a new developed application based on Leap Motion and Unity3D is developed and presented. To test the usage availability of this application, a pilot study was carried out at Central University Hospital (CHU) Grenoble. Two types of hand model, (normal human-like) skin and silver skin), for both right and left hands, were used in the performed tests. Five subjects (one healthy volunteer, two healthy physical therapists, one healthy hospital practitioner and one patient) participated in the tests. During the tests subjects were asked to perform separately wrist and finger movements (four fingers movement except the thumb), for each type of hand model. The rendered hand motion (visual feedback) was shown with different ratios between the real subject's physical hand motion and the rendered avatar's hand motion. The rotation angles of avatar hand for the subjects were recorded and the range of movement calculated. All the subjects gave their feedback about the experiment. In particular the Medical staff expressed a strongly interest in using the application for kinesiological therapy.

3.1 Introduction

Motor disorder or movement disorder is a concept proposed in the mid of 19th century, although many motor disorder related diseases have been discovered [Lans09]. Generally, it affects the nervous system and causes unrests as abnormal and involuntary movements. CRPS (Complex Regional Pain Syndrome) is a disease which may companied with the motor disorder symptom. Although the reasons of CRPS are not very clear yet, it is believed that it is caused by the damage to the central nervous system [JäBa02]. The latter is composed by brain, spinal cord nervous system and peripheral nervous system and is responsible for the motor control. For the patients with motor disorder related diseases, the sensory restoring on the limbs or other affected parts engaged in the movement of daily life is the main purpose for rehabilitation.

Sandroni et al. [SBML03] estimated the incidence at *5.5* cases per *100,000* person years (database period from 1989-1999) while De Mos et al. [DDHD07] reported that an estimated overall incidence rate of CRPS was *26.2* per *100,000* person years (database period from January 1996 to June 2005).. Note, that CRPS can happen at any one, although the results in [DDHD07, SBML03] indicate that the number of affected women is higher than the affected men. CRPS can affect any age but it is more common between 40 and 49 years [Seba11].

The limited range of motion of the affected limb due to inhibition of intolerant pain of CRPS patients is the main obstacle which prevents them from actively using their affected limb in the physical therapy and daily life. Ervilha et al. [EFAG05] have investigated the relationship between the muscle pain and the motor control strategies in a dynamic task. The results showed that the different level of pain changes/influences the motor strategy of painful muscle and the synergistic muscles during performing a maximum speed dynamic exercise. Adaptation to pain (Figure 3.1) has a short-term benefit, such as reducing the pain temporally, but has deleterious long-term negative consequences [HoTu11, HuLe16]. While performing daily live painful movements, the peripherical adaptation may happen on the muscles involved in the movement of affected CRPS joints. This implies that the pain can create irreversible alterations in skeletal muscle. In this optic, Bank et al. [BPMB13] have experimentally proved that the structural alterations in skeletal muscle tissue and pain-induced adaptations of motor function may contribute to the loss of voluntary modulation of muscle activity. In this context, increasing the muscle activity which is maladapted into an abnormal posture can help CRPS patients to improve their motion functions.

Hodges et al. [HoTu11] proposed a new theory of motor adaptation to pain (Figure 3.1). They indicate evidence of redistribution of muscle activation at micro and macro levels with a common goal of protection limit further pain or injury. For achieving this goal, one possibility is to change the redistribution of muscles activities or the mechanical behavior of the muscles which are caused by changes in the nervous system. Especially, Moseley [Mose04a] and Geisser et al. [GGRG93] noted that changes in nervous system may be at different levels, such as: pain cognition, behavioral factors or somatic vigilance. The latter is related to pain tolerance. Virtual reality technologies may be used to change the visual feedback during the limb movement, which in turn confuse the central nervous system for the motor control of movements. One interesting and open question is thus: Can virtual reality help to adapt motor control at multiple levels of the nervous system in order to splint a painful part? Or, in other words, does the pain tolerance increase while using visual feedback with virtual reality technology to confuse the central nervous system for improving the patient rehabilitation to return to the initial no pain pattern? To our knowledge, no study has addressed this point.

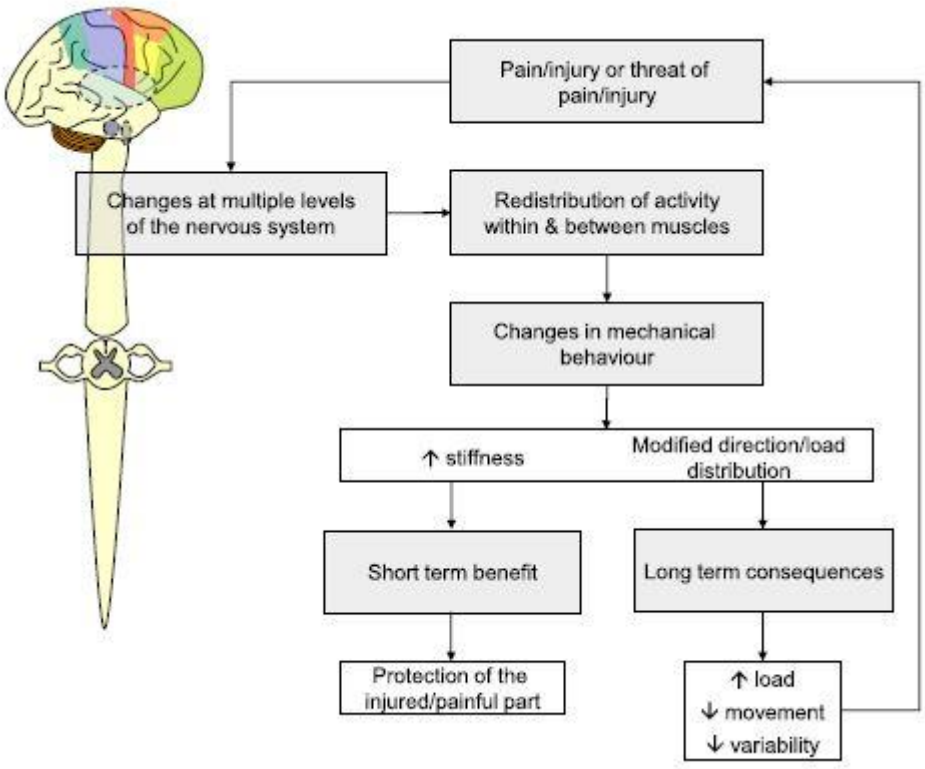

Figure 3.1 New theory of motor adaptation to pain [HoTu11].

Although the treatment of mirror therapy on CRPS (see details in section 3.3.1.1) has been proved it still has some drawbacks such as: fixed head orientation and necessity to ignore

the intact limb. Different from mirror reflection, VR or computer-based applications can provide more possibility to patients in particular for visualizations.

Thus, inspired from the previous work of Murray et al. [MPCH06] and Won et al. [WTCK15], an application based on the Leap Motion and Unity3D was developed and is presented in the following sections.

3.2 Symptoms and treatments of CRPS

3.2.1 Symptoms of CRPS

CRPS has six main symptoms:

- pain,
- autonomic dysfunction,
- edema,
- dyskinesia,
- malnutrition
- and atrophy.

There are two types of CRPS, called CRPS-I and CRPS-II, with similar symptoms and treatments. Patients suffering from CRPS-I have all the main symptoms, but without definable nervous injuries, while CRPS-II (called Causalgia) have definable nervous injuries.

The symptoms of the CRPS-I with dyskinesia are:

- motor weakness,
- general weakness,
- tremor,
- muscle spasm and
- dystonia.

It has been rarely seen that both upper and lower limbs are affected. Although some researchers have identified the evident nervous injury in the CRPS-I, the essential differences between CRPS-I and CRPS-II are still waiting for validation.

CRPS is often associated with surgery of the distal of upper limb [Seba11]. The diagnose conditions for the hand CRPS are:

1. Most of patients had hand injuries before;

2. The symptoms in the early stage exhibit as:

- feeling pain and swelling in the end of the fingers,

- inflexible motor in the finger joints,

- unstable temperature of the skin in the end of fingers,

- pallor or dark red color in the skin.

The delay between the injury and the appearing of the CRPS may vary from a few hours, a few weeks or a few days after the injury. The course of the disease is divided into different phases:

- acute,
- dystrophic,
- atrophic.

Note that there is no obvious link between any two phases of the disease. For example, a patient has pain in the affected hand while in the next phase he/she has autonomic dysfunction which means that he/she cannot normally move the affected limb.

The key physiological symptoms of the CRPS patient is the prolonged pain which can be unbearable in some extremely cases. Except the pain, the other common physiological symptoms are:

- Changed stiffness in the affected joint, due to the abnormal tissue growing around the joint.
- Sensitive skin to light touch.
- Edema in the affected region (Figure 3.2).
- Abnormal posture of the affected limb (mainly flexion of fingers and wrist) (Figure 3.3), sometimes accompanied with jerking and tremors [BPMB13].

Figure 3.2 CRPS patient with swelling wrist joints [BPMB13].

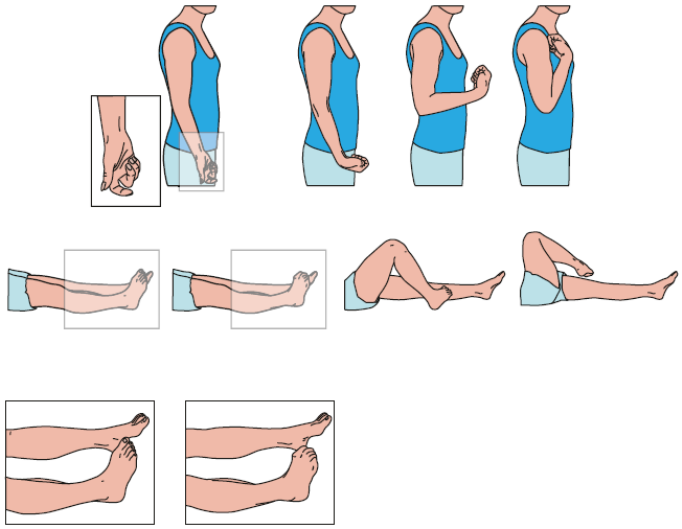

Figure 3.3 Dystonic postures in CRPS. Most common postures in arm and leg in CRPS-related dystonia arranged to the severity from left to right [AMMA11].

Note that apart the physiological symptoms there are also some psychological symptoms in CRPS patients, including:

- Depression.
- Difficulties to relax.
- Unconfident feeling in himself/herself.
- Difficulty to accept the help from family and friends.

No matter the physiological or psychological symptoms, their existences are big obstacles for preventing the patients from normally engaging in their social and professional lives.

3.2.2 Treatment

The core of the therapy is to decrease the sympathetic excitability of the nervous system in the affected limb. The sympathetic nervous system is causing the pain and sensitive skin. Thus, there are some techniques allowing to block or remove a part of sympathetic nervous system [ScMc87]:

- transcutaneous nervous stimulation therapy,
- bier block technique,
- partial blocking sympathetic,
- paravertebral sympathetic block technique,
- removal of peripheral arterial sympathectomy.

For patients in early stage Paravertebral sympathetic block technique is the better solution. For severe patients and patients on long-term Removal of peripheral arterial sympathectomy is recommended.

Excepting treatment which perform operation on patient's nervous system, physical exercise therapy is also widely used. This method is focusing on improving limb's mobility by asking the patient to do physical exercises including kinesiological rehabilitation and occupational rehabilitation tasks. Improving the motor functions of the affected limb through exercising the motor component in the affected limbs is the key point on this treatment. Concerning the physical exercise therapy, once the patients being able to accept it, they are encouraged to exercise the affected limb. One of the most famous physical therapy is the mirror therapy (see details in section 3.3.1.1).

3.3 Previous work

3.3.1 Traditional rehabilitation for CRPS

3.3.1.1 Mirror therapy

Mirror therapy was introduced first time by Ramachandra and Rogers-Ramachandra in 1996 [ViDi96] to treat the so called *phantom limb pain syndrome*. This is a method which uses the visual feedback of the patient's healthy limb reflection in the mirror to effect on the brain in order to reduce the pain associated with the phantom limb. The mirror therapy consists in:

- placing a mirror in the sagittal plane of patient body,
- presenting patient healthy limb and move it in front of the mirror while the residual limb is hiding behind the mirror and trying to symmetrically do the same movement as the healthy limb (Figure 3.4).

This therapy gives patient's the illusion that his/her lost limb still exist and can move as normally as before. The effect of the mirror therapy in reducing the pain associated with the phantom limb. It was proved by a randomized, sham-controlled trial of *mirror therapy* versus *imagery therapy* involving patients with phantom limb pain after the amputation of a leg or foot [CWCM07]. In the imagery therapy group patients close their eyes and imagine performing movements with their amputated limb. The number of the patients in the mirror therapy group who report a decrease in pain was significantly higher than in the imagery group. This results prove that visual feedback of mirror is indeed important comparing with the imagery therapy

alone. Simply saying, having an indeed visual feedback of limb motion is better than just imaging the motion in the mind for the phantom limb patients.

Figure 3.4 Example of mirror therapy [RaAl09].

After the successful application of mirror therapy in the treatment of phantom limb pain, it has recently been applied into the treatment of CRPS. Moseley [Mose04b] conducted a clinical trial incorporating the mirror therapy into a three stage motor imagery program (MIP). The latter consisted of:

- hand laterality recognition task,

- imagery therapy,

- and mirror therapy.

The results show that there is significant treat effect on the patient in pain and movement function. Other successive research proved the efficiency of applying the mirror therapy in reducing the pain and improving the motor functions of the affected limb. Thus, Moseley [Mose05] proved that the mirror therapy has decreased pain and increased the motor function of *20* patients with CRPS type I. Cacchio et al. [CDND09] proved that the mirror therapy significantly improved the motor function and decreased the pain after performing mirror therapy in 24 patients with CRPS type I. .

3.3.1.2 Mirror neuron system

Although the mechanism behind the mirror therapy is not known yet, we might propose question why observing the same action can influence our nervous system and reduce pain? The answer should be find in a particular type of neuron which is called mirror neuron. A mirror neuron is a neuron that fires when an animal observe the same action performed by another animal [RiCr04]. The mirror neuron was first discovered by Giacomo Rizzolatti, et al. in the ventral premotor cortex of monkey [DFFG92, RFGF96]. Later, Molenberghs et al. [MoCM09] found that it also exists in human perception system. Although there is no widely accepted model for explaining how the mirror neuron is supporting the cognitive functions, its possible functions include:

- understanding intentions,
- learning facilitation,
- human self-awareness,
- automatic imitation,
- motor mimicry etc.

Although the mechanism of how the does visual feedback can reduce the pain is not clear yet, the relation between the visual and motor properties is an important functional aspect of mirror neuron or mirror neuron system [RiCr04]. One fact is that observing the action of the healthy limb during the mirror therapy influences the cortical and spinal motor neuron excitability. H-reflex (or Hoffmann's reflex) is a reflectory reaction of muscle induced by electrical stimulations. It is a valuable tool for assessing the monosynaptic reflex activity in the spinal cord [PaIH04]. Baldissera et al. [BCCF01] measured the value of the H-reflex while observing healthy subjects opening and closing their hands. The H-reflex of the antagonist muscle (flexors in the forearm when opening the hand) increases during hand opening and decreases during hand closuring. For the extensors, the conclusion is opposite as the flexor. That means that there exists an inhibitory mechanism which can prevent subjects to do as what they observe.

3.3.2 Computer-based rehabilitation for CRPS

Although the positive effect of mirror therapy on rehabilitation has been proved, it still has some disadvantages:

- The spatial dimension is narrow and the patient's head is required to be oriented into the mirror with the body held in midi-sagittal plane.

- The patient have to ignore the intact limb which provides the reflection.

Different from mirror reflection, Virtual Reality (VR) can create a virtual scenario with complete vision on both healthy and affected limbs thus giving a stronger visual impact on patient. With VR applications more and more physical activities can be simulated and feed-back visualized to the patient thus providing more possibilities than mirror. For those reasons, more and more researchers and physical therapists apply VR or computer-based applications in rehabilitation activities.

Based on the effect of the mirror box therapy in the phantom limb pain, Eynard et al. [EyMB05] developed an augmented reality (AR) application which copy the movement of the healthy limb and symmetrically apply on the residual limb with adapting its positon and orientation. The mechanism of the application is shown in Figure 3.5. In this way, patient is allowed to have a desynchronized movement between the healthy arm and phantom arm.

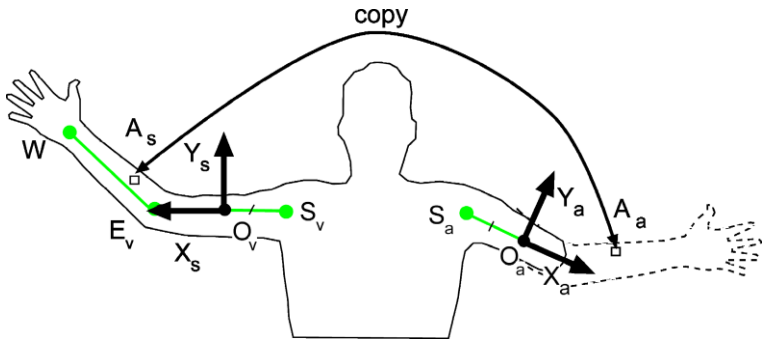

Figure 3.5 Copy movement of the part of healthy limb and symmetrically displayed on the residual limb side [EyMB05].

A year later, Murray et al. [MPCH06] replaced the mirror with VR environment. They created a platform involving the transposition of the movements of healthy limb into the movements of the virtual representor of residual limb in the VR environment (Figure 3.6). The main equipment includes:

- 5DT-14 dataglove,

- position sensors for monitoring the movements of upper-limb amputees,

- sensors for the movements of the legs.

Three patients with phantom limb were involved into the experiment. The results show that two of them reported a pain decrease. The missing hand was visualized to patients with head-mounted display. The movement of the virtual limb (left hand) is the symmetrical transposition of the healthy limb (right hand). Although this platform is not dedicated for CRPS rehabilitation

yet, it provides a good exhibition on how to build a virtual scenario to afford a visualization on the limb movement.

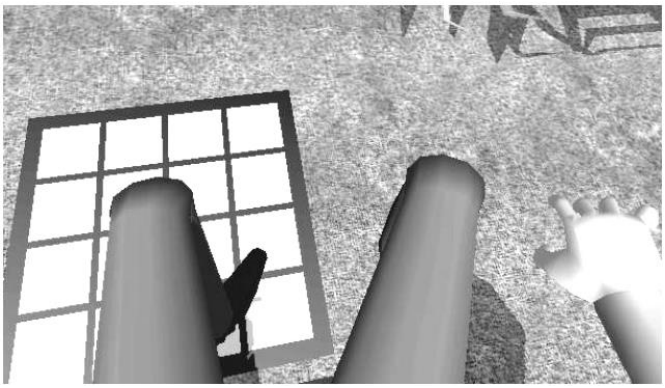

Figure 3.6 VR environment for transposition of the movements of healthy limb [MPCH06].

Although some patients in [MPCH06] reported the relief of the pain in the residual limb after performing the therapy in the VR platform, it still has some limitations.

- Firstly, head oriented into the mirror and ignoring the intact limb are not the key elements of restricting the effect of mirror box. The key problem is that mirror box in mirror therapy cannot arouse the voluntary movements of the stump which directly cause the restriction of its normal activities. Note that this problem exists not only in the mirror therapy for the phantom limb pain, but also for the CRPS patients.
- Secondly, in both mirror therapy and virtual reality therapy system the patient has to associate the proprioception of movement of the healthy limb in the reality with the visual perception of the affected limb in the virtual reality.

As the motor pattern of right hand stored in the corpus striatum is different with the left hand, how does the mismatch between the proprioception in one side of the body and the visual perception of another side influence the patient is not known yet.

Note, that CRPS patients, have a complete limb comparing with the phantom limb pain patients. As previously said, because of the swelling and the pain in the affected joint, they normally have a limited range of movement in the affected limb [Seba11] (Figure 3.7) which discourage them to actively use it in the physical therapy and the daily lift. The patient shown in Figure 3.7 was diagnosed to have CRPS I at the wrist and fingers and started on gabapentin and oxycodone in May 2010. From the picture taken in Oct.2010, her wrist and finger show an evident limited movement range comparing with the beginning of the first report of CRPS.

Figure 3.7 Evolution of CRPS patient hand movement [Seba11].

In the frame of a pilot study, realized in parallel with our work, Won et al. [WTCK15]invited three patients, with pediatric CRPS in unilateral lower limb, to participate into a VR therapy. Patients' head and ankles positions were tracked. They can see a silver-color and undetailed avatar from first person perspective in the HMD (Figure 3.8, the dark human shape is the avatar and the deep one is the subject). Wearing head-mounted display patients were asked to use their limbs to manipulate the avatar in order to hit balloons. Won and his team proposed three conditions during the experiment:

- normal condition; the leg of the avatar has the same movement as the tracked subject leg (Figure 3.8.a),
- extended condition: the avatar's leg has an amplified by *1.5* gain factor movement to the movement of subject's leg (Figure 3.8.b.),
- switched condition: participant's physical leg controls the avatar arm (Figure 3.8.c).

During the experiment the movement distance of patients' affected legs are recorded. The data shown that the total distance performance by the affected limb of patients was improved as more sessions has been performed by them (patients). It was also reported that all patients were remarkably calm while engaging in the experiment and this behavior were different from their behavior during standard physical therapy sessions. From the feedback of the participants, it seems that VR therapy proposed by Won et al. was tolerated by them. However, their experiment cannot confirm the efficacy of using the virtual reality therapy to reduce the pain. In this experiment, effects of using different avatars haven't been tested and the reason for using the silver undetailed avatar was not given either.

The discussion about using human-like avatar or unhuman-like avatar have started after the concept of *uncanny valley* proposed by Mori [Mori70]. The uncanny valley theory is making a hypothesis that human replicas that appear almost, but not exactly, like real human beings elicit feelings of eeriness and revulsion among some observers. When humans observe and interact with a robot, for instance, they have different expectations and movement predictions based on appearance of the robot. Once the behavior of robot does not meet the brain's expectation, human will generate the prediction error. Saygin et al. [SCID12] proved that this error increases when the robot appears like human but doesn't move biologically. That means if robot looks too human, we will expect too much from it. This conclusion may also fit the situation of using avatar in VR environment. But what is the effect or subject's feeling when he/she sees different avatars with similar motion is worth to be tested.

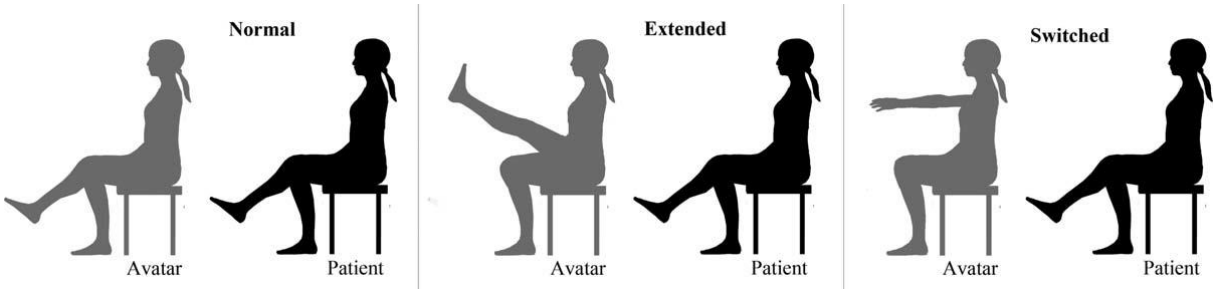

a). b). c).

Figure 3.8 (a). Normal condition; (b). Extended condition; (c). Switched condition [WTCK15].

Thus, based on the existing virtual reality platforms, a part of which were presented here above, we think that applying such platforms in CRPS physical therapy can provide more flexibility for the rehabilitation task design and potential application for CRPS rehabilitation without wearing pain, or with less pain.

3.3.3 Hand tracking devices for movement reconstruction

3.3.3.1 Based on glove system

The early works about hand tracking started from tracking the position and the orientation of whole user's hand. For example, LaViola and Zeleznik [LaZe99] created a Flex and Pinch glove whit eight sensors (Figure 3.9.a). It can recognize the palm flexion angle and pinch movement between thumb and index finger.

Through almost 20 years' development, there are several data gloves available today such as:

- wireless *Cyberglove* (Figure 3.9.b) with twenty-two sensors allowing to measure the rotations of fingers, palm and wrist. The *Cyberglove* was firstly commercialized in 1992.
- *Humanglove* (Figure 3.9.c) is equipped with twenty sensors to measure flexion/extension of five fingers, thumb abduction/adduction, wrist flexion and abduction/adduction.
- *5DT data glove* (Figure 3.9.d) whit one sensor in each finger to measure the overall flexion of the five fingers [DiSD08].
- *Multi-colored* low-cost glove [WaPo09] (Figure 3.9.e) which can estimate the user hand pose.

Note, that for patients with a sensitive or painful skin, there are not available data gloves yet allowing tracking their motions.

(a) (b)

(c) (d)

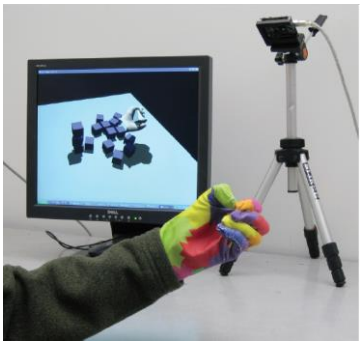

(e)

Figure 3.9 Glove tracking systems: a). Flex and Pinch glove [LaZe99]; b). Cyberglove, Immersion Corporation; c). Humanglove, Image courtesy Humanware; d). 5DT data glove www.5DT.com; e). Multi-colored glove [WaPo09].

3.3.3.2 Based on marker tracking system

Putting makers on fingers and using motion capture system is another way for tracking the motion hand's joint. In order to explore a new way for user to have a direct interaction with the virtual object during a computer-aided sculpting task, Sheng et al. [ShBS06] used *Vicon* motion capture system to track the movements of three fingers attached with markers (Figure 3.10). However, the complexity of using markers and the expensive cost limit its usage in tracking all joints of the hand.

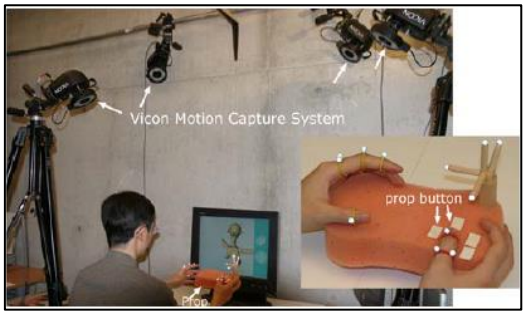

Figure 3.10 Marker tracking System [ShBS06].

3.3.3.3 Based on EMG signals

When subjects move fingers while performing different hand gestures, there exists different combinations of EMG signals for flexors and extensors muscles in the forearm. Saponas et al. [STMB09] proposed to use these signals to reconstruct the user's hand gesture. The basic idea is to use machine learning technology to offline train the artificial neural network which is supposed to automatically recognize the finger gestures by analyzing the EMG signals detected from user's forearm (Figure 3.11.a). The platform, developed by the team of Saponas defines three scenarios (Figure 3.11.b) to perform the finger gesture recognition:

- hand free,
- holding a mug,
- lifting a travel bag.

The recognized finger gesture can be used as different commands. However, this technology is difficult to be applied in fine task of dexterous manipulation. The finger gesture that can be recognized strictly depends on those have been defined before artificial neural network offline training.

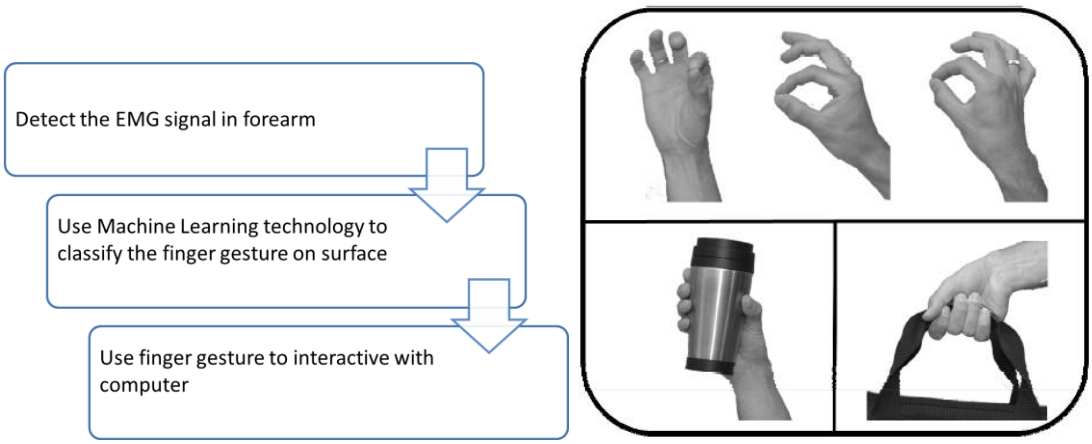

(a) (b)

Figure 3.11 Finger gesture recognition platform in [STMB09]: a). The frame of the platform in; b). Three finger-gesture sets.

3.3.3.4 Based on the image of hand

The hand motion can be also tracked by the image of hand captured by a camera. In this optic, Oikonomidis et al. [OiKA11] applied the *Particle Swarm Optimization method* for processing the image of the hand obtained from Kinect sensor and achieved a robust 3D tracking of hand articulations with a frequency of 15Hz. Note, that this frequency is not smooth enough for a real-time hand tracking application. One year later, Kim et al. [KHIB12] presented a device for reconstructing fingers movement based on infrared camera and laser (Figure 3.12.a). The infrared light-emitting diode (LED) is for uniformly illuminating the user's hand by extracting the 2D position of the fingertip. The infrared laser line projector is used for sampling a single 3D point on each point. Finally, the infrared camera is used in the background subtraction. IMU (inertial measurement unit) provides absolute tri-axis orientation data of the forearm. The flow-chart of the signal processing for reconstructing the finger movement is shown in Figure 3.12.b. The results of the test for reconstructing the five fingers gesture pre-defined are shown in (Figure 3.12.c). Despite its performances, there still exist some limitations for this device.

- The movement reconstruction for the thumb has very large error. It may be because the camera treats the thumb as a regular finger while the thumb has a more complex motion in reality.
- The pinky finger movement reconstruction also has a relatively big error. The reason may be that based on the position of the camera, the pinky finger may be not visible in certain positions.

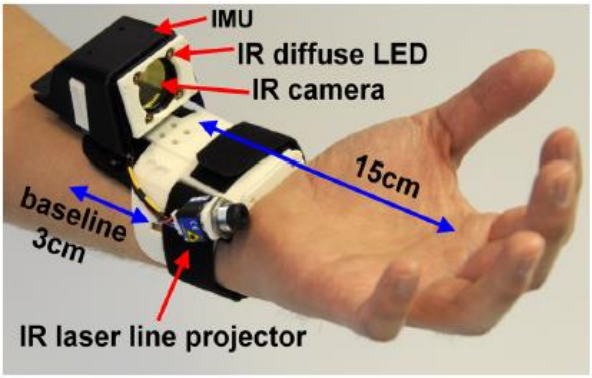

(a)

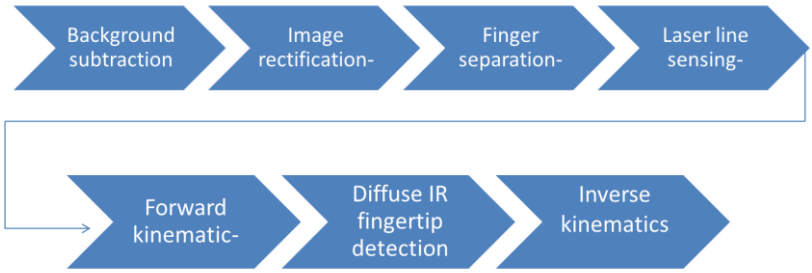

(b)

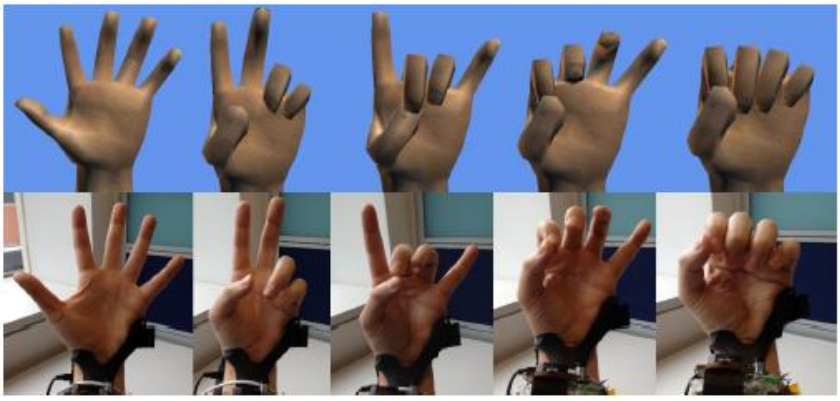

(c)

Figure 3.12 Hand image based tracking device in [KHIB12]: a). Main hardware of the device; b). Signal processing steps for reconstructing the finger movements; c). The finger movement reconstruction results of five finger gesture.

Leap Motion™ is a low-cost device whit two monochromatic infrared cameras and three infrared LEDs allowing to detect a hemispherical area, of about 1 meter, situated above it. The coordinate system of Leap Motion is shown in Figure 3.13.a. The hand is represented by a twenty-six points model as shown in Figure 3.13.b. To each detected point an ID is allocated. Thus, with Leap Motion SDK (software development kit), we consider that it will be easy to

obtain the position of each joint detected on fingers and wrists. The vertical working distance of Leap Motion ranges from *25mm* to *600 mm*.

Note that one of Leap Motion limitations is when some parts of two hands are overlapping or are too close to each other. In the case of overlapping far parts of the hand are disappearing (Figure 3.14, red circle marks the missing part of avatar hand). Another limitation is that if the palm is parallel to ZY plan (see Figure 3.13), the motion tracking is unstable for all the fingers.

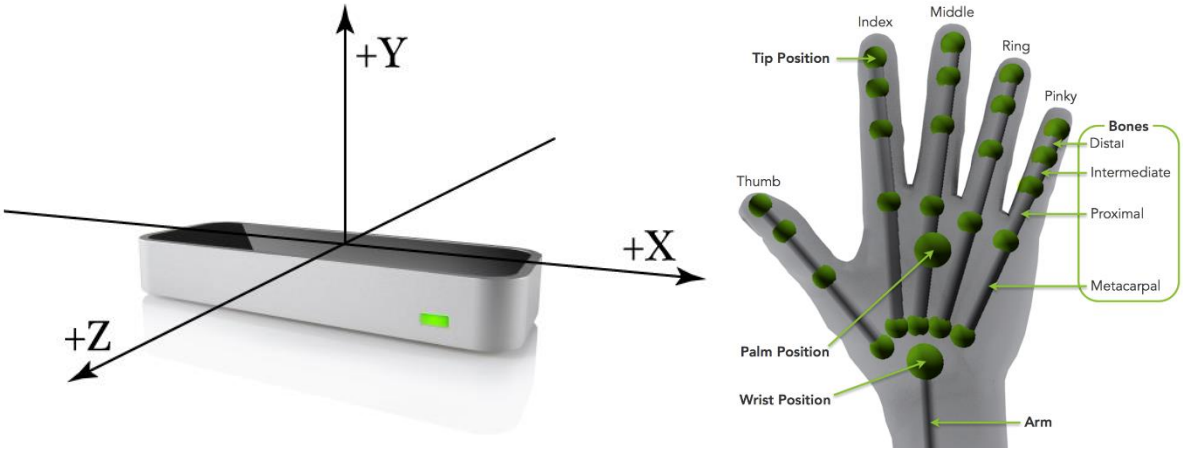

Figure 3.13 Leap Motion: a). Leap Motion coordinate system, [www.leapmotion.com]; b). Leap Motion hand model, [www.leapmotion.com].

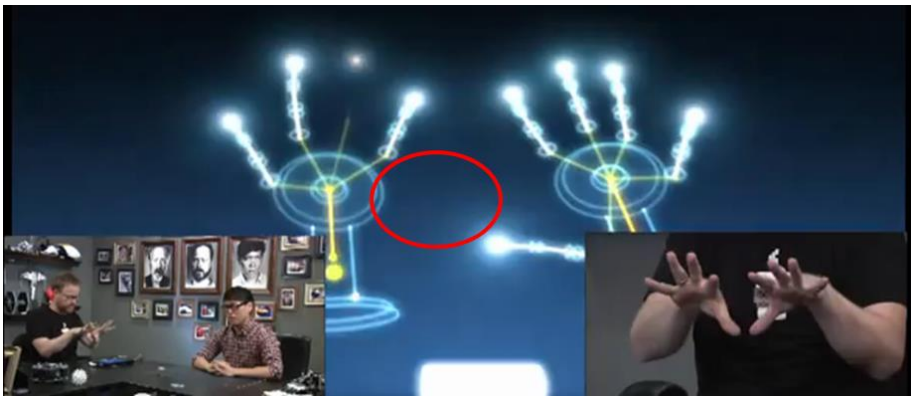

Figure 3.14 Leap motion limits. The left thumb disappears because of overlapping of two thumbs.

3.4 Experimental application

The application used in the performed experiment of this chapter was developed by Charles-Henry Dufetel in the frame of his mater thesis [Dufe15].

In our opinion virtual reality can significantly increase the interest of the patients to actively devote themselves into physical therapy and consequently encourage them to actively use their affected limbs during rehabilitation.

The main purpose for applying virtual reality into CRPS rehabilitations is to encourage them to participate in the physical therapy thanks of its advantages. Namely, the possibility to amplify the patient's movements thus letting them to see some movements that they cannot achieve in the physical world.

3.4.1 Software environment and hardware

As our work focusses on the development of low-cost computer-based application for hand rehabilitation of CRPS patients, hand movement tracking and reconstruction is our first challenge.

Comparing with the available technologies for hand tracking, some of which were shortly presented here above, we consider that Leap Motion does not need the preset figure gesture. However, it has acceptable reconstruction results for tracking the thumb and pinky fingers with a relatively lower cost. Note also, that Leap Motion can work in a relatively high accuracy of movement reconstruction with high frequency. The different applications can be built for Windows, iOS and Android systems. For the design of computer-based application for physical therapy, Unity3D can provide a strong support for the development of the human-computer interaction scenario. Thus, the development of the application is based on Unity3D™ which is a comprehensive software and widely applied for game developments and 3D animations.

In order to realize functions in the application, several scripts have been developed based on C# by Charles-Henry DUFETEL [Dufe15] in the frame of his MS training study. Figure 3.15 presents the communications amongst the scripts. *HandControl* in Leap Motion API is detecting the actual motion of the hand. The detected motion parameters of palm center and fingers are transferred to *PseudoHapticHandController* in *Core* part. Then based on the amplification coefficients *PseudoHapticHand* and *PseudoHapticFinger* the avatar's hand and fingers rotations are calculated and consequently applied on the *HandModel* and *FingerModel* of avatar's hand. The relationship between the actual rotation angle of user hand joint θ_U and the rotation angle of the same joint in avatar hand θ_A is:

$$\theta_A = C_A \cdot \theta_U \tag{3-1}$$

where: C_A is the joint amplification coefficient set in the interface of Unity3D.

Finally, the rotation angles of each joint of fingers and wrist of the avatar hand are recorded by the application.

For C_A <1 the joint movement of avatar's hand is reduced comparing with the physical joint of user's hand. For C_A >1 the joint movement is amplified thus the rendered movement of avatar's hand has a possibility to beyond the normal range of movement of human hand and becomes a weird hand posture.

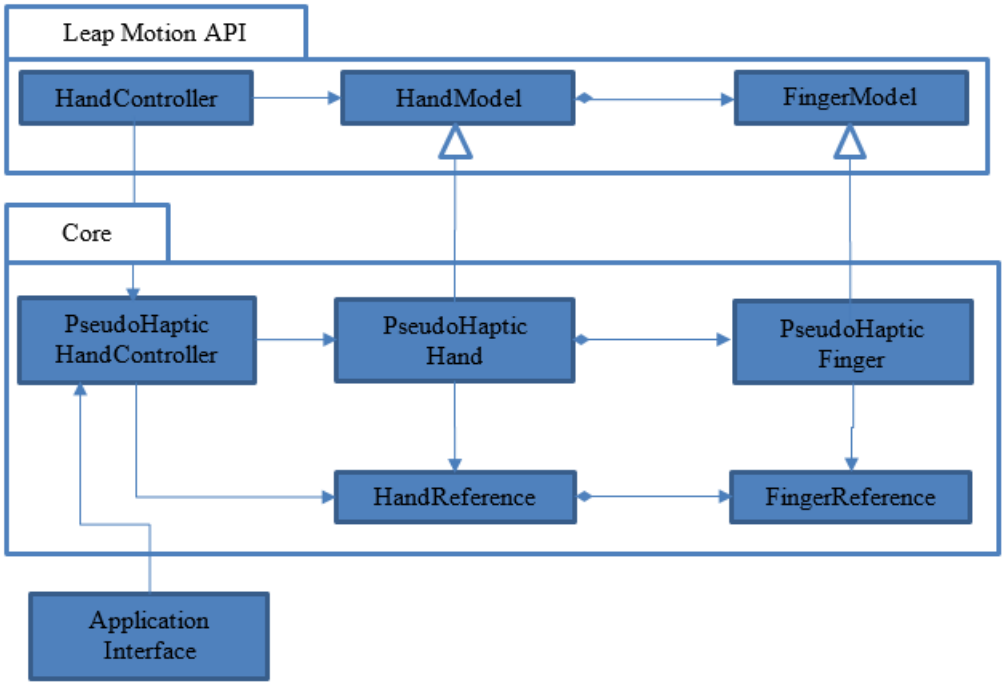

Figure 3.15 Application script diagramme [Dufe15].

A screen view of the interface is presented in Figure 3.16. On the right side is situated the control panel allowing to modify the amplification coefficients of wrist and MCP joint of each finger. On the left side is displayed the application scenario including the avatar hand and background.

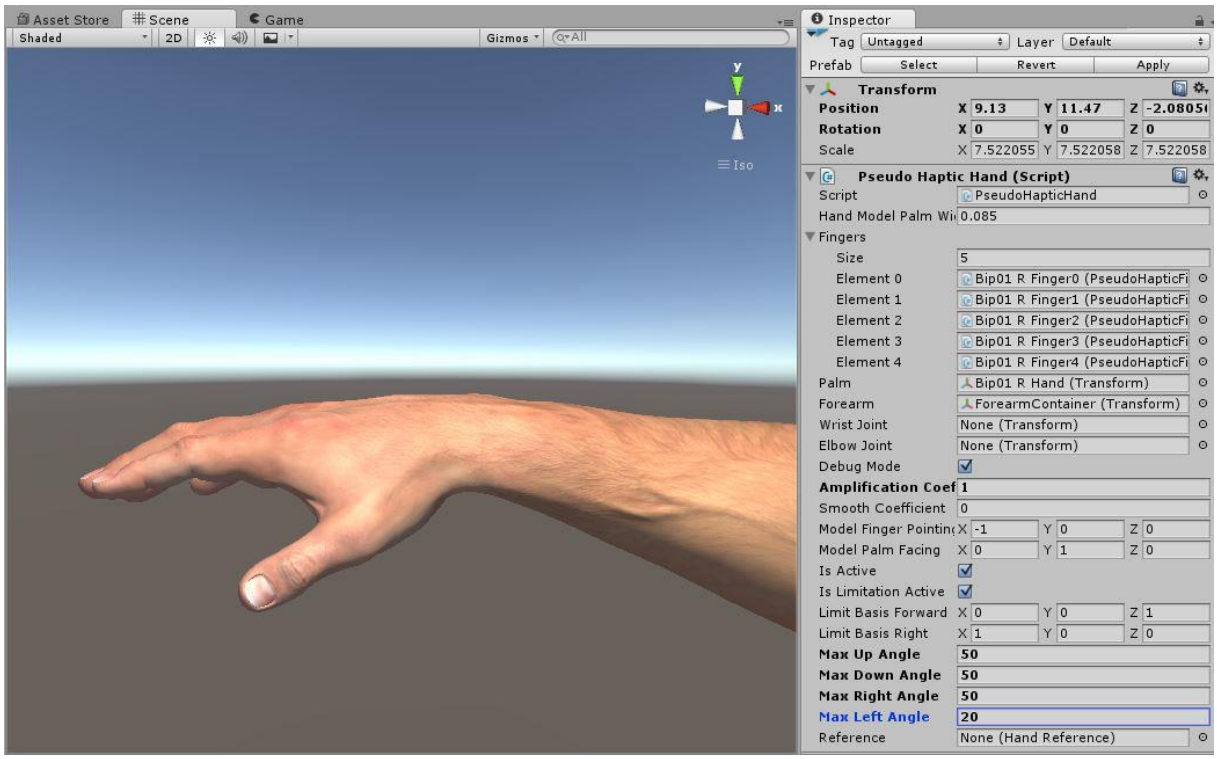

Figure 3.16 Virtual platform interface.

3.4.2 Hand Model

As the Leap Motion is not able to detect the movement of the whole arm, the hand model in the developed application is only limited of forearm. As mentioned in section 3.3.2, subjects have different feelings when they observe different avatars. High-quality human-like avatar hand might let the subject have high expectation on avatar movement. That means decreasing the similarity between the avatar hand and the subject hand might let the subject have more satisfaction on the avatar movement. There are two types of hand models used in the application:

- hand model with normal skin texture (normal hand model) shown in Figure 3.17.a,
- hand model with silver skin texture (silver hand model) shown in Figure 3.17.b.

The normal hand looks more-like human hand while the silver one does not. With those two different models, we can get subjects' feedback about whether the human-like skin or not detailed human skin help them to better associate the avatar motion with their own hand motion. Both the normal and silver hands have left and right models. Note that women hand models are not developed in this stage of the study.

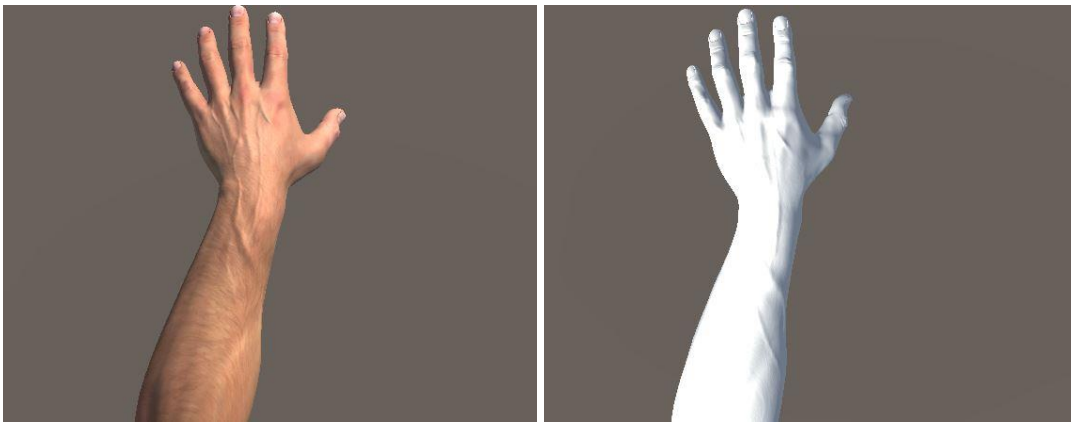

(a) (b)

Figure 3.17 Two types of left hand models: a). with normal skin texture; b). with silver skin texture.

In order to prevent the avatar hand moving beyond the normal range of human hand, limitations for rotation in flexion, extension, abduction and adduction have been imposed to wrist joint and metacarpophalangeal (MCP) of fingers according to [Appl93]. Table 3.1 presents the rotation angles limitations for wrist and MCP of index finger. The limitations for MCP of the other four fingers are the same as the MCP of index finger.

Table 3.1 Rotation angle limitations for the wrist and the MCP of index finger of avatar hand.

	Flexion	Extension	Abduction	Adduction
Wrist	60°	50°	50°	20°
MCP of index finger	20°	90°	20°	20°

3.5 Experiment in CHU Grenoble

3.5.1 Experimental task

The experiment includes two parts:

- I. Using normal hand model to perform the experiment.
- II. Using silver hand model to perform the experiment.

For each part of experiment, subjects were asked to perform two movement tasks:

- *Wrist movement task*: subjects perform flexion and extension around the wrist of right (or left) hand for 10 times with five different amplification coefficients (Figure 3.18. a). All fingers should keep straight at the same plan as the palm.

- *Fingers movement task*: subjects perform flexion and extension around the first finger joint of index, middle, ring and pinky fingers of right (or left) hand for 10 times with the same five amplification coefficients (Figure 3.18.b). The thumb should keep static without rotation for distal interphalangeal joint (DIP) and proximal interphalangeal joint (PIP).

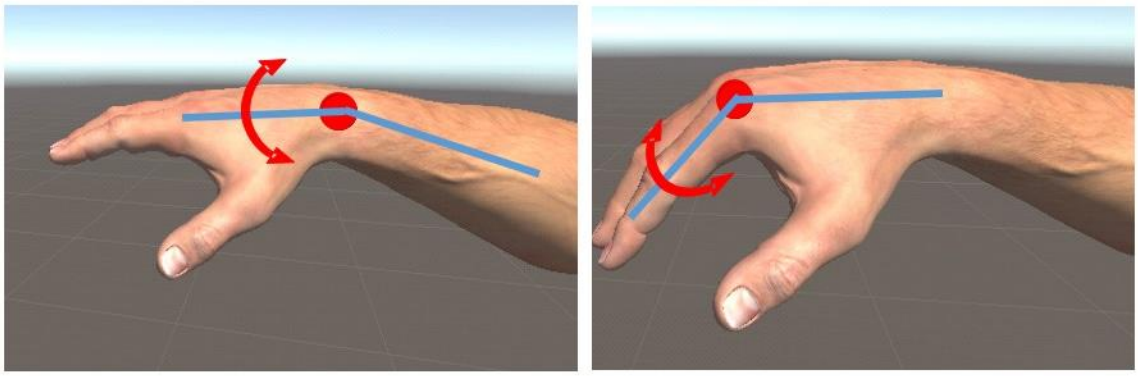

(a) (b)

Figure 3.18 Movement tasks: a) Flexion and extension of wrist; b) Flexion and extension of first finger joint of index, middle, ring and pinky finger.

There are five amplification coefficients from ranging from *0.25* to *4*, namely: *0.25*, *0.5*, *1*, *2* and*4*. When subjects performed the wrist movement task, the C_A of each finger is *1*. When subjects performed the finger movement task, C_A of the wrist is 1. In order to avoid the influence of sequence, the order of five amplification coefficients were randomly applied. They were the same for both wrist movement and finger movement tasks.

3.5.2 Experimental protocol

In order to let the avatar hand and user's actual hand have the same size from the user's point of view, it needs to fix the position of the experiment setup and subject as in Figure 3.19.a. During the experiment subjects (in fixed siting position, their palms situated in about *20 cm* above the Leap Motion) were asked to look at the computer screen while performing the motion tasks (Figure 3.19). A hand supporter was used in order to support subject's hand in a fixed position.

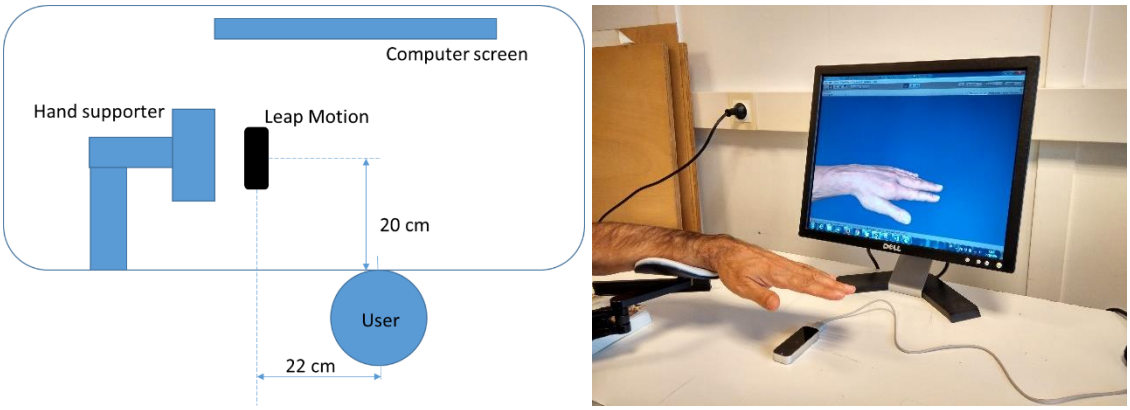

(a) (b)

Figure 3.19 Experiment setup: a). top view. The user was located 20 cm in front and 22 cm near the hand support; b). scene.

In order to evaluate subject's feeling, especially the pain, they were asked to fill in a questionnaire before and after the experiment while using normal and silver hand models, (see Appendix 3). The pain assessment scale utilized in here is Wong-Baker FACES Pain Rating Scale [HoWW01]. The experimental process consists in:

1. Answering the part of questionnaire '*Before experiment'*
2. Using the hand model with normal skin texture to perform the experiment. Asking the subject to perform the wrist movement under different amplification coefficients and recording:

   - the wrist's rotation angles,

   - fingers' rotation angles.
3. Answering the part of questionnaire '*After experiment I'*.
4. Using the hand model with silver skin to perform the experiment. All operations are the same as in step 2.
5. Answering the part of questionnaire '*After the experiment II*'.

In each trail, subject performs one movement task with one amplification coefficient by using one hand model. As there are two types of hand model, two movement tasks and five amplification coefficients, totally each subject had to perform twenty trails.

3.5.3 Participants

Five subjects (one healthy volunteer, two healthy physical therapists, one healthy hospital practitioner and one patient), aged from *31* to *61* participated in the experiments performed at CHU Grenoble. The patient had undergone a surgery on the left hand and is currently accepting the kinesiological training. Except the patient, none of subjects reported hand motor function problems. All subjects, except one physical therapist, declared not having previous experience on using virtual reality.

3.5.4 Data analysis

The range of movement of the wrist and the MCP joint of index finger of avatar hand in flexion and extension plan were calculated for all the subjects. Figure 3.20 shows the raw data of the rotation angles recorded for the avatar's wrist. The peak and valley was detected by using the *findpeaks* function of MATLAB. To avoid the detection of two closed peaks, the minimal sample number between two peaks or valley was set as:

$$D_{min} = \frac{L_D}{n} \tag{3-2}$$

where:

- L_D is the length of the recorded data, equal with the recording time multiplied by the sampling frequency (*50 Hz*).
- n is the total number for flexion and extension movements (here *n=10*).

The range of movement for the wrist of the avatar hand during the wrist movement task and the range of movement of MCP of index finger of the avatar hand during the finger movement task were calculated as well. The ranges of movement for both wrist and MCP of fingers are calculated as:

$$ROM_i = \theta_{pi} + |\theta_{si}| \qquad (i = 1, 2, \dots, 10) \tag{3-3}$$

where: - θ_p is the peak of the recorded angle,

- θ_s is the valley value of the record angle,

- i is the number of flexions or extensions.

The range of movement of the joint for one trial is:

$$\overline{ROM} = \sum_{i=1}^{n} ROM_i \tag{3-4}$$

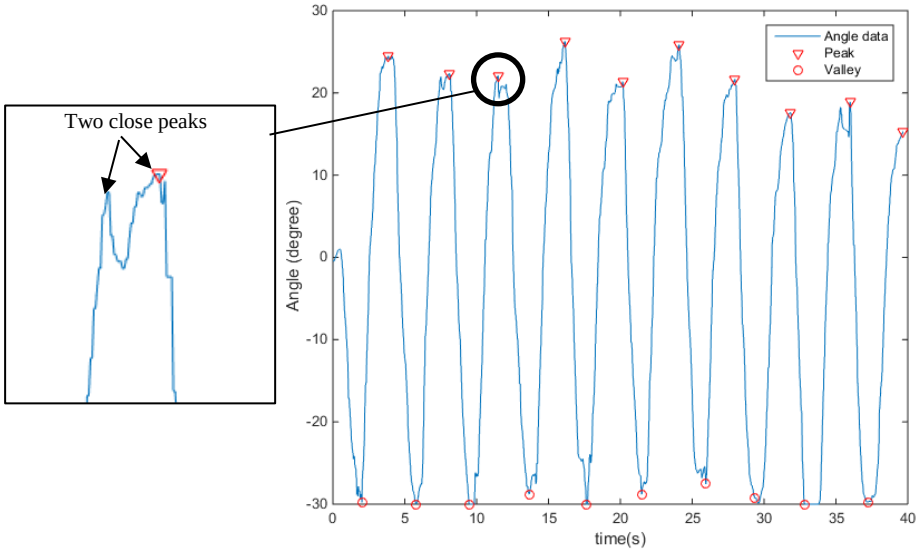

Figure 3.20 Raw signal of angle rotation detected on the wrist with marked peak and valley for one subject as example.

When the amplification coefficient of each joint is *1*, the motion of avatar hand is the same as subject's hand. In this condition, the raw signal of angle rotation recoded by the application have been verified with goniometer.

3.6 Results

3.6.1 Range of movement

As the physical therapists and the hospital practitioner are healthy subjects and the number of subjects are not enough to perform a statistical analysis, only the data on healthy subject and the patient were presented for individual level quantitative analysis and qualitative comparison.

Figure 3.21 shows the range of movement of wrist (healthy subject and the patient) during performing wrist movement task with different amplification coefficients on the avatar hand. From Figure 3.21.a is seen that the wrist rotation angle of avatar hand controlled by the healthy subject ranges from *29.63*° to *110*° when the amplification coefficient increased from *0.25* to *2*, for the normal hand model. The wrist of the silver hand model controlled by healthy subject with a range of movement increased from *26.6*° to *110*°. No obvious difference has been observed between the data of normal hand avatar and silver hand avatar during the wrist movement. That means that the healthy subject had the similar range of movement of wrist for the two hand models.

Figure 3.21.b shows that following the increase of amplification coefficient, avatar hand movement controlled by the patient ranges from *20.20*° to *110*° with normal hand model and from *21.48*° to *110*° with silver hand model.

The avatar hand controlled by both healthy subject and patient arrived at the limitation of flexion and extension when the amplification coefficient was *2*.

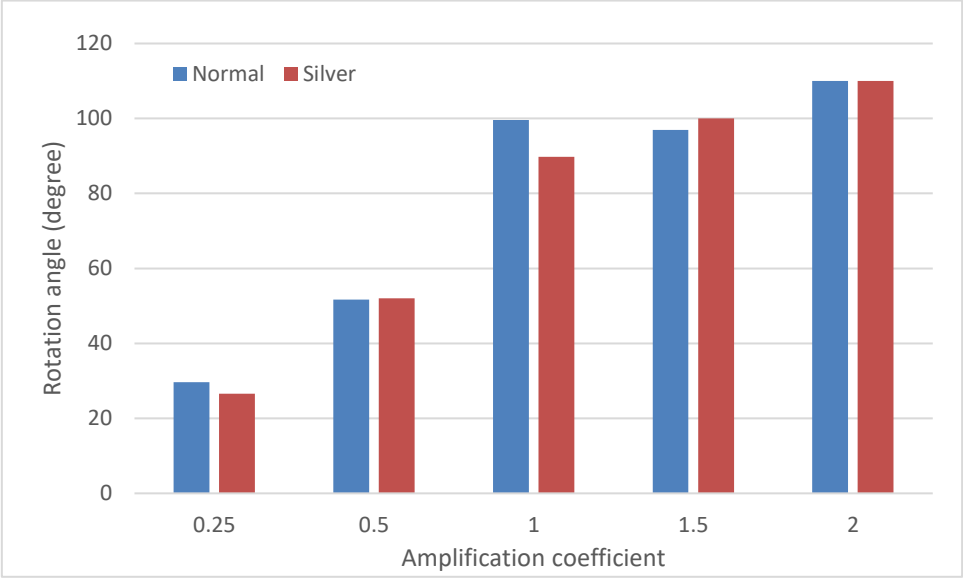

(a)

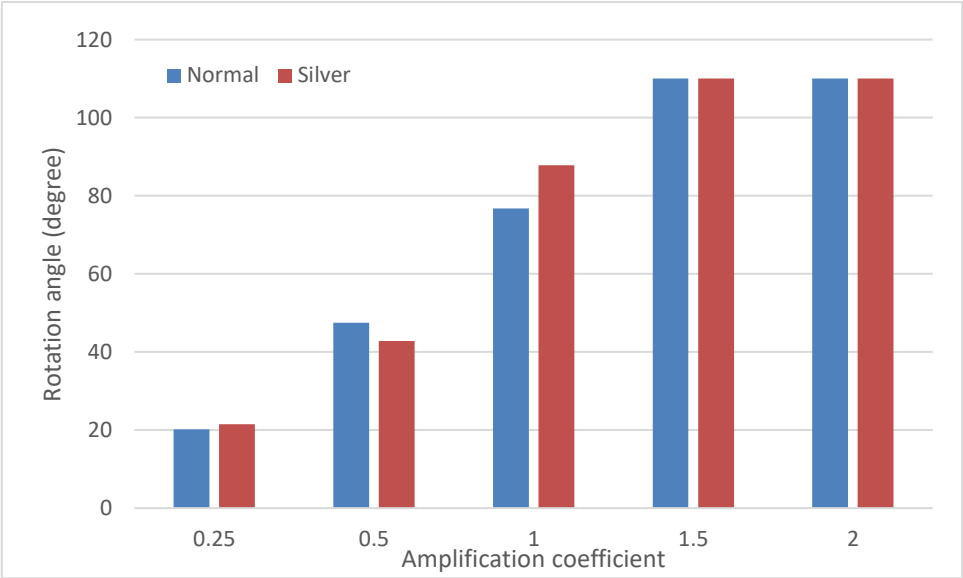

(b)

Figure 3.21 Ranges of movement of subjects' wrist: a). Healthy subject; b). Patient.

Figure 3.22 shows the range of movement of the MCP of index finger of avatar hand during finger movement. No matter the healthy subject or the patient, the range of movement

of MCP of index finger increases when the amplification coefficient increases which is similar with the wrist movement. Avatar hand controlled by both patient and healthy subject arrived at the limitation of flexion and extension of MCP of index finger when the amplification coefficient was *2*.

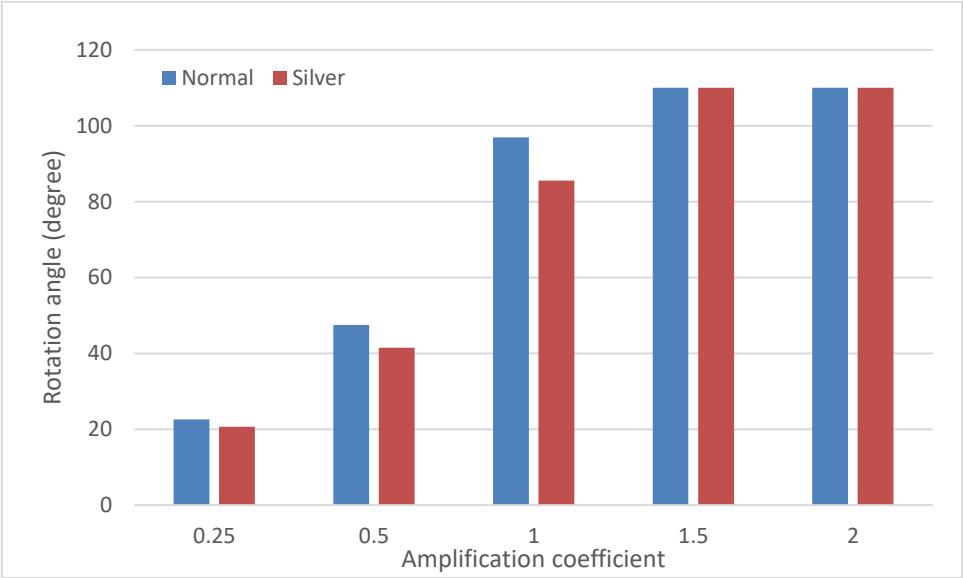

(a)

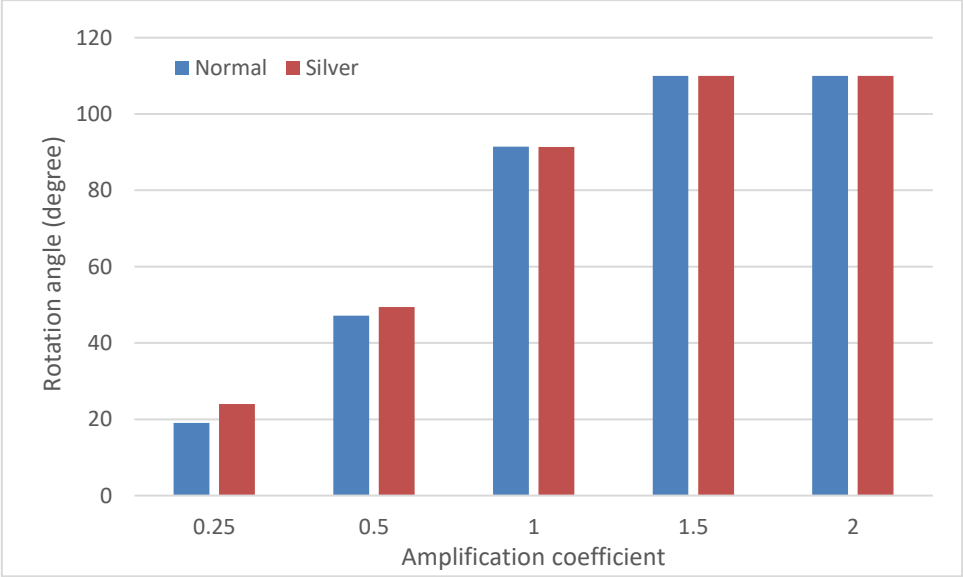

(b)

Figure 3.22 Ranges of movement of subjects' MCP of index finger: a). Healthy subject; b). Patient.

3.6.2 Pain estimation and feelings of participants

All subjects have evaluated their pain states before the experiment, and after experiment I and experiment II. As presented in Table 3.2, there is no change between pain states before and after

the experiments which means that no one had uncomfortable feeling during the experiment. For the only patient among subjects, he has light pain in the hand.

Table 3.2 Pain evaluation results before and during experiments.

	Before experiment	During experiment I	During experiment II
Healthy subject	No Hurt	No Hurt	No Hurt
Patient	Light pain	Light pain	Light pain
Physical therapist 1	No Hurt	No Hurt	No Hurt
Physical therapist 2	No Hurt	No Hurt	No Hurt
Hospital practitioner	No Hurt	No Hurt	No Hurt

From Table 3.3, three subjects thought that the normal hand model makes them more uncomfortable. It means that they found the avatar undetailed silver hand better.

Table 3.3 Subject's feeling about uncomfortable hand avatar.

	Normal hand avatar	Silver hand avatar
Healthy subject		√
Patient	The same	The same
Physical therapist 1	√	
Physical therapist 2	√	
Hospital practitioner	√	

Table 3.4 presents subjects' suggestions for improving the application. The suggestions focus on how to increase the identity of avatar hand. The hospital practitioner and the physical therapists focus mostly on increasing the robustness of the application and applicable conditions for future applications. However, due to some limitations of Leap Motion device, as its robustness, it may limit its medical application in short time period.

Table 3.4 Subjects' suggestions for improving the application.

Subject	Suggestions
Healthy subject	That the movements on the screen are more in tune with the real movement of the hand.
Patient	1. There exist some conflicts between the proprioceptive feedback about the hand position and the visual feedback from the avatar hand motion. 2. To cover the hand in order to not see it will be better; 3. To have a scenario closer to the real environment (for example add a table inside a kitchen room, desk in an office…) 4. To put a specific marker, such as tattoo drawing, on both user's and avatar hands to increase user's identification of avatar hand.

Physical therapist 1	1. The applicable situations for different amplification coefficients: - Amplification coefficient bigger than 1: Maintenance of the motor cortex of patient whose symptoms are restricted movements because of the damaged motor organs such as: tendons, section, stents; - Amplification coefficient less than 1: For patients with higher stiffness which results in a decreased range of movement; 2. Coupling the device to a detection of activity such as: - muscular activity (EMG signal), - motor cortex (EEG (electroencephalogram) signal). 3. Raises the question of rings, scars.
Physical therapist 2	1. To fix the shoulder and the elbow in order to suppress fluctuation of the forearm. 2. To improve the bending movement which is more disturbed while approaching the Leap Motion. 3. With the amplification of the movement, we could imagine allow patients to improve the mobility of their fingers and wrist. 4. Less applications for amplitude's rehabilitation. Can be for people who are obliged to move their fingers in a precise and limited angulation (Ex. Expander Rehabilitation, Movement meta- Corpo phalangeal *0-30*°). There are other constraints as passive return in extension. 5. Interest to add objects at virtual hand: we are more in functional training, in the field of occupational therapy, while without object, we are on the analytical motorization (this is a plus for physiotherapy).
Hospital practitioner	Fixing the forearm more stably on the hand support.

3.7 Discussion

From the results of avatar hand movements, no matter for the wrist or the MCP of fingers, the range of rendered movements increases when the amplification coefficient increases. This means that the application has successfully created a rendered hand motion which changes following the change of amplification coefficients.

As there are rotation limits for rendered motion of the avatar hand joints, it is possible to have an unused zone where the user's hand is still moving while the avatar hand stops. For example, if the amplification coefficient for the wrist is 2, the avatar hand will stop when the user's hand performs flexion more than*30*°. Thus, for user's wrist the zone between *30*° and *60*° flexion is an unused zone (see Figure 3.23).

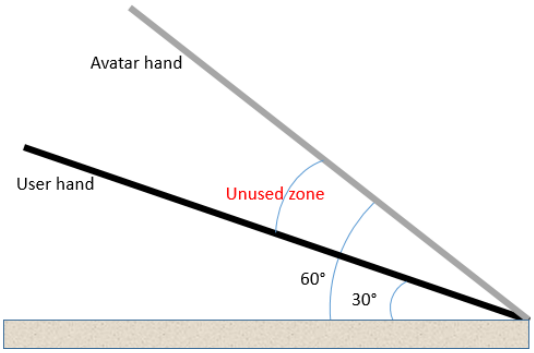

Figure 3.23 Unused zone for user.

In order to avoid the unused zone, the amplification coefficient of each joint of the avatar hand should depend on corresponding user's joint range movement. Assuming β_j is the range of movement of joint j of avatar hand, then the constrain is:

$$C_{Aj} \times \beta_{Sj} \leq \beta_j \Rightarrow C_{Aj} \leq \frac{\beta_j}{\beta_{Sj}} \tag{3-5}$$

where: C_{Aj} is the amplification coefficient of joint j,

β_{Sj} is the user's range of movement of joint j.

From equation (3-5), is seen that for given β_j a smaller β_{Sj} allows bigger range of C_{Aj}. This result indicates that coefficient superior than 1 may be used just at the beginning of the rehabilitation process when patient cannot move his limb with a great amplitude, while this coefficient should decrease as the range of restored movement increases.

Concerning the pain evaluation, the results shown that subjects did not feel any pain during the experiments, no matter the hand model or amplification coefficient are. This proves that the application can be tolerated by the patients and consequently may be potentially useful for rehabilitation.

More than half of subjects felt that using the normal hand avatar is less comfortable, despite its human hand details (hair, skin color, blood vessel, …). From the subjects' suggestion, the reason might be that more details that we provide on the avatar hand, more evidences are available for subject to deny similarity between his own hand and the avatar hand. From this aspect, the silver hand obviously provides less characteristics and subjects focus more on the movement of the avatar hand instead of appearance details. This conclusion is in agreement with the uncanny valley and the conclusion presented by Saygin et al. in [SCID12]. As the silver hand model looks less human, subjects' have less expectation on the avatar movement.

Note, that different from the mirror therapy, the patient's hand is not hidden with a box. Previously performed test shown that covering the hand by a box changes the light environment around the hand which influences the operation of Leap Motion.

Two physical therapists, specialized in hand movement reconstruction, have shown their interests for potential application when the movement of hand is amplified. They think that this can encourage patients to perform large movements in rehabilitation activities. When the amplification coefficient is less than *1*, one physical therapist thinks that the proposed environment can be useful to force patients to perform bigger ranges of movements when he thinks it is necessary to accelerate the training process while the patients do not want to.

3.8 Conclusion

In this chapter CRPS with its symptoms and available treatments were introduced. The most important thing after the medical treatment of CRPS patients is that they are encouraged to actively use their affected limbs once they can perform the physical therapy.

However, for participating in the physical therapy, the biggest obstacle for CRPS patients is the limited range of movement of the affected joints resulting from swelling, abnormal tissue growth or pain. Mirror therapy efficacy on releasing the pain of CRPS has been proved (see the reference cited in section 3.2.2.1), however the problem is that patients have to ignore the healthy limb or at least have a healthy limb which can be reflected on the mirror.

For humans, the visual feedback can influence the motor neuron excitability or directly the motor behavior because of mirror neuron system. In order to provide more flexibility and increase the functionalities in physical therapy scenario, virtual reality environment has been used in development of computer-based physical therapy application for CRPS. Several researchers have utilized the virtual reality for creating a rendered motion different from the real motion of patient's affected limb. The positive feedback from the patients implies that is meaningful to explore deeper on how to create a virtual reality or computer-based scenario which can better encourage CRPS patients to actively use their affected limbs.

Thus, an application based on Leap Motion for CRPS rehabilitation has been developed. With this application, the user hand motion can be tracked and reconstructed on avatar hand. The relationship between user's physical hand motion and rendered motion of avatar hand can be modified also. In order to test the usage availability of this application for CRPS patients, an experiment has been performed as a pilot study at Grenoble CHU. In the experiment, two types

of hand models, normal and silver hand model, have been controlled by subjects to perform the wrist and finger movement while the rotated joints of avatar hand were either amplified or decreased. Even if lacking of sufficient number of subject, three of them indicated that the silver hand model is more comfortable to use.

The range of movement of the avatar changed following different amplification coefficients, no matter for patient or healthy subjects. That means that we have successfully provided a rendered hand motion. However, the choice of amplification coefficients depends on the actual range of movement of user in order to avoid the unused zone of avatar hand.

The developed application did not worse subjects' pain during the experiments which proves its potential application for CRPS patients' rehabilitation. As the no evident pain in the patient among the tested subjects, how the CRPS patient will react to the application need to be verified in the future. With this application, patient can perform the rehabilitation task in his/her home, and the recorded motion data can be sent back to the practitioner at the hospital. This is helpful for decentralizing the patient treatment from the hospital and realizing the remote monitoring rehabilitation which can save medical resource and time. However, before definitive conclusions can be drawn, further studies need to be performed with more subjects and with different pathologies.

General conclusion

Some limitations of the available techniques and unknown physiological aspects for VR-based concepts and applications stimulated this research on understanding and evaluating the effect of simulated haptic feedback on the human perception and behavior in general, and its application for CRPS rehabilitation in particular. Different existing research methods and available tools in the field of fatigue evaluation in VR-based operations, and the effect of VR-based concept in haptic simulation were presented. Some existing classical and computer-based methods for CRPS rehabilitation are also presented. We pointed out that a simple method for evaluation of muscle fatigue levels associated with disassembly operations is needed for disassembly sequence evaluation during product design phase. There exist two main problems in this field:

- One is the evaluation model using parameters obtained in a subjective way without corresponding physical considerations of the operator.
- The other one is the evaluation method requiring some physiological parameters with poor availability.

Stiffness simulation, being one of the key aspect in pseudo-haptics, has attracted some researchers to provided prospects on better understanding its effect on human perception and consequently human behavior. As we are aware there is no work which analyzes the pseudo-haptic from a biomechanical point of view. For the CRPS rehabilitation, VR has been applied to create more possibilities of manipulating the visual feedback and overcome some drawback of the existing classical physical therapy methods.

We think that a low-cost device for hand tracking and movement reconstruction with acceptable accuracy is ideal for decentralizing the CRPS hand rehabilitation from hospital. Thus, we have led a biomechanical analysis of different aspects of Virtual Reality and its potential application for rehabilitation. Thus, the aim of our work was to contribute in better understanding the human perception and behavior under the influence of VR-based concepts, and to apply our findings in further studies into the design of low-cost computer-based solution for CRPS hand rehabilitation.

In Part I, entitled “Biomechanical analysis of haptic-based concepts and tasks”, we investigated the evaluation of operator’s muscle fatigue in disassembly operation simulation with haptic device in VR environment, and studied a stiffness discrimination task and its influence on human perception and behavior.

First, we focused on muscle fatigue evaluation of the operator while performing disassembly task in VR environment with using haptic device. In here a new method for disassembly task evaluation which aims at using the expenditure volume of metabolic energy to quantify fatiguing disassembly tasks was proposed. The method is based upon four hypothesizes proved by experimental tests. The proposed model was employed to calculate the associated fatigue levels while performing different tasks. For this purpose, the RMS value of EMG signals were recorded and analyzed. In order to verify the validity of the proposed method, series of experiments, consisting in performing basic operations with haptic device in VR environment, were performed. The theoretical results were compared with the experimental ones. The agreement between them indicated that the proposed method is pertinent for estimating the level of peripheral fatigue induced while performing disassembly tasks in VR environment. As a conclusion, the use of the current method should be extended to different VR tasks when fatigue evaluation is required.

Secondly, we focused on the investigation for better understand the pseudo-haptic effect on human perception and motor behavior through a stiffness discrimination experiment between a real spring and a virtual one (pseudo-haptic spring). The PSE point analysis confirmed the underestimation of the stiffness of virtual spring which was firstly evoked in [LCKR00]. Hand pressing force, some kinematic parameters of pressing movement, EMG signals on flexor and extensor, and muscle co-activation during pressing the real and virtual springs have been analyzed and compared. One major and novel result concerns the force behavior aspect, since both real and virtual springs have increased the subjects’ pressing force with the increase of the stiffness, with different rates. Corresponding to the same stiffness, the force on virtual spring is higher than on the real, but the gap decreases following the increase of the stiffness. During pressing on real spring, which is a dynamic task, since the fingertip moves, both the maximal pressing velocity and the muscle co-activation decrease following the increase of the stiffness. This phenomenon was also found while pressing the virtual spring which means that pseudo-haptic feedback can induce the muscle co-activation as in a dynamic task for finger even if the fingertip is static. These results are strong enough to indicate that pseudo-haptic effect is a tool that makes possible to manipulate pressing force and co-activation in the involved joints.

Finally, in Part II, entitled “Application in CRPS rehabilitation”, CRPS disease and the existing challenges in its physical therapy have been introduced. In order to help patients to improve performance in the rehabilitation task, a low-cost application based on Leap Motion device, has been introduced and applied in a pilot study at CHU Grenoble to test its availability of usage.

This part of the study focusses on manipulating the visual feedback in the VR-based application to encourage CRPS patients to actively participate in physical therapy and better perform rehabilitation. For this purpose, as previously said, an application based on Leap Motion for CRPS rehabilitation has been developed. With this application, the relationship between user’s physical hand motion and rendered motion of avatar hand can be modified. In order to test the potential usage of this application for CRPS patients, experiments have been performed at CHU of Grenoble. The results shown that the range of movement of the avatar has changed following the applied amplification coefficients. This proved that the application successfully provides a rendered hand motion which changes following the values of the amplification coefficients. Through evaluating subjects’ pain during performing the experiment, it is shown that the application is safe to be use for CRPS patients in rehabilitation.

Future work

Our research contributed to better understand the influence of haptic-based concepts and applications on human perception and behavior. However, there are still some improvements which can be considered in short time extended study:

- Concerning the fatigue evaluation, its levels were calculated/estimated knowing the disassembly path of each component. One of the parameters appearing in the proposed mechanical model, angle θ_1 (between the forearm and the horizontal frame) had to be measured. In future work, instead of using Kinect to measure this angle, a geometrical model for its calculation should be built and after then integrated into the proposed mechanical model.
- Concerning the pseudo-haptic it has been proved that through manipulating the visual feedback, different motor behaviors of user including pressing force and co-activation in the involved joints can be induced. As the performed experiments are only in the stiffness discrimination, this limits the generation about the conclusions obtained in pseudo-haptics. There are many physical properties and parameters that have been simulated by using pseudo-haptic feedback, such as: friction, texture, shape, weight, force filed, torque etc. How the pseudo-haptic feedback influence on the human behavior during the simulation of those physical properties and parameters are unknown yet which can be investigated in the future. Moreover, before drawing conclusions about co-activation changes with pseudo-haptic feedback, further studies should be conducted on a simpler biomechanical joint, as the elbow joint which has less muscles involved in its rotations.
- Concerning the CRPS rehabilitation, all the subjects involved in the performed experiments expressed that the hand movement of the avatar was not always stable. We suppose that this is due may be of the accuracy or some limitations of Leap Motion device. In future, the improvement of the hand tracking and reconstruction with using other existing low-cost devices can be done in order to render avatar hand movement more robust. User's identity may be also improved by using more personalized avatar hand model in the application. For instance, 3D scanner model may be used to rapidly generate a customized avatar hand. Note, that at this stage of the study, it is not known yet whether such a model or an undetailed one is better for CRPS patients. We have

used two hand models in the application. However, lacking of sufficient number of patients, and relative investigation on which model has better effect on improving patient motor functions and reducing the pain, makes these questions still open for future work.

Let us recall, that there are two main types of rehabilitations: kinesiological and occupational. The first one focuses more on the basic motor function recover while the second one focuses more on motor function rehabilitation in occupational scenario.

- We believe that the possibilities offered by the virtual reality environments with their rich sources of information and high level of innovative interaction may augment the patients' interest to performing simple and repeated rehabilitation task. Thus, comparing with kinesiology rehabilitation training, the occupational rehabilitation training may provide scenarios which are closer to the daily or professional life. A disassembly task simulation, for instance, in virtual reality can be used as a rehabilitation task. Instead of traditional rehabilitation tasks which are often annoying and repeatable, a disassembly operation can give the patient a kind of feeling of great achievement which can enormously encourage him/her to perform the rehabilitation task. Due to the motor abnormal function of CRPS patients and chronic pain, their fatigue endurance is bigger or lower than the healthy people. This requires to consider the fatigue factor in the design and usage of the rehabilitation task according to the fatigue endurance capacity of each patient. We consider that the method proposed here for evaluating the fatigue levels associated with different disassembly tasks may allow the physical therapist to choose rehabilitation task for specific patient in order to consider patient's fatigue tolerant capacities.
- For the CRPS patients, the abnormal co-contraction, as the deficient activation, is resulting in their abnormal limb posture, as mentioned in [BPMB13]. In order to deal with the loss voluntary modulation of muscle activity or deficient muscle co-activation of CRPS patients, there is a chance for us to try to manipulate the relationship between the actual motion and rendered motion in virtual reality. It will induce a different motor strategy to compensate the lost voluntary of muscle activity, especially in kinesiological therapy which is principally aiming at helping the patients to recover the basic movement functions of their affected limbs.
- The developed application for CRPS patients' rehabilitation based on the Leap Motion can be useful in kinesiological therapy. When the rendered motion (visual feedback) is

bigger than the real motion of patient's hand, it can encourage him/her to overcome the limited range of movement. However, the choice of amplification coefficients depends on the actual range of movement of user in order to avoid the unused zone. On the other hand, when the rendered motion is smaller than the motion of patient's hand, it can induce the patient to move in a bigger range in order to accelerate the rehabilitation process.

References

[AGLN09] ABATE F.A. ; GUIDA M. ; LEONCINI P. ; NAPPI M. ; RICCIARDI S.: A haptic-based approach to virtual training for aerospace industry. In: *Journal of Visual Languages & Computing*, *Multimodal Interaction through Haptic FeedbackMultimodal Interaction through Haptic Feedback*. Bd. 20 (2009), Nr. 5, pp. 318–325

[AlCa10] ALEOTTI J. ; CASELLI S.: Physics-based virtual reality for task learning and intelligent disassembly planning. In: *Virtual Reality* Bd. 15 (2010), Nr. 1, pp. 41–54

[AMMA11] ALEXANDER G. MUNTS ; MUGGE W. ; MEURS S.T. ; ALFRED C. S. ; MARINUS J. ; MOSELEY G. L. ; VAN DER HELM F.C.T ; VAN DER HILTEN J. J.: Fixed dystonia in complex regional pain syndrome: a descriptive and computational modeling approach. In: *BMC neurology* Bd. 11 (2011), Nr. 1, pp. 1

[Appl93] APPLETON B.: Stretching and flexibility. In: *Retrieved on May* Bd. 31 (1993), pp. 2013

[BCCF01] BALDISSERA F. ; CAVALLARI P. ; CRAIGHERO L. ; FADIGA L.: Modulation of spinal excitability during observation of hand actions in humans. In: *The European Journal of Neuroscience* Bd. 13 (2001), Nr. 1, pp. 190–194. — PMID: 11135017

[BoGu14] BOYAS S. ; GUEVEL A. ; NAIK R.G. (Hrsg.): *Endurance time prediction using electromyography, in Applications, Challenges, and Advancements in Electromyography Signal Processing:* Bd. v. 219-233 : IGI Global, 2014 — ISBN 978-1-4666-6090-8

[BPMB13] BANK J.M.P. ; PEPER C. L. E. ; MARINUS J. ; BEEK J.P. ; VAN HILTEN J.J.: Deficient muscle activation in patients with Complex Regional Pain Syndrome and abnormal hand postures: an electromyographic evaluation. In: *Clinical Neurophysiology: Official Journal of the International Federation of Clinical Neurophysiology* Bd. 124 (2013), Nr. 10, pp. 2025–2035. — PMID: 23692976

[BrKP03] BRAIN R. U. ; KARIN G.M. G. ; PHILIP E. M.: A Model of Human Muscle Energy Expenditure. In: *Computer Methods in Biomechanics and Biomedical Engineering* Bd. 6 (2003), Nr. 2, pp. 99–111

[BSHG11] BISI M.C. ; STAGNI R. ; HOUDIJK H. ; GNUDI G.: An EMG-driven model applied for predicting metabolic energy consumption during movement. In: *Journal of Electromyography and Kinesiology: Official Journal of the International Society of Electrophysiological Kinesiology* Bd. 21 (2011), Nr. 6, pp. 1074–1080. — PMID: 21840224

[BuCo03] BURDEA C. G. ; COIFFET P.: *Virtual Reality Technology* : John Wiley & Sons, 2003. — Google-Books-ID: 0xWgPZbcz4AC — ISBN 978-0-471-36089-6

[CDND09] CACCHIO A. ; DE BLASIS E. ; NECOZIONE S. ; DI ORIO F. ; SANTILLI V.: Mirror therapy for chronic complex regional pain syndrome type 1 and stroke. In: *New England Journal of Medicine* Bd. 361 (2009), Nr. 6, pp. 634–636

[CDPS07] CAPPELLI F. ; DELOGU M. ; PIERINI M. ; SCHIAVONE F.: Design for disassembly: a

methodology for identifying the optimal disassembly sequence. In: *Journal of Engineering Design* Bd. 18 (2007), Nr. 6, pp. 563–575

[CLSM04] CRISON F. ; LÉCUYER A. ; SAVARY A. ; MELLET-D'HUART D. ; BURKHARDT J.-M. ; JEAN-LOUIS DAUTIN: The use of haptic and pseudo-haptic feedback for the technical training of milling. In: *EuroHaptics Conference poster, Munich, Germany*, 2004

[CMCQ16] CHEN J. ; MITROUCHEV P. ; COQUILLART S. ; QUAINE F.: Disassembly task evaluation by muscle fatigue estimation in a virtual reality environment. In: *The International Journal of Advanced Manufacturing Technology* (2016), pp. 1–11

[CWCM07] CHAN L.B. ; WITT R. ; CHARROW P. A. ; MAGEE A. ; HOWARD R. ; PASQUINA F. P. ; HEILMAN M.K. ; TSAO W.J.: Mirror therapy for phantom limb pain. In: *New England Journal of Medicine* Bd. 357 (2007), Nr. 21, pp. 2206–2207

[DDHD07] DE MOS M. ; DE BRUIJN A. G.J. ; HUYGEN F. J.P.M. ; DIELEMAN J. P. ; STRICKER C.B.H. ; STURKENBOOM M.C.J.M.: The incidence of complex regional pain syndrome: A population-based study: In: *Pain* Bd. 129 (2007), Nr. 1, pp. 12–20

[DeMi03] DESAI A. ; MITAL A.: Evaluation of disassemblability to enable design for disassembly in mass production. In: *International Journal of Industrial Ergonomics* Bd. 32 (2003), Nr. 4, pp. 265–281

[DFFG92] DI PELLEGRINO G. ; FADIGA L. ; FOGASSI L. ; GALLESE V. ; RIZZOLATTI G.: Understanding motor events: a neurophysiological study. In: *Experimental Brain Research* Bd. 91 (1992), Nr. 1, pp. 176–180

[DGBA99] DON B.C. ; GUNNAR B. J. A. ; BERNARD J. M. ; ANDERSSON GUNNAR B.J.: *Occupational Biomechanics*. 3–rd. Aufl. : WILEY-INTERSCIENCE, 1999 — ISBN 0-471-24697-2

[DGKR10] DE LUCA C. J. ; GILMORE L. D. ; KUZNETSOV M. ; ROY S. H.: Filtering the surface EMG signal: Movement artifact and baseline noise contamination. In: *Journal of Biomechanics* Bd. 43 (2010), Nr. 8, pp. 1573–1579

[DiSD08] DIPIETRO L. ; SABATINI A.M. ; DARIO P.: A Survey of Glove-Based Systems and Their Applications. In: *IEEE Transactions on Systems, Man, and Cybernetics, Part C (Applications and Reviews)* Bd. 38 (2008), Nr. 4, pp. 461–482

[DLBR05] DOMINJON L. ; LÉCUYER A. ; BURKHARDT J.-M. ; RICHARD P. ; RICHIR S.: Influence of control/display ratio on the perception of mass of manipulated objects in virtual environments. In: *IEEE Proceedings. VR 2005. Virtual Reality, 2005.* : IEEE, 2005, pp. 19–25

[DNHÅ11] DAWSON D. ; NOY Y. I. ; HÄRMÄ M. ; ÅKERSTEDT T. ; BELENKY G.: Modelling fatigue and the use of fatigue models in work settings. In: *Accident Analysis & Prevention* Bd. 43 (2011), Nr. 2, pp. 549–564

[Dufe15] DUFETEL C.-H.: *Plateforme de réalité virtuelle pour la rééducation de l'algodystrophie*, Arts et Métiers Paristech, Master thesis, 2015

[EFAG05] ERVILHA F.U. ; FARINA D. ; ARENDT-NIELSEN L. ; GRAVEN-NIELSEN T.: Experimental muscle pain changes motor control strategies in dynamic contractions. In: *Experimental Brain Research* Bd. 164 (2005), Nr. 2, pp. 215–224

[EnDg92] ENOKA R. M. ; D. G. STUART: Neurobiology of muscle fatigue. In: *Journal of Applied*

Physiology (Bethesda, Md.: 1985) Bd. 72 (1992), Nr. 5, pp. 1631–1648. — PMID: 1601767

[Endo16] ENDO H.: Pressing movements and perceived force and displacement are influenced by object stiffness. In: *Physiology & Behavior* Bd. 163 (2016), pp. 203–210

[ErBa02] ERNST O M. ; BANKS S M.: Humans integrate visual and haptic information in a statistically optimal fashion. In: *Nature* Bd. 415 (2002), Nr. 6870, pp. 429–433

[ErGD12] ERVILHA, U. F. ; GRAVEN-NIELSEN, THOMAS ; DUARTE, M.: A simple test of muscle coactivation estimation using electromyography. In: *Brazilian Journal of Medical and Biological Research* Bd. 45 (2012), Nr. 10, pp. 977–981

[EyMB05] EYNARD L. ; MEYER A. ; BOUAKAZ S.: Virtual arm for the phantom pain therapy. In: *International Conference on Machine Intelligence (ACIDCA-ICMI)*, 2005

[FaWi85] FALCONER K. ; WINTER D. A.: Quantitative assessment of co-contraction at the ankle joint in walking. In: *Electromyography and Clinical Neurophysiology* Bd. 25 (1985), Nr. 2–3, pp. 135–149. — PMID: 3987606

[FrAv13] FREY-LAW A.L. ; AVIN G.K.: MUSCLE COACTIVATION: A GENERALIZED OR LOCALIZED MOTOR CONTROL STRATEGY? In: *Muscle & nerve* Bd. 48 (2013), Nr. 4, pp. 578–585. — PMID: 24037745PMCID: PMC4180747

[Fuji04] FUJITA K.: Control strategies in human pinch motion to perceive the hardness of an elastic object. In: *Electronics and Communications in Japan (Part II: Electronics)* Bd. 87 (2004), Nr. 11, pp. 28–37

[Gesc97] GESCHEIDER G. A.: *Psychophysics: The Fundamentals* : Psychology Press, 1997. — Google-Books-ID: gATPDTj8QoYC — ISBN 978-1-134-80122-0

[GGRG93] GEISSER M. E. ; GASKIN M. E. ; ROBINSON M. E. ; GREENE A. F.: The relationship of depression and somatic focus to experimental and clinical pain in chronic pain patients. In: *Psychology & Health* Bd. 8 (1993), Nr. 6, pp. 405–415

[GiFa07] GIUDICE F. ; FARGIONE G.: Disassembly planning of mechanical systems for service and recovery: a genetic algorithms based approach. In: *Journal of Intelligent Manufacturing* Bd. 18 (2007), Nr. 3, pp. 313–329

[GoZa99] GOMES DE SÁ AN. ; ZACHMANN G.: Virtual reality as a tool for verification of assembly and maintenance processes. In: *Computers & Graphics* Bd. 23 (1999), Nr. 3, pp. 389–403

[GPRS14] GONZÁLEZ-FRANCO M. ; PECK C.T. ; RODRÍGUEZ-FORNELLS A. ; SLATER M.: A threat to a virtual hand elicits motor cortex activation. In: *Experimental brain research* Bd. 232 (2014), Nr. 3, pp. 875–887

[GrOs98] GRIBBLE L.P. ; OSTRY J.D.: Independent coactivation of shoulder and elbow muscles. In: *Experimental Brain Research* Bd. 123 (1998), Nr. 3, pp. 355–360

[GuGu97] GUNGOR A. ; GUPTA S. M.: An evaluation methodology for disassembly processes. In: *Computers & Industrial Engineering*, *Proceedings of the 21st International Conference on Computers and Industrial Engineering*. Bd. 33 (1997), Nr. 1–2, pp. 329–332

[HDPC00] HOFFMAN H. G. ; DOCTOR J. N. ; PATTERSON D. R. ; CARROUGHER G. J. ; THOMAS A. FURNESS III: Virtual reality as an adjunctive pain control during burn wound care in adolescent patients. In: *Pain* Bd. 85 (2000), Nr. 1, pp. 305–309

[HéDA91] HÉBERT L.J. ; DE SERRES S.J. ; ARSENAULT A.B.: Cocontraction of the elbow muscles during combined tasks of pronation-flexion and supination-flexion. In: *Electromyography and clinical neurophysiology* Bd. 31 (1991), Nr. 8, pp. 483–488. — PMID: 1797544

[HFMS99] HERMENS H. J. ; FREIKS B. ; MERLETTI R. ; STEGEMAN D. ; BLOK J. ; RAU G. ; DISSELHORST-KLUG C. ; HÄGG G.: *European Recommendations for Surface Electromyography: Results of the SENIAM Project* : Roessingh Research and Development, 1999. — Google-Books-ID: w7HgOwAACAAJ — ISBN 978-90-75452-15-0

[HoTu11] HODGES P. W. ; TUCKER K.: Moving differently in pain: A new theory to explain the adaptation to pain: In: *Pain* Bd. 152 (2011), Nr. Supplement, pp. S90–S98

[HoWW01] HOCKENBERRY J.M. ; WILSON D. ; WINKELSTEIN L.M.: *Wong's Essentials of Pediatric Nursing* : Elsevier Mosby, 2001. — Google-Books-ID: FTJqAAAAMAAJ — ISBN 978-0-323-02593-5

[HuLe16] HUG F. ; LE SANT G.: Adaptations du mouvement à la douleur : objectifs et conséquences. In: *Kinésithérapie, la Revue* Bd. 16 (2016), Nr. 170, pp. 2–9

[JäBa02] JÄNIG W ; BARON R: Complex regional pain syndrome is a disease of the central nervous system. In: *Clinical Autonomic Research* Bd. 12 (2002), Nr. 3, pp. 150–164

[JAOM14] JAUREGUI D.A.G. ; ARGELAGUET F. ; OLIVIER A.-H. ; MARCHAL M. ; MULTON F. ; LÉCUYER A.: Toward „Pseudo-Haptic Avatars": Modifying the Visual Animation of Self-Avatar Can Simulate the Perception of Weight Lifting. In: *IEEE transactions on visualization and computer graphics* Bd. 20 (2014), Nr. 4, pp. 654–661

[JiPu06] JIMENO A. ; PUERTA A.: State of the art of the virtual reality applied to design and manufacturing processes. In: *The International Journal of Advanced Manufacturing Technology* Bd. 33 (2006), Nr. 9–10, pp. 866–874

[JJSK06] JAYARAM U. ; JAYARAM S. ; SHAIKH I. ; KIM Y.J. ; PALMER C.: Introducing quantitative analysis methods into virtual environments for real-time and continuous ergonomic evaluations. In: *Computers in Industry*, *Advanced Computer Support of Engineering and Service Processes of Virtual EnterprisesAdvanced Computer Support Special Issue*. Bd. 57 (2006), Nr. 3, pp. 283–296

[KeAP03] KELLIS E. ; ARABATZI F. ; PAPADOPOULOS C.: Muscle co-activation around the knee in drop jumping using the co-contraction index. In: *Journal of Electromyography and Kinesiology: Official Journal of the International Society of Electrophysiological Kinesiology* Bd. 13 (2003), Nr. 3, pp. 229–238. — PMID: 12706603

[KHIB12] KIM D. ; HILLIGES O. ; IZADI S. ; BUTLER A. D. ; CHEN J. ; OIKONOMIDIS I. ; OLIVIER P.: Digits: freehand 3D interactions anywhere using a wrist-worn gloveless sensor. In: *Proceedings of the 25th annual ACM symposium on User interface software and technology* : ACM, 2012, pp. 167–176

[Koch08] KOCHERRY J. J.: *Comparison of Muscle Behavior While Using Real and Virtual*

Applications : ProQuest, 2008. — Google-Books-ID: WI4qGQP9fcUC — ISBN 978-0-549-73627-1

[KoGu05] KONGAR E. ; GUPTA S. M.: Disassembly sequencing using genetic algorithm. In: *The International Journal of Advanced Manufacturing Technology* Bd. 30 (2005), Nr. 5–6, pp. 497–506

[KSCK09] KOCHERRY J. J. ; SRIMATHVEERAVALLI G. ; CHOWRIAPPA A. J. ; KESAVADAS T. ; SHIN G.: Improving haptic experience through biomechanical measurements. In: *World Haptics 2009 - Third Joint EuroHaptics conference and Symposium on Haptic Interfaces for Virtual Environment and Teleoperator Systems*, 2009, pp. 362–367

[KWHC10] KARADOGAN E. ; WILLIAMS R. L. ; HOWELL J. N. ; CONATSER R. R.: A Stiffness Discrimination Experiment Including Analysis of Palpation Forces and Velocities. In: *Simulation in Healthcare: The Journal of the Society for Simulation in Healthcare* Bd. 5 (2010), Nr. 5, pp. 279–288

[LaFP10] LADEVEZE N. ; FOURQUET J.Y. ; PUEL B.: Interactive path planning for haptic assistance in assembly tasks. In: *Computers & Graphics* Bd. 34 (2010), Nr. 1, pp. 17–25

[Lans09] LANSKA D. J.: The history of movement disorders. In: *Handbook of Clinical Neurology* Bd. 95 (2009), pp. 501–546. — PMID: 19892136

[LaZe99] LAVIOLA J. ; ZELEZNIK R.: Flex and pinch: A case study of whole hand input design for virtual environment interaction. In: *Proceedings of the Second IASTED International Conference on Computer Graphics and Imaging*, 1999, pp. 221–225

[LBCC01] LECUYER A. ; BURKHARDT J.M. ; COQUILLART S. ; COIFFET P.: „Boundary of illusion“: an experiment of sensory integration with a pseudo-haptic system. In: *Proceedings IEEE Virtual Reality 2001*. Yokohama, Japan : IEEE, 2001, pp. 115–122

[LCKR00] LECUYER A. ; COQUILLART S. ; KHEDDAR A. ; RICHARD P. ; COIFFET P.: Pseudo-haptic feedback: can isometric input devices simulate force feedback? In: S. FEINER ; D. THALMANN (Hrsg.): : IEEE Comput. Soc., 2000 — ISBN 978-0-7695-0478-0

[LéBE04] LECUYER A. ; BURKHARDT J.-M. ; ETIENNE L.: Feeling bumps and holes without a haptic interface: the perception of pseudo-haptic textures. In: *Proceedings of the SIGCHI conference on Human factors in computing systems* : ACM, 2004, pp. 239–246

[LéCC01] LECUYER A. ; COQUILLART S. ; COIFFET P.: *Simulating haptic information with haptic illusions in virtual environments* : DTIC Document, 2001

[Lécu01] LECUYER A.: *Contribution à l'étude des retours haptique et pseudo-haptique et de leur impact sur les simulations d'opérations de montage/démontage en aéronautique*, Paris 11, Orsay, 2001

[Lécu09] LECUYER A.: Simulating haptic feedback using vision: a survey of research and applications of pseudo-haptic feedback. In: *Presence* Bd. 18 (2009), Nr. 1, pp. 39–53

[Leou14] LEOUFFRE M.: *Extraction de sources d'électromyogrammes et évaluation des tensions musculaires*, Université Grenoble Alpes, phdthesis, 2014

[Lind00] LIND A.R.: Muscle fatigue and recovery from fatigue induced by sustained

contractions. In: *The Journal of Physiology*

[LLLS12] LI M. ; LIU H. ; LI J. ; SENEVIRATNE D.L. ; ALTHOEFER K.: Tissue stiffness simulation and abnormality localization using pseudo-haptic feedback. In: *Robotics and Automation (ICRA), 2012 IEEE International Conference on* : IEEE, 2012, pp. 5359–5364

[LXGK13] LI W. D. ; XIA K. ; GAO L. ; K. -M. CHAO: Selective disassembly planning for waste electrical and electronic equipment with case studies on liquid crystaldisplays. In: *Robotics and Computer-Integrated Manufacturing* Bd. 29 (2013), Nr. 4, pp. 248–260

[MaSa94] MASSIE H.T. ; SALISBURY J.K.: The phantom haptic interface: A device for probing virtual objects. In: *Proceedings of the ASME winter annual meeting, symposium on haptic interfaces for virtual environment and teleoperator systems*. Bd. 55 : Chicago, IL, 1994, pp. 295–300

[Mert54] MERTON P. A.: Voluntary strength and fatigue. In: *The Journal of Physiology* Bd. 123 (1954), Nr. 3, pp. 553–564. — PMID: 13152698PMCID: PMC1366225

[MiWC16] MITROUCHEV P. ; WANG C. ; CHEN J.: Disassembly Process Simulation in Virtual Reality Environment. In: , 2016, pp. 631–638.

[MJBT02] MERIANS S.A. ; JACK D. ; BOIAN R. ; TREMAINE M. ; BURDEA C.G. ; ADAMOVICH V.S. ; RECCE M. ; POIZNER H.: Virtual reality-augmented rehabilitation for patients following stroke. In: *Physical Therapy* Bd. 82 (2002), Nr. 9, pp. 898–915. — PMID: 12201804

[MoAr13] MOHAPATRA S. ; ARUIN S.A.: Static and dynamic visual cues in feed-forward postural control. In: *Experimental Brain Research* Bd. 224 (2013), Nr. 1, pp. 25–34

[Mori70] MORI M.: The Uncanny Valley. In: *Energy* Bd. 19 (1970), Nr. 2, pp. 98–100

[Mose04a] MOSELEY G. L.: Evidence for a direct relationship between cognitive and physical change during an education intervention in people with chronic low back pain. In: *European Journal of Pain (London, England)* Bd. 8 (2004), Nr. 1, pp. 39–45. — PMID: 14690673

[Mose04b] MOSELEY G.L.: Graded motor imagery is effective for long-standing complex regional pain syndrome: a randomised controlled trial. In: *Pain* Bd. 108 (2004), Nr. 1, pp. 192–198

[Mose05] MOSELEY G. L.: Is successful rehabilitation of complex regional pain syndrome due to sustained attention to the affected limb? A randomised clinical trial. In: *Pain* Bd. 114 (2005), Nr. 1, pp. 54–61

[MoZG09] MO J. ; ZHANG Q. ; GADH R.: Virtual disassembly. In: *International Journal of CAD/CAM* Bd. 2 (2009), Nr. 1

[MPCH06] MURRAY C. D. ; PATCHICK E. L. ; CAILLETTE F. ; HOWARD T. ; PETTIFER S.: Can immersive virtual reality reduce phantom limb pain. In: *Stud Health Technol Inform* Bd. 119 (2006), S. 407–12

[MWLL15] MITROUCHEV, P. ; WANG, C. G. ; LU, L. X. ; LI, G. Q.: Selective disassembly sequence generation based on lowest level disassembly graph method. In: *The*

International Journal of Advanced Manufacturing Technology Bd. 80 (2015), Nr. 1–4, pp. 141–159

[OHLR86] OSTERNIG L. R. ; HAMILL J. ; LANDER J. E. ; R. ROBERTSON: Co-activation of sprinter and distance runner muscles in isokinetic exercise. In: *Medicine and Science in Sports and Exercise* Bd. 18 (1986), Nr. 4, pp. 431–435. — PMID: 3747804

[OiKA11] OIKONOMIDIS I. ; KYRIAZIS N. ; ARGYROS A. A.: Efficient model-based 3D tracking of hand articulations using Kinect. In: *BmVC*. Bd. 1, 2011, pp. 3

[PaBC04] PALJIC A. ; BURKHARDTT J.-M. ; COQUILLART S.: Evaluation of pseudo-haptic feedback for simulating torque: a comparison between isometric and elastic input devices. In: *Haptic Interfaces for Virtual Environment and Teleoperator Systems, 2004. HAPTICS'04. Proceedings. 12th International Symposium on* : IEEE, 2004, pp. 216–223

[PaIH04] PALMIERI M.R. ; INGERSOLL D.C. ; HOFFMAN A.M.: The Hoffmann reflex: methodologic considerations and applications for use in sports medicine and athletic training research. In: *Journal of athletic training* Bd. 39 (2004), Nr. 3, pp. 268

[PCDS14] PAGGETTI G. ; CIZMECI B. ; DILLIOGLUGIL C. ; STEINBACH E.: On the discrimination of stiffness during pressing and pinching of virtual springs. In: *Haptic, Audio and Visual Environments and Games (HAVE), 2014 IEEE International Symposium on* : IEEE, 2014, pp. 94–99

[PDSM14] PONTONNIER C. ; DUMONT G. ; SAMANI A. ; MADELEINE P. ; BADAWI M.: Designing and evaluating a workstation in real and virtual environment: toward virtual reality based ergonomic design sessions. In: *Journal on Multimodal User Interfaces* Bd. 8 (2014), Nr. 2, pp. 199–208

[PJHS14] PALMERIUS L. K. ; JOHANSSON D. ; HÖST G. ; SCHÖNBORN K.: An Analysis of the Influence of a Pseudo-haptic Cue on the Haptic Perception of Weight. In: *Haptics: Neuroscience, Devices, Modeling, and Applications* : Springer, 2014, pp. 117–125

[PKVD13] PERRET J. ; KNESCHKE C. ; VANCE J. ; DUMONT G.: Interactive assembly simulation with haptic feedback. In: *Assembly Automation* Bd. 33 (2013), Nr. 3, pp. 214–220

[PPTC04] POMARES J. ; PUENTE S. T. ; TORRES F. ; CANDELAS F. A. ; GIL P.: Virtual disassembly of products based on geometric models. In: *Computers in Industry* Bd. 55 (2004), Nr. 1, pp. 1–14

[PSBM13] PONTONNIER C. ; SAMANI A. ; BADAWI M. ; MADELEINE P. ; DUMONT G.: Assessing the Ability of a VR-based Assembly Task Simulation to Evaluate Physical Risk Factors. In: *IEEE Transactions on Visualization and Computer Graphics* (2013)

[PuMC08] PUSCH, A. ; MARTIN, O. ; COQUILLART, S.: HEMP-Hand-Displacement-Based Pseudo-Haptics: A Study of a Force Field Application. In: *IEEE Symposium on 3D User Interfaces, 2008. 3DUI 2008*, 2008, pp. 59–66

[RaAl09] RAMACHANDRAN S.V. ; ALTSCHULER L.E.: The use of visual feedback, in particular mirror visual feedback, in restoring brain function. In: *Brain* Bd. 132 (2009), Nr. 7, pp. 1693–1710

[RaMS99] RAGHAVAN V. ; MOLINEROS J. ; SHARMA R.: Interactive evaluation of assembly

sequences using augmented reality. In: *IEEE Transactions on Robotics and Automation* Bd. 15 (1999), Nr. 3, pp. 435–449

[RFGF96] RIZZOLATTI G. ; FADIGA L. ; GALLESE V. ; FOGASSI L.: Premotor cortex and the recognition of motor actions. In: *Cognitive Brain Research*, *Mental representations of motor acts*. Bd. 3 (1996), Nr. 2, pp. 131–141

[Rich94] RICHARD G. LANZARA: Weber's Law Modeled by the Mathematical Description of a Beam Balance. In: *Mathematical Biosciences* (1994)

[RiCr04] RIZZOLATTI G. ; CRAIGHERO L.: THE MIRROR-NEURON SYSTEM. In: *Annual Review of Neuroscience* Bd. 27 (2004), Nr. 1, pp. 169–192

[RNHK14] ROSE L. M. ; NEUMANN W. P. ; HÄGG G. M. ; KENTTÄ G.: Fatigue and recovery during and after static loading. In: *Ergonomics* Bd. 57 (2014), Nr. 11, pp. 1696–1710

[RoFD04] ROACH G. D. ; FLETCHER A. ; DAWSON D.: A model to predict work-related fatigue based on hours of work. In: *Aviation, space, and environmental medicine* Bd. 75 (2004), Nr. Supplement 1, pp. A61–A69

[Roge01] ROGER M. E.: *Neuromechanics of Human Movement 3rd edition*. Third Edition. Aufl. U.S.A : HUman Kinetics, 2001 — ISBN 0-7360-0251-0

[RuSe91] RUBE N. ; SECHER N. H.: Effect of training on central factors in fatigue following two-and one-leg static exercise in man. In: *Acta physiologica scandinavica* Bd. 141 (1991), Nr. 1, pp. 87–95

[SBML03] SANDRONI P. ; BENRUD-LARSON M.L. ; MCCLELLAND L.R. ; LOW A.P.: Complex regional pain syndrome type I: incidence and prevalence in Olmsted county, a population-based study. In: *Pain* Bd. 103 (2003), Nr. 1, pp. 199–207

[SCID12] SAYGIN P.A ; CHAMINADE T. ; ISHIGURO H. ; DRIVER J. ; FRITH C.: The thing that should not be: predictive coding and the uncanny valley in perceiving human and humanoid robot actions. In: *Social Cognitive and Affective Neuroscience* Bd. 7 (2012), Nr. 4, pp. 413–422. — PMID: 21515639

[ScMc87] SCHWARTZMAN J.R. ; MCLELLAN L.T.: Rreflex Sympathetic Dystrophy: A review. In: *Neurological Review* Bd. 44 (1987), pp. 555–561

[Seba11] SEBASTIN S.J.: Complex regional pain syndrome. In: *Indian Journal of Plastic Surgery* Bd. 44 (2011), Nr. 2, pp. 298

[ShBS06] SHENG J. ; BALAKRISHNAN R. ; SINGH K.: An interface for virtual 3D sculpting via physical proxy. In: *GRAPHITE*. Bd. 6, 2006, pp. 213–220

[ShWi65] SHAPIRO S. S. ; WILK M. B.: An analysis of variance test for normality (complete samples). In: *Biometrika* Bd. 52 (1965), Nr. 3–4, pp. 591–611

[SHWP15] SONNE M.W. ; HODDER J.N. ; WELLS R. ; POTVIN J.R.: Force time-history affects fatigue accumulation during repetitive handgrip tasks. In: *Journal of Electromyography and Kinesiology: Official Journal of the International Society of Electrophysiological Kinesiology* Bd. 25 (2015), Nr. 1, pp. 130–135. — PMID: 25465984

[SmCh11] SMITH S. S. ; CHEN W.H.: Rule-based recursive selective disassembly sequence

planning for green design. In: *Advanced Engineering Informatics*, *RFID and sustainable value chains*. Bd. 25 (2011), Nr. 1, pp. 77–87

[SMRB09] STINS J. F. ; MICHIELSEN M. E. ; ROERDINK M. ; BEEK P. J.: Sway regularity reflects attentional involvement in postural control: Effects of expertise, vision and cognition. In: *Gait & Posture* Bd. 30 (2009), Nr. 1, pp. 106–109

[SoKn00] SODERBERG G. L. ; KNUTSON L. M.: A guide for use and interpretation of kinesiologic electromyographic data. In: *Physical Therapy* Bd. 80 (2000), Nr. 5, pp. 485–498. — PMID: 10792859

[SrBB96] SRINIVASAN M. A. ; BEAUREGARD G.L. ; BROCK D.L.: The impact of visual information on the haptic perception of stiffness in virtual environment (1996)

[SrFG99] SRINIVASAN H. ; FIGUEROA R. ; GADH R.: Selective disassembly for virtual prototyping as applied to de-manufacturing. In: *Robotics and Computer-Integrated Manufacturing* Bd. 15 (1999), Nr. 3, pp. 231–245

[SSGO01] SUZUKI, MASATAKA ; SHILLER, DOUGLAS M. ; GRIBBLE, PAUL L. ; OSTRY, DAVID J.: Relationship between cocontraction, movement kinematics and phasic muscle activity in single-joint arm movement. In: *Experimental Brain Research* Bd. 140 (2001), Nr. 2, pp. 171–181

[STMB09] SAPONAS T.S. ; TAN S.D. ; MORRIS D. ; BALAKRISHNAN R. ; TURNER J. ; LANDAY A.J.: Enabling always-available input with muscle-computer interfaces. In: : ACM Press, 2009 — ISBN 978-1-60558-745-5, pp. 167

[SYMM97] SUZUKI M. ; YAMAZAKI Y. ; MIZUNO N. ; MATSUNAMI K.: Trajectory formation of the center-of-mass of the arm during reaching movements. In: *Neuroscience* Bd. 76 (1997), Nr. 2, pp. 597–610. — PMID: 9015341

[TaHi08] TANIKAWA T. ; HIROSE M.: A Study of Multi-modal Display System with Visual Feedback. In: : IEEE, 2008 — ISBN 978-0-7695-3433-6, pp. 285–292

[TDBS95] TAN H. Z. ; DURLACH N. I. ; BEAUREGARD G. L. ; SRINIVASAN M. A.: Manual discrimination of compliance using active pinch grasp: the roles of force and work cues. In: *Perception & Psychophysics* Bd. 57 (1995), Nr. 4, pp. 495–510. — PMID: 7596747

[TLKC12] TIAN G. ; LIU Y. ; KE H. ; CHU J.: Energy evaluation method and its optimization models for process planning with stochastic characteristics: A case study in disassembly decision-making. In: *Computers & Industrial Engineering*, *Energy Management and Economics*. Bd. 63 (2012), Nr. 3, pp. 553–563

[TsYH11] TSENG, YUAN-JYE ; YU, FANG-YU ; HUANG, FENG-YI: A green assembly sequence planning model with a closed-loop assembly and disassembly sequence planning using a particle swarm optimization method. In: *The International Journal of Advanced Manufacturing Technology* Bd. 57 (2011), Nr. 9–12, pp. 1183–1197

[UDFV96] UNNITHAN V. B. ; DOWLING J. J. ; FROST G. ; VOLPE AYUB B. ; BAR-OR O.: Cocontraction and phasic activity during GAIT in children with cerebral palsy. In: *Electromyography and Clinical Neurophysiology* Bd. 36 (1996), Nr. 8, pp. 487–494. — PMID: 8985677

[Vand10] VAN DER HELM A.P.: Weber-Fechner behavior in symmetry perception? In:

Attention, Perception, & Psychophysics Bd. 72 (2010), Nr. 7, pp. 1854–1864

[Vern29] VERNON H. M.: The influence of rest pauses and changes of posture on the capacity for muscular work. In: *A.R. industr. Fatig. Res. Bd., Lond* (1929), Nr. No. 54, Part B

[ViDi96] VILAYANUR S. RAMACHANDRAN ; DIANE ROGERS-RAMACHANDRAN: Synaesthesia in phantom limbs induced with mirrors. In: *Proceedings of the Royal Society of London B: Biological Sciences* Bd. 263 (1996), Nr. 1369, pp. 377–386

[Vøll95] VØLLESTAD N. K.: Metabolic correlates of fatigue from different types of exercise in man. In: *Advances in Experimental Medicine and Biology* Bd. 384 (1995), pp. 185–194. — PMID: 8585450

[Wang14] WANG C.: *Disassembly sequences generation and evaluation. Integration in a virtual veality environment*. Grenoble, University Grenoble Alpes, 2014

[WaPo09] WANG Y. R. ; POPOVIĆ J.: Real-time hand-tracking with a color glove. In: *ACM transactions on graphics (TOG)*. Bd. 28 : ACM, 2009, pp. 63

[WMLL15] WANG C. ; MITROUCHEV P. ; LI G. ; LU L.: Disassembly operations' efficiency evaluation in virtual environment. In: *International Journal of Computer Integrated Manufacturing, Ed. Taylor & Francis*, *29(3)*. (2015), pp. 1–14

[WTCK15] WON, ANDREA STEVENSON ; TATARU, CHRISTINE A. ; COJOCARU, CRISTINA M. ; KRANE, ELLIOT J. ; BAILENSON, JEREMY N. ; NISWONGER, SARAH ; GOLIANU, BRENDA: Two Virtual Reality Pilot Studies for the Treatment of Pediatric CRPS. In: *Pain Medicine (Malden, Mass.)* Bd. 16 (2015), Nr. 8, pp. 1644–1647. — PMID: 25930099

[WuBS99] WU W. ; BASDOGAN C. ; SRINIVASAN M.A.: Visual, Haptic, and Bimodal Perception of Size and Stiffness in Virtual Environments. In: *Proceeding of the ASME Dynamic Systems and Control Division* Bd. 67 (1999)

[YaWi83] YANG J.F. ; WINTER D.A.: Electromyography reliability in maximal and submaximal isometric contractions. In: *Archives of physical medicine and rehabilitation* Bd. 64 (1983), Nr. 9, pp. 417–420. — PMID: 6615179

[YoAE11] YOUSSIF M. M. ; ALKADEEM R. A. ; EL DARDIRY M. A.: Incorporating ergonomic factors in disassembly sequence planning. In: *Alexandria Engineering Journal* Bd. 50 (2011), Nr. 3, pp. 213–217

[YTFS13] YUKI B. ; TAKUJI N. ; FUJII T. ; SAKURAI S. ; IMURA J. ; TANIKAWA T. ; HIROSE M.: Augmented endurance: controlling fatigue while handling objects by affecting weight perception using augmented reality. In: *Proceedings of the SIGCHI Conference on Human Factors in Computing Systems* : ACM, 2013, pp. 69–78

[ZBHR11] ZHOU L. ; BAI S. ; HANSEN M. R. ; RASMUSSEN J.: Modeling of Human Arm Energy Expenditure for Predicting Energy Optimal Trajectories. In: *Modeling, Identification and Control: A Norwegian Research Bulletin* Bd. 32 (2011), Nr. 3, pp. 91–101

Appendixes

Appendix 1. Experimental plan

Human arm muscles and Position of the strain sensors

There are six sets of electrodes distributed on the operator's hand in order to detect the EMG on each point (two for the flexor and extensor wrist muscles, one for the biceps and one for the triceps muscle). The electrode on the wrist is used as ground to reduce the noise.

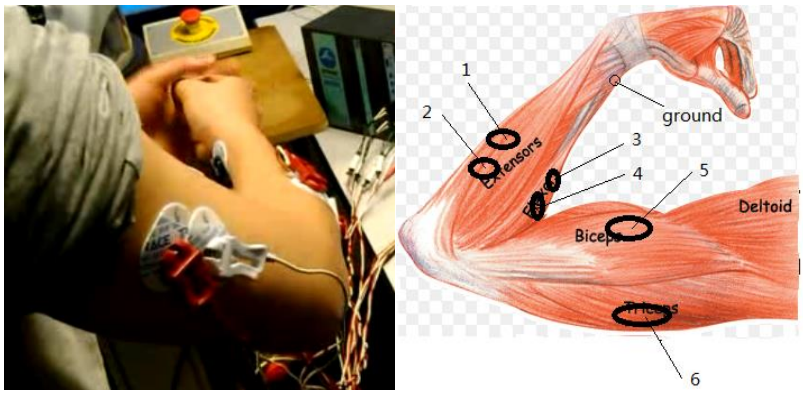

Figure 1. Position of the electrodes.

Parameters to be measured

1. Operation completing time while each disassembly sequence is performed by each operator.

2. EMG curve of each operator's arm muscle involved to manipulate the haptic device.
3. The velocities of some points on the operator's arm.

Experimental steps

1. Each operator (subject) should be familiar with the basic operations including selecting component, achieve translation of component in any directions and rotations around any orientations. For this purpose, every operator has three minutes to get familiar with the haptic device before the experiment.
2. To locate six sets of electrodes in the corresponding places of operator's arm.
3. Let the operator do the nine basic exertions to obtain the values of MVC of each joint. The movements are show in the following figures.

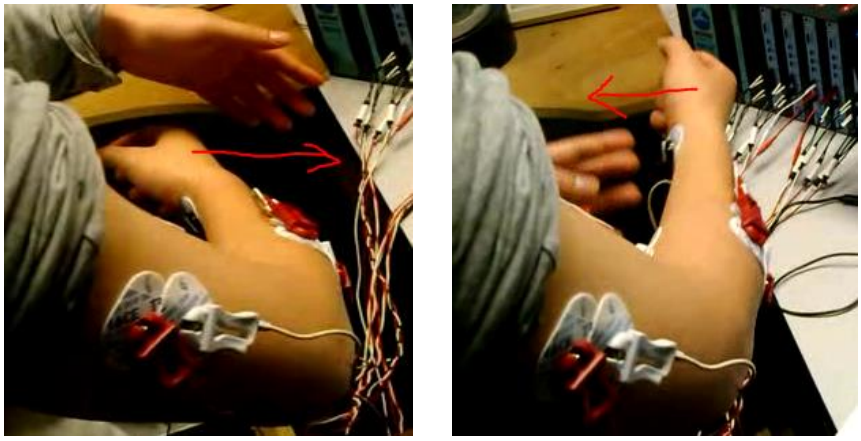

Figure 2. MVC 1 (left) and MVC 2 (right).

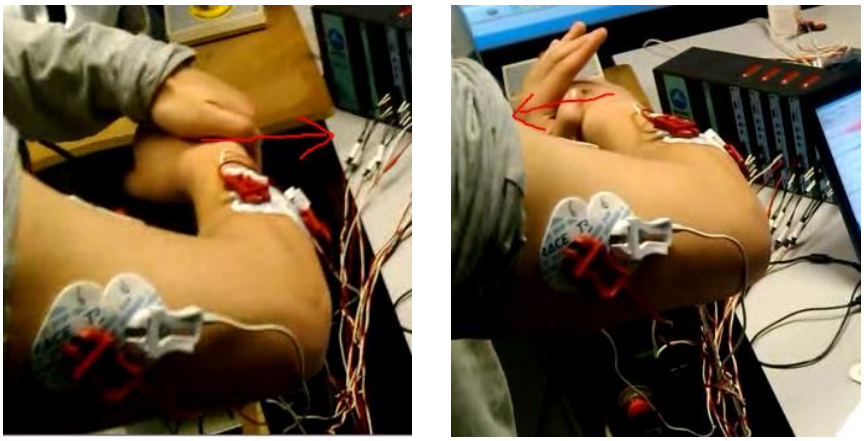

Figure 3. MVC 3 (left) and MVC 4 (right).

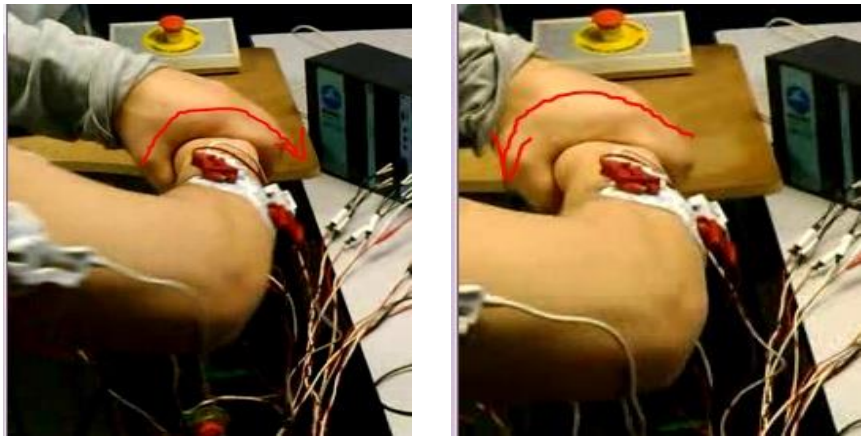

Figure 4. MVC 5 (left) and MVC 6 (right).

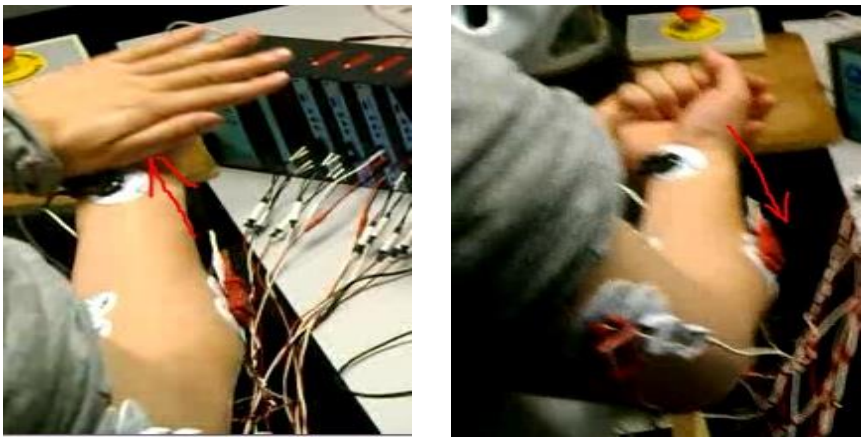

Figure 5. MVC 7 (left) and MVC 8 (right).

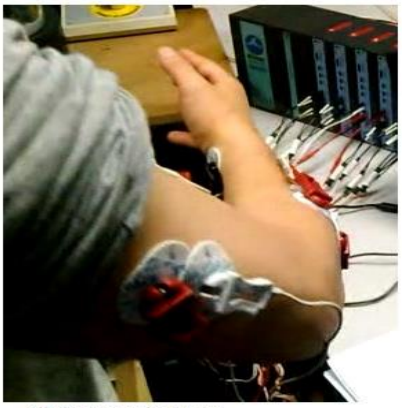

Figure 6. MVC 9.

4. Let the operator to repeatedly manipulate the motor from the bottom of frame to the top of the frame for five minutes with standing position.
5. To record the EMG signals for the six sets of electrodes of EMG system.
   Use the Kinect scanner to measure some angles of rotation and the speed of some points on the muscles.

Appendix 2. Experimental protocol

1. Questionnaire

1) Did you already hear about the experiment (from colleagues…)?
   □ Yes □ No

2) Gender: □ Male □Female
3) Your age: □18-20 □21-30 □31-40 □41-50 □51-60 □ 61 and above
4) Your dominant hand: □Left □Right
5) I conform that I have no:
   a. corrected visual impairments,
   b. impairments of haptic sensivity (sensivity of touch, numbness of the fingers, loss of finger location…)
   c. diseases or symptoms which induce hand movement disorders.

2. Instructions

The purpose of the experiment is to compare the stiffness of two simulated springs. A simulated spring (spring for short) is composed of a button (Fig.1.b), and a piston visualized on the screen (Fig.1.a).

For each trial, you will be asked to perform a stiffness discrimination task between two springs.

The pistons of two compared springs will be displayed on the screen titled “Spring A” and “Spring B”. For each spring, the ID of the corresponding button is indicated just below “Button N°i/ Button N° j”. In Figure 3a, the button associated with piston A is button No. 1 and the button associated with piston B is button No. 4. For each trial, you have to press spring B first.

a). b).

Fig. 1 Stiffness discrimination interface.

The information presented on the top of the screen (Fig.1a) indicates that you are performing Trial 1 and you have spent 10s. To evaluate a spring during the stiffness discrimination task, you have to use your index finger to press the button inside the box while continuously looking at the rendered piston movement on the computer screen.

The experiment, includes 198 trials in total.

The protocol for each trial is the following:

1. You compare the stiffness of each of the two given springs (you can switch back and forth between the two springs as you wish). It is recommended to give your answer within 20 seconds.
2. Once you have made your decision of which spring is stiffer, you have to push key 'S' to *Stop* the trial.
3. Then the computer will ask the question '*Which spring is stiffer*?' (Fig. 2.a).
4. Pushing key 'A' indicates that you found that spring A is stiffer (harder) than spring B. Pushing key 'B' indicates that you found spring B stiffer than spring A.
5. The system will then ask you to confirm your answer (Fig. 2b). To confirm your answer, you have to push key 'Y' (Yes). Otherwise, you can push key 'N' (No), and it will return to the question in order to let you correct your answer.
6. You have to give an answer for each trial.

3. Pay attention:

1. As previously said, when you press the simulated spring's button, you have to look at the computer screen. When the "STOP PRESSING" message is appearing on the screen, you have to stop pressing immediately. If not, you may reach unoperational part of the spring.
2. Your forearm must always be in contact with the two black blocks.
3. After the experiment, please do not speak about the experiment with your colleagues (they may also be invited as subjects, and have to be *naive* to the purpose of the *experiment.*

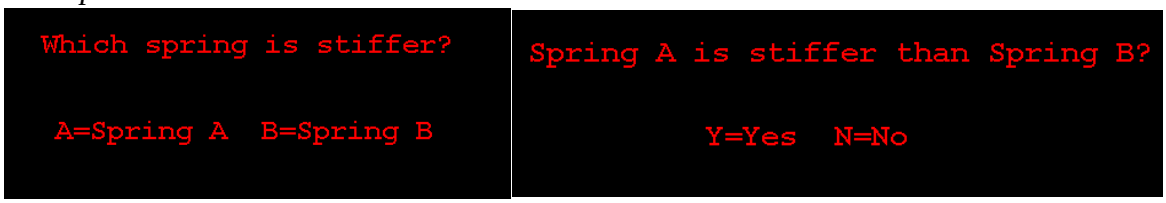

a). b).

Fig. 2 Interactive "question" and "answer" interface.

Appendix 3. Questionnaire

Before Experiment

1. Gender: Male □ Female □
2. Your age:
3. Before the experiment, does your hand have pain? Please evaluate your pain, before the experiment; by crossing one of the following faces :

After Experiment 1 (Normal skin)

4. Please indicate your pain level during using the application by crossing one of the following faces :

After Experiment 2 (Silver skin)

5. Please indicate your pain level during using the application by crossing one of the following faces :

6. Do you have previous experience with using virtual reality? Yes□ No□
7. During the experiment, do you have any uncomfortable feeling? Yes□ No□
   If 'yes', indicate which one make you more uncomfortable
   Normal skin □ Silver skin □
8. Do you think using this application will encourage you to better participant in the physical therapy? Yes□ No□
9. What is the most interesting thing that you want to do by controlling the hand in computer screen as physical therapy scenario?

Summary:
Nowadays, Virtual reality (VR) is being more and more integrated into many fields of our daily life thus influencing some practices such as: human behavior, communication methods, cognition… amongst others. In this context, our research aimed to better understand how VR is influencing on human behavior with using biomechanical analysis methods and its application for Complex Regional Pain Syndrome (CRPS) rehabilitation in particular. Firstly, the muscle fatigue levels associated with different disassembly task simulations by using haptic device in VR environment are evaluated. For this purpose, a new analytical model for mechanical energy expenditure is proposed where the required mechanical work is used as main parameter. After then, the proposed method is validated by analyzing the recorded electromyography (EMG) signals on operator' arm performed in a VR environment. Secondly, we focus to understand the effect of pseudo-haptic on human behavior. The task consisted in discriminating the stiffness between a real and a virtual spring. For this purpose, series of experiments were performed on the specially designed test bench. The pressing force, some kinematic parameters of the test and the EMG signals recorded from the involved muscles of subjects' arms were analyzed and compared. It was found that pressing forces on both real and virtual springs have similar behavior and the muscle co-activation induced by pseudo-haptic spring behavior is as in dynamic task, even though subjects' fingers were static while pressing on the virtual spring. Pain and muscular maladaptation, due to the abnormal posture of affected limbs, are big obstacles for CRPS patients in their physical therapy and daily lives. Thus, in order to overcome some drawbacks of the traditional physical therapy, an application based on Leap Motion and Unity3D was developed allowing to manipulate the relationship between the user's physical hand motion and the rendered avatar virtual motion. The application was validated by a pilot study performed at University Hospital Center (CHU) Grenoble in the Service of Hand surgery. During the experiments the rendered avatar hand motion is shown identical, amplified or reduced compared to the users' real hand motion. Users' feedback, after each experience, allowed to positively conclude for the possibility to use the application in rehabilitation process.

Key words: disassembly task evaluation; muscle fatigue; virtual reality; force; muscle co-activation; pseudo-haptic feedback; stiffness discrimination; Complex Regional Pain Syndrome; rehabilitation.

Résumé :
Aujourd'hui la réalité virtuelle (RV) est de plus en plus intégrée dans de nombreux aspects de notre vie quotidienne et, par conséquent, elle influence certaines pratiques comme : le comportement humain, les méthodes de communication, la cognition… entre autres. Dans ce contexte, notre recherche a visé à mieux comprendre comment la réalité virtuelle (RV) influence le comportement humain en utilisant les méthodes d'analyse de la biomécanique et son utilisation dans la réhabilitation du Syndrome douloureux régional complexe (SDRC) en particulier. Premièrement les niveaux de fatigue musculaire associés à différentes tâches de désassemblage en utilisant un dispositif haptique dans un environnement RV ont été évalués. A cet effet, un nouveau modèle analytique pour la dépense d'énergie mécanique est proposé où le travail mécanique requis est utilisé comme paramètre principal. Ensuite, la méthode proposée a été validée par l'analyse des signaux EMG (électromyographie) enregistrés sur le bras de l'opérateur lors d'un exercice réalisé dans l'environnement de RV. En second lieu, nous nous sommes concentrés sur la compréhension de l'effet d'un retour pseudo-haptique sur le comportement humain. La tâche consistait à discriminer la raideur d'un ressort simulé par rapport à un ressort réel. A cet effet des expériences ont été effectuées sur un banc d'essai spécialement conçu. La force de compression, certains paramètres cinématiques du test et les signaux EMG, enregistrés sur les muscles impliqués des bras des sujets ont été analysés et comparés. Il a été constaté que les changements des forces de pression sur les ressorts réels et le ressort virtuel ont un comportement similaire tandis que la co-activation musculaire induite par le comportement du ressort virtuel est la même que dans le cas du test de ressort réel correspondant (tâche dynamique), en dépit du fait que les doigts des sujets étaient immobiles en appuyant sur le ressort virtuel. La douleur et la mal-adaptation musculaire associées à une posture anormale constituent des obstacles importants pour les patients souffrant de CRPS dans leur thérapie physique et leur vie quotidienne. Ainsi, afin de surmonter certains inconvénients de la thérapie physique traditionnelle, une application basée sur le Leap Motion et Unity3D a été développée permettant de manipuler la relation entre le mouvement de l'utilisateur et le mouvement virtuel rendu de l'avatar. L'application a été validée par une étude pilote menée au Centre Hospitalier Universitaire (CHU) de Grenoble (Service chirurgie de la main). Au cours des expériences, le mouvement de la main de l'avatar est rendu identique, amplifié ou réduit par rapport au mouvement réel de l'utilisateur. Les commentaires des utilisateurs, après chaque expérience, ont permis de conclure positivement sur la possibilité d'utiliser l'application dans le processus de réhabilitation.

Mots-clés : évaluation des tâches de désassemblage; fatigue musculaire; réalité virtuelle; force; co-activation musculaire; retour pseudo-haptique; discrimination de raideur ; Syndrome douloureux régional complexe; réhabilitation ;